PhD degree in Molecular Medicine

European School of Molecular Medicine (SEMM),

University of Milan and University of Naples "Federico II"

Faculty of Medicine

Settore disciplinare: MED/04

Dissecting the Transformation Process in Mammary Stem Cells

Cristina Elisabetta Pasi

IFOM-IEO Campus, Milan

Matricola n. R07399

Supervisor: **Prof. Pier Giuseppe Pelicci, MD, PhD**

IFOM-IEO Campus, Milan

Added co-Supervisor: **Dr. Stefano Casola, PhD**

IFOM-IEO Campus, Milan

Academic Year 2010-2011

To my parents

Contents

1 List of Abbreviations

Nomenclature

4-OHT 4-Hydroxy Tamoxifen

ALDH Aldheyde Dehydrogenase

AML Acute Myeloid Leukemia

aPKC atypical Protein Kinase C

BMP Bone Morphogenetic Proteins

Brat Brain tumour

BSA Bovine Serum Albumin

CD44 Cluster of Differentiation 44

CML Chronic Myeloid Leukemia

CMV Cytomegalovirus

CSC Cancer Stem Cell

DAPI 4',6-Diamidino-2-Phenylindole

DIC Differential Interference Contrast

dlg Disc Large

DMEM Dulbecco's Modified Eagle Medium

DMSO Dimethyl Sulfoxide

EGF Epidermal Growth Factor

EMT Epithelial to Mesechimal Transition

ER Estrogen Receptor

FAP Familial Adenomatous Poliposis

FBS Fetal Bovine Serum

FD Familial Dysautonomia

FGF Fibroblast Growth Factor

FVB Friend Virus B-Type

GFP Green Fluorescent Protein

GMC Ganglion Mother Cell

HBS HEPES Buffer Saline

HEPES 4-(2-hydroxyethyl)-1-piperazineethanesulfonic acid

HRP Horse Radish Peroxidase

i.p. Intra Peritoneal

IEO Istituto Europeo di Oncologia

iPS induced Pluripotent Stem

K5 Cytokeratin 5

K8 Cytokeratin 8

KO KnockOut

Lgl Lethal giant larvae

LIF Leukemia Inhibitory Factor

MEF Mouse Embryo Fibroblasts

miRNAs microRNA

MMTV Mouse Mammary Tumour Virus

Mud Mushroom body defect

NA Numerical Aperture

NuMA Nuclear Mitotic Apparatus protein 1

PAR Partitioning factor

PBS Phosphate Buffered Saline

Pins Prtner of inscuteable

PML Promyelocytic Leukemia

PON Partner of Numb

RFP Red Fluorescent Protein

scrib Scribbled

SCs Stem Cells

SDS Sodium Dodecyl Sulfate

SDS-PAGE Sodium Dodecyl Sulfate-Polyacrylamide Gel Electrophoresis

TBS-T Tris Buffered Saline-Tween

TEBs Terminal End Buds

WB Western Blot

WT Wild Type

2 List of Figures and Tables

List of Figures

List of Tables

3 Abstract

Stem Cells (SCs) may play a critical role in cancer development, yet the direct demonstration is still lacking. The characterization of mechanisms that sustain and regulate Cancer Stem Cells (CSCs) may help elucidating their role in tumors. Using a MMTV-ErbB2 breast cancer mouse-model, we had previously shown that CSCs, through multiple rounds of symmetric divisions and extended self-renewal, drive tumor growth and the expansion of the CSC pool. Critical for this property is the lack of functional p53, that drives CSCs to symmetric divisions. Here we show that symmetric divisions and extended self-renewal in CSCs are due to the activation of c-myc as direct consequence of the loss of functional p53. In particular, c-myc is upregulated in transformed and p53-/- immortalized SCs, and enforced expression of c-myc in normal mammary SCs induces symmetric divisions and extended self-renewal, but does not transform. We show that mammary progenitors expressing c-myc acquire *in vitro* self-renewal properties (mammosphere formation and expansion) and *in vivo* regenerative potential (formation of normal mammary gland upon transplantation). Our data suggest that c-myc is critical for the maintenance of CSCs in ErbB2-mammary tumors and their aberrant self-renewing properties. This is achieved through its binary effect on CSCs (induction of symmetric divisions) and progenitors (reprogramming into CSCs). Recent studies demonstrate that c-myc over-expression in epithelial tissues induces an abnormal transcriptional pattern, similar to that of embryonic SCs, and that the same is activated in epithelial cancers and CSCs. This suggests that c-myc may be a general regulator of CSCs and their altered self-renewing properties.

4 INTRODUCTION

4.1 The Origin and Nature of Cancer

Cancer is a widespread disease that comprises a number of different lesions characterised by uncontrolled cell proliferation. What univocally describes these lesions is their very heterogeneity. Not only they can arise in different tissues with different mechanisms, but within each single lesion cells with several phenotypical and functional differences coexist (Campbell and Polyak, 2007; Reya et al., 2001; Visvader and Lindeman, 2008). These cellular subtypes differ in size and morphology, cell surface marker expression, membrane composition as well as in proliferation rate, cell-cell interaction, metastatic proclivity, and sensitivity to chemotherapy. Three models have been postulated to explain the underlying mechanisms and to describe the onset and progression of cancer: the cancer stem cell model, the clonal evolution model and the interconversion model. These theories have important implications from a therapeutic point of view, as they identify very different putative targets for therapies that can be specifically directed against those cells that contribute to the progression of the disease.

4.1.1 The Cancer Stem Cell Theory

The CSC theory postulates that only a subset of cells that possess stem properties accounts for the maintenance and the growth of a tumoural mass .SCs are a long-lived cell population responsible for tissue formation, homeostasis and repair. SCs have been identified in several tissues like blood, breast, colon, lung, liver and brain but, in light of recent findings, it seems plausible that every tissue is maintained by specific SCs. These cells are defined by their ability to perpetuate themselves through self-renewal and to generate mature cells of a particular tissue through differentiation. Because tumours can be considered as hierarchically organized tissues, it is reasonable to propose that a subset of cells with analogous properties is responsible for the sustenance of the malignant cellular mass. Due to their extended life span, normal SCs or their direct progenies represent an ideal target of cell transformation, and may explain the appearance of CSCs (Fig. 4.1) .

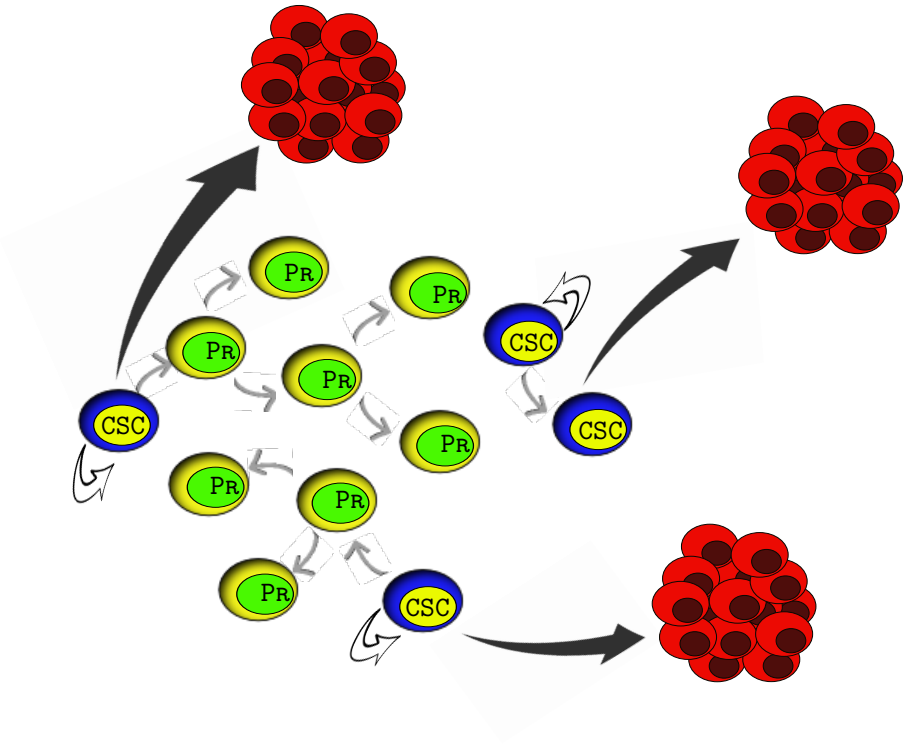

Figure 4.1: **The Cancer Stem Cell Theory.**
In the cancer stem cell theory, the only tumorigenic cells, CSCs, are able to sustain their growth (outlined arrow) and to give rise to differentiated cells (Pr) that cannot support the growth of the tumour mass (in red).

Therefore, according to this theory, cancers are supported by transformed SCs, which retain the same self-renewing and differentiating properties of their normal counterparts (Reya et al., 2001; Shipitsin and Polyak, 2008). Just as normal SCs, they can differentiate into phenotypically different progeny with limited proliferative potential through irreversible epigenetic changes that are accompanied by the loss of tumorigenic capacities. Consistently with this model, several tumours have been shown to be subfractionable into populations of tumorigenic and non tumorigenic cells, suggesting that indeed there is a phenotipic and functional hierarchy within the tumour mass.

The first demonstration of the existence of a rare population of cancer-initiating cells came from studies performed in 1994 on acute myeloid leukemia (AML) patients, by the group of John Dick in Toronto (Lapidot et al., 1994). In this study, the authors describe the purification of a subpopulation of cancer cells that possess tumour-initiating properties. Using the fluorescence-activated cell sorting (FACS) technique, they were able to fractionate different subsets of tumour cells based on the expression of surface markers. Of these subpopulations, only the CD34 +/CD38- cell fraction was able to form a new AML upon xeno-transplantation in mice, leading to the formal demonstration that only specific cell subsets in the tumour mass were able to recapitulate the disease upon engraftment. These cells showed differentiating and self-renewing abilities, as they were able to form tumours with the same cell heterogeneity of the

tumour of origin, and could be serially transplanted to obtain tertiary tumours. In addition, the surface markers that prospectively identified the AML-initiating cells were found to be specifically expressed in the corresponding normal SCs. Because these AML-initiating cells represented less than the 0,01% of the total leukemia cells, the authors concluded that rare cells in tumours share the same features of normal SCs and can be referred to as Cancer SCs (Campbell and Polyak, 2007; Visvader and Lindeman, 2008).

Further evidences supporting the CSC theory have come from several human diseases including malignant germ cell cancers (Illmensee and Mintz, 1976; KLEINSMITH and PIERCE, 1964), breast cancers (Al-Hajj et al., 2003), brain cancers (Singh et al., 2004) and colon cancers (Ricci-Vitiani et al., 2007; O'Brien, 2007; Dalerba et al., 2007). All these works describe the identification of a subpopulation of cells isolated from the bulk of the tumour mass which possessed the ability to reproduce the disease if engrafted in recipient mice. In particular, the identification of cancer cells with stem properties in breast cancers was the first report of the existence of these cells in solid malignancies. In 2003 Al-Hajj and colleagues isolated from human breast cancer samples a CD44+/ CD24- population that was highly enriched in cells able to re-generate breast carcinoma upon transplantation into the mammary tissue of NOD-SCID mice (Al-Hajj et al., 2003). This work made way for the subsequent identification of cell surface markers that have been used to purify human cancer SCs in different tumours . Although it is still unclear whether all cancers exhibit the same hierarchical organization and are sustained by cells with stem properties, some of the identified markers were found to be expressed by cancer SCs derived from different types of tumours. For example, CD44 has been used to fractionate cancer SCs in breast, colon and pancreas tumours, whereas CD133 can separate cancer SC subsets in brain (both glioblastoma and medulloblastoma), colon, pancreas and lung tumours. Interestingly, CD44 is expressed in a variety of epithelial basal layer cells, where SCs and less differentiated precursors are usually situated (Tan et al., 2006), and CD133 is also expressed in normal neural SCs (Uchida et al., 2000), thus supporting the idea that cancer SCs may arise from the transformation of normal SCs or their direct progenies.

In summary, the CSC hypothesis implies that a particular subset of tumour cells with stem cell-like properties drives tumour initiation, progression, and is responsible for the high recurrence incidence of this malignancy. These cells share with normal adult SCs the ability to self-renew indefinitely and to differentiate, two properties that lead to the generation of nontumorigenic differentiated cells, thereby accounting for tumour heterogeneity. Because of the described similarities, the origin of CSCs is often attributed to the transformation of normal SCs, although there is no formal proof to confirm this. These cells are thought to persist as a small fraction of the total cells in the tumour and to sustain its growth with their constant expansion (Visvader and Lindeman, 2008; Campbell and Polyak, 2007).

4.1.2 The Clonal Evolution Model

The CSC theory is supported by very strong data, however, there are some limitations to this theory and some of its points still remain to be demonstrated. As previously described, this theory identifies a small subset of tumour cells as responsible for tumour growth and sustenance. According to the model, these cells are the only ones that can propagate the disease if transplanted, however, recapitulation of the heterogeneity of the original tumour upon transplantation has only ever been evaluated by the analysis of few surface markers, and genetic alterations in the primary tumour has never been studied. Furthermore, transplantation in NOD/SCID mice of human tumour cells has been shown to dramatically underestimate the frequency of tumorigenic cells in some cancers (Quintana et al., 2008) suggesting that the population of tumorigenic cells may be dramatically underestimated. The CSC theory postulates that CSCs are responsible for the tumour growth and they can originate differentiated progeny which has undergone epigenetic modifications and is no longer tumorigenic. Nonetheless, the observed tumour heterogeneity, in fact, can arise also if cells that compose it differ genetically rather than epigenetically, and these genetic alterations may result in the loss of tumorigenicity (Shackleton et al., 2009). If this were the case, the process of tumour formation and growth may be explained by a model that identifies as potential target of transformation any cell in a given tissue. Transformation occurs through the accumulation of multiple stochastic genetic mutations and results in the generation of an heterogeneous population of cancer cells within the same tumour; this model has been named the clonal evolution model (Fig. 4.2).

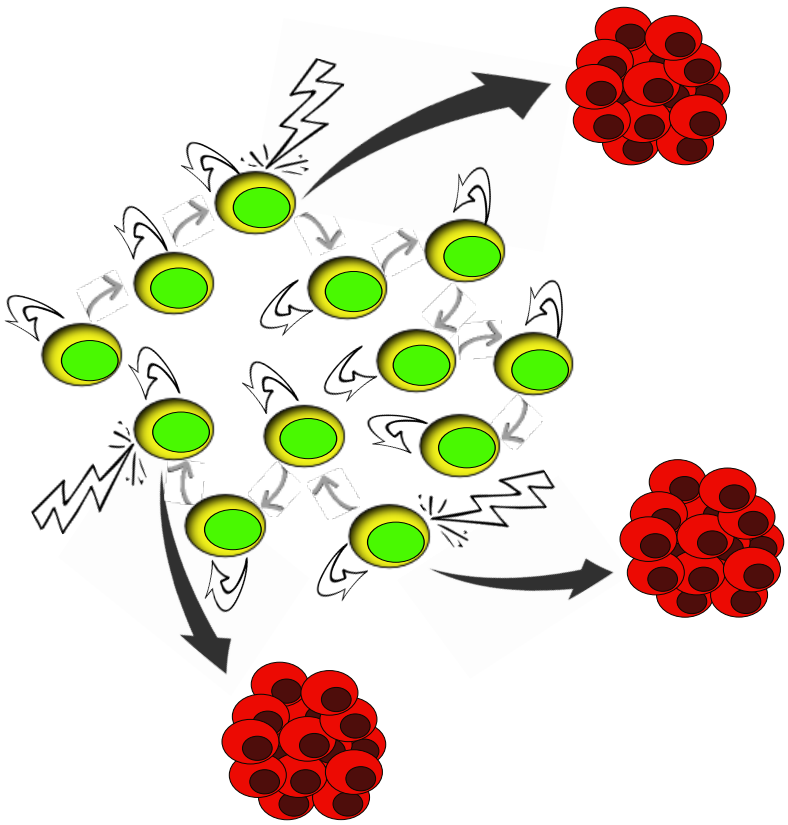

Figure 4.2: **The Clonal Evolution Model.**
In the clonal evolution model, phenotypically distinct cancer cells are endowed with the same malignant potential and the potential to propagate themselves (outlined arrows), and are equally likely to acquire the ability to propagate the tumour (in red) by accumulation of further genetic mutations (bolts).

Based on this theory, different subpopulations arise continuously within the tumour mass by accumulation of mutations of genes that control cellular checkpoints, which favors the onset of additional genetic mutations and the selection of new phenotipic traits, thus accounting for tumour heterogeneity. Furthermore, any new mutation can potentially increase invasiveness, thus conferring to the tumour metastatic properties or resistance to therapies (Campbell and Polyak, 2007).

In summary, the clonal evolution model states that heterogeneity in a tumoural mass may not be necessarily due to a hierarchical organization of cells. Accumulation of genetic mutations and epigenetic modifications can account for the generation of subpopulations with different phenotype, function and response to therapy. The clonal evolution model can explain several tumour features, including its clonal origin, morphological and functional heterogeneity, tumour progression, metastasis and reoccurrence.

4.1.3 The Interconversion Model

A third and more novel model for cancer development hypothesises that cancer cells may interconvert between different tumorigenic states. This model has been proposed in response to the CSC tumour model as more and more evidences suggest that the fraction of CSCs in human tumours (defined as tumorigenic cells capable of spawning non-tumorigenic cells) may not be as exiguous as the current SC-validation methods allow to establish. Moreover, the number of CSCs in a tumour may vary depending on the level of its differentiation, within different subtypes arising from the same tissues and in the same tumour in response to factors that are intrinsic or extrinsic to the cells of origin like cell type, stromal microenvironment, somatic mutations and stage of tumour progression (Gupta et al., 2009). In light of these observations, it has been proposed that cancer cells may exist in two phenotypical states with different tumorigenic potential. The acquisition of tumorigenic and metastatic potential has been often associated with a specific state of differentiation at least in the mammary gland. Accordingly, epithelial to mesenchimal transition (EMT) in transformed cells induces the enrichment in CSCs(Morel et al., 2008; Mani et al., 2008). Interestingly, EMT has been shown to be a reversible process, that can be undone upon removal of the environmental cues that initially triggered it (Hugo et al., 2007). This cellular plasticity may occur also in the context of CSCs, generating cells that are endowed with tumorigenic potential or that are unable to sustain tumour growth depending on their differentiation state and ultimately on the stimuli that they receive from their microenvironment. Indeed, analogous mechanisms may also govern normal tissues. A first suggestion of the existence of this mechanism comes from intra-vital studies of melanomas where researchers have shown oscillation between metastatic and non-metastatic status,

expression of stem-associated gene Brn-2 and pigmentation of melanoma cells (Pinner et al., 2009) (Fig. 4.3).

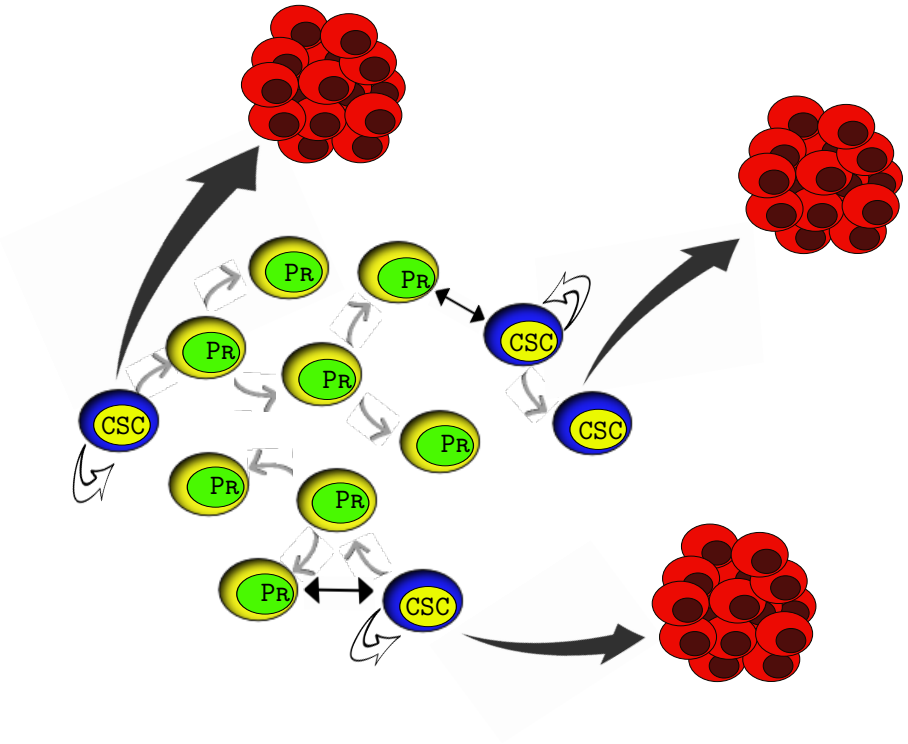

Figure 4.3: **The Interconversion Model.**
In the interconversion model cells with tumorigenic abilities (blue) give rise to more differentiated cells (yellow) with no potential to sustain the tumour mass (in red). However, in response to external cues and depending on their differentiation state, these cells are able to convert to tumorigenic cells (jagged arrow).

Because all three theories are supported experimental evidences, it is reasonable to hypothesise that all the above mechanisms coexist during tumour growth. In fact, tumours that follow a CSC model may contain cells that undergo clonal selection during self-renewal and differentiation, and the non-tumorigenic cells that they originate may acquire further mutations that somehow restore self-renewing and cancer-promoting abilities through genetic changes and epigenetic alterations. The result of this scenario is an heterogeneous population of cancer cells that dominate the tumour growth and continuously reiterate processes of mutation and differentiation, giving rise to all tumour cell types.

Regardless of the origin of the cells that comprise the tumoural mass and of the mechanisms with which they evolve, it is clear that tumours arise because of the existence of cells with deregulated self-renewing mechanisms. This is why the study of self-renewal in SCs may help the understanding of the alterations that are at the basis of carcinogenesis.

4.2 Pathophysiology of Breast Stem Cells

4.2.1 Stem Cells in Breast Tissues

The existence of mammary SCs has been first described by Deome et al. in 1959, with transplantation studies on mice that showed how cells with the ability to repopulate a mammary gland could be found in adult tissues (DEOME et al., 1959). Several years later, Kordon and Smith showed in a very elegant, yet indirect, way how the mouse mammary gland can be repopulated by a single cell and that the mammary epithelium contains three distinct multipotent progenitors(Kordon and Smith, 1998). These studies paved the way for many others and have rendered the mammary gland, especially in the mouse, a very potent system for the study of SCs and their role in tissue homeostasis as well as in cancer.

There are five pairs of mammary glands in the mouse. These comprise two different cellular compartments: the epithelium, which consists of ductal and alveolar cells, and the stroma, also called the mammary fat pad, that is composed mainly of adipocytes, but also of other cell types, like fibroblasts, haematopoietic cells, blood vessels and neurons. The epithelial cells are organized into a system of branched ducts that progressively decrease in diameter and terminate in lobular complexes of alveoli. Ducts and alveoli possess a central lumen that opens to the body surface through the nipple. In the alveoli, the luminal epithelial cells undergo functional differentiation during pregnancy to produce milk. The basal myoepithelial cells, whose contraction facilitates the milk release, surround both ducts and alveoli. This complex system of ducts and alveoli is embedded in the mammary fat pad (Hennighausen and Robinson, 2001, 2005; Smalley and Ashworth, 2003) (Fig. 4.4).

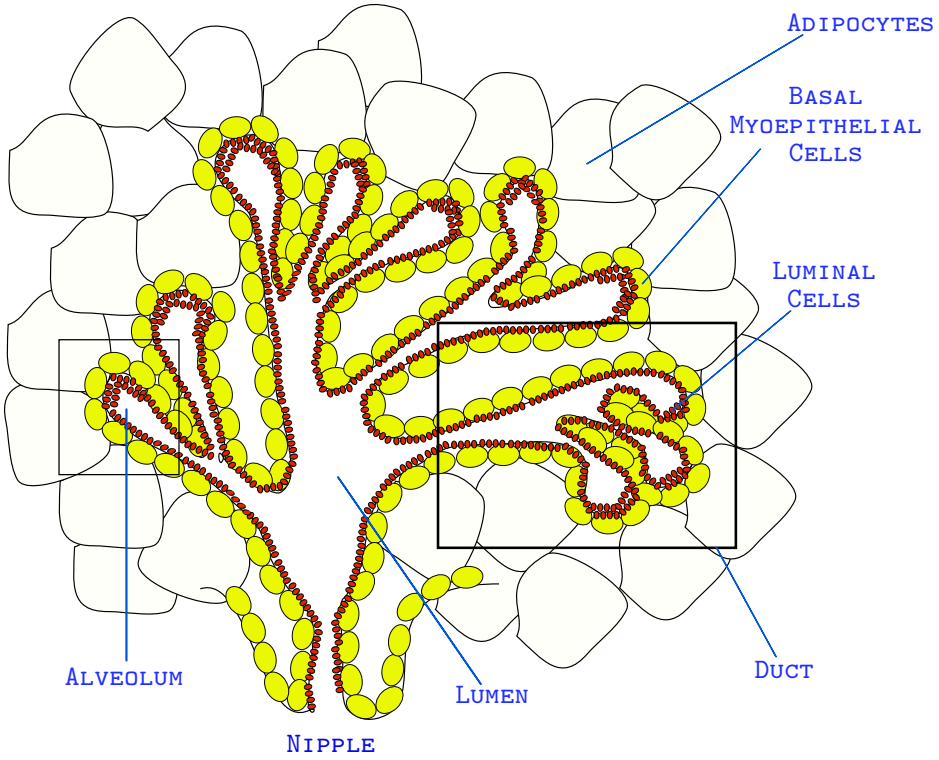

Figure 4.4: **Structure of the mammary gland.**
The mammary epithelial tree is organized in a series of ducts that terminate in alveolar clusters. These structures have a hollow lumen paved with luminal epithelial cells (red) that are responsible for the secretion of milk during lactation. The system of basal myoepithelial cells (yellow) that surround the ducts and alveoli favour the milk secretion with their contraction. The complex structure of ducts convey to the nipple, where the milk is expelled. The mammary epithelium is embedded in a fat-pad comprised by adipose cells, but also other stromal components and blood vessels, that sustain its growth.

The mammary gland undergoes massive rearrangements in defined stages that are connected to sexual development and reproduction. These are embryonic, prepuberal, puberal, pregnancy, lactation and involution. During puberty the epithelial ducts grow and branch further, to reach a complete penetration of the fat pad in maturity. During pregnancy, the alveolar compartment expands and matures, and is the site of milk secretion during lactation. Lactation is followed by an involution stage, during which the alveoli undergo apoptosis and remodeling to restore a simple ductal structure. Alveolar expansion and maturation, lactation and involution initiate with every new pregnancy (Smalley and Ashworth, 2003; Hennighausen and Robinson, 2001, 2005). The complex turnover that characterizes the mammary gland is a functional proof of the existence of cells endowed with the ability to sustain and regenerate the tissue for several cycles. Such cells are responsible for the generation of all the cells that form the epithelial compartment of the gland. They have the capacity to self-renew and give rise to progenitor cells destined to either a basal or a luminal fate. It is generally believed that in the mammary gland of puberal mice

these SCs reside in the terminal end buds (TEBs), the growing units at the end of the ducts. TEBs are composed of a mass of cells surrounded by a layer of cap cells that are the putative SCs. Cap cells generate transit cells on the outer side of the TEB that will differentiate in the myoepithelium, and transit cells that form the body cells and will differentiate into luminal epithelial cells. The ductal lumen is formed following apoptotic events in the mass of the developing body/luminal cells. TEBs disappear at the end of the puberty, when the mammary gland reaches its full development (Smalley and Ashworth, 2003).

Great effort has been put into the isolation of mammary SCs in the past few years, and the use of different methods has led several research groups to purify a population of cells highly enriched in cells with stem properties. These include: *i)* the side-population method, which relies on the increased activity of membrane transporters that is specific to SCs and enables their isolation based on dye exclusion assays (Alvi et al., 2003); *ii)* FACS sorting of SCs based on the expression of surface markers as pioneered by the haematopoietic system; *iii)* the mammosphere culturing system, which, based on an analogous protocol used for neural stem cells, enriches the cell population in stem and progenitor cells.

All the methods mentioned above and all the surface markers that have been described for the purification of mammary SCs allow for the isolation of a population of cells enriched in SCs, nevertheless, no technique has been established for the identification of *bona fide* SCs.

4.2.2 Breast Cancer Stem Cells

In the last few years we have witnessed a drastic reduction in the mortality of breast cancer patients. This has been possible due to the improvement in the techniques for early detection and the use of more effective adjuvant therapies and therapies that efficiently target specific molecular subtypes of this disease. Nevertheless, many women affected by this malignancy experience relapse after treatment, a phenomenon that renders metastatic breast cancer a widely incurable disease. The high frequency of relapses in breast cancers, as well as in many other types of cancer, has been attributed to the presence of a subset of cells that escape these treatments, thanks to properties that render them similar to SCs. This is why understanding the properties of normal SCs may shed light on the alterations that these cancer SCs undergo and may help in defining targeted therapies against these cells.

The human breast cancer was the first solid malignancy for which the cancer stem model was described. Breast cancer SCs were isolated based on the expression of the cell surface markers ESA and CD44 and on the absence of CD24(Al-Hajj et al., 2003). Since then other markers have been described to isolate human breast CSCs, as for example the expression of aldehyde dehydrogenase (ALDH)(Ginestier et al., 2007), however, there are evidences that show that different breast cancers are sustained by CSCs that express different cell surface markers(Charafe-Jauffret et al., 2009; Wright et al., 2008). Because very little is known about cell surface markers that may allow for a perspective identification of normal and tumour human breast SCs (Cariati and Purushotham, 2008), and because the expression of surface

markers is highly dependent on the cell microenvironment, other methods that rely on the functional characterization of CSCs have been adopted. Taking advantage of protocols that have been established for neural SCs (Reynolds and Weiss, 1996; Weiss et al., 1996), a population enriched in SCs was isolated from the normal mammary gland and propagated *in vitro* as non-adherent spheroids called mammospheres. Mammospheres are enriched in undifferentiated cells that: *i)* are able to growth in anchorage-independent manner, *ii)* can be serially propagated showing self-renewal ability and *iii)* are capable of multilineage differentiation upon plating in a differentiation-promoting matrix (Dontu et al., 2003). Interestingly, mammospheres arising from primary human breast tumours are composed of cells that show a CD44+/ CD24- phenotype and are greatly enriched in tumour initiating cells, thus indicating that mammosphere assay is also a good system to propagate cancer SCs (Ponti et al., 2005). All the methods that have been adopted for the purification of tumour SCs rely on the potent tool that the mammary gland offers, to validate the stem properties of mammary epithelial cells based on their ability to repopulate the cleared fat pad upon xenotransplantation in the mammary gland of immunocompromised mice. Although this technique is considered the gold standard assay for the validation od CSCs, it does not take into account the role that the immune system plays in regulating cancer onset and progression, suggesting that indeed this method may have some important limitations.

Tumour type	CSC marker	Tumour cells expressing CSC marker, %	Minimal number of cells expressing CSC markers for tumour formation	Transplantation site	Strain
Breast	$CD44^+/CD24^{-/low}$	11–35	200	Mammary fat pad	NOD-SCID
Breast	$CD44^+/CD24^-$	ND	2×10^3	Mammary fat pad	NOD-SCID
Breast	$ALDH1^+$	3–10	500	Mammary fat pad	NOD-SCID
Brain	$CD133^+$ (GBM) $CD133^+$ (MB)	19–29 6–21	100 100	Brain Brain	NOD-SCID NOD-SCID
Brain	$CD133^+$	2–3	500	Brain	nu/nu
Colon	$CD133^+$	1.8–25	200	Kidney capsule	NOD-SCID
Colon	$CD133^+$	0.7–6	3×10^3	Subcutaneous	SCID
Colon	$EpCAM^{hi}/CD44^+$	0.03–38	200	Subcutaneous	NOD-SCID
Head and neck	$CD44^+$	0.1–47	5×10^3	Subcutaneous	$Rag2/\gamma^{-/-}$DKO, NOD-SCID
Pancreas	$CD44^+/CD24^+/ESA^+$	0.2–0.8	100	Pancreas	NOD-SCID
Pancreas	$CD133^+$	1–3	500	Pancreas	NMRI-nu/nu
Lung	$CD133^+$	0.32–22	10^4	Subcutaneous	SCID
Liver	$CD90^+$	0.03–6	5×10^3	Liver	SCID/Beige
Melanoma	$ABCB5^+$	1.6–20	10^6	Subcutaneous	NOD-SCID
Mesenchymal	Side population (Hoechst dye)	0.07–10	100	Subcutaneous	NOD-SCID

Table 4.1: **Prospective isolation of CSCs from different tumour types based on the expression of surface markers.**
Cancer subpopulations enriched in CSCs have been isolated from different tumour subtypes and the presence of tumorigenic cells evaluated by transplantation in immunocompromised mice. The table indicates the enrichment of cancer-forming cells as percentage of cells expressing the CSC marker and the minimum number of cells required for the development of tumours in recipient mice(adapted from Visvader and Lindeman, 2008).

It was recently shown in a variety of transgenic mouse models that murine mammary tumours too follow a CSC model. Various degrees of cancer SC enrichment, in fact, were documented in the $CD24^{pos}Thy1^{pos}$ (Cho et al., 2008) or $CD29^{low}CD24^{pos}CD61^{pos}$ (Vaillant et al., 2008) breast cancer fractions from MMTV-Wnt-1 transgenic mice; in the $CD24^{high}CD29^{high}$(Zhang et al., 2008) or $CD29^{low}CD24^{pos}CD61^{pos}$ breast cancer fractions from p53-null mice; and in the $CD24^{pos}$ breast cancer fraction from transgenic mice overexpressing the non-mutated form of ErbB2 (Liu et al., 2007a), though the same was not observed in another report (Vaillant et al., 2008). More recently, Grange and colleagues reported the prospective isolation of cancer SCs from transgenic mice expressing the mutated form of ErbB2 (Grange et al., 2008). In particular, they show enrichment of CSCs associated with positivity to the surface marker Sca1 (3 positive transplants out of 6 injections with 100 Sca1+ cells; no positive transplants out of 6 injections with 10,000 Sca1− cells).

Collectively, these reports confirm the great heterogeneity of the markers expressed by CSCs in human tumours as well as in transgenic mouse models, these markers being also often different from those expressed by normal SCs. Moreover, in all the analyzed breast tumours derived from transgenic models, except those from mutated ErbB2-transgenic mice, the negative subpopulations (those that did not express the selected markers) were also able to transplant, although with a lower frequency compared to the positive fractions, confirming the great heterogeneity of CSCs in tumour tissues.

4.2.3 Targeting Breast Cancer Stem Cells

The confirmation of the existence of cells with stem properties within the bulk of a tumour mass has important therapeutic implications. Conventional anti cancer therapies rely on the property of tumour cells to be actively proliferating; however, CSCs that like normal SCs are slowly dividing, survive this kind of treatment and are likely to give rise to relapses (Gil et al., 2008; Reya et al., 2001; Visvader and Lindeman, 2008).

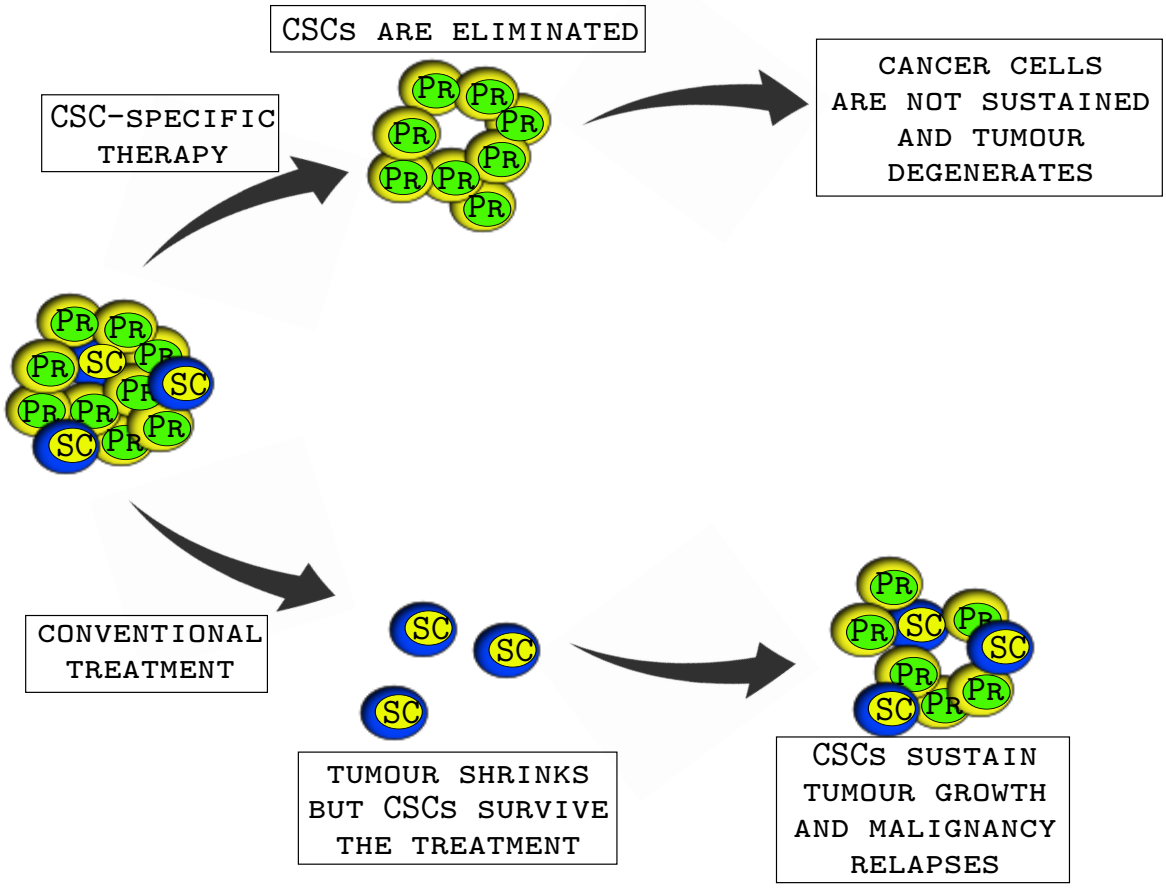

Figure 4.5: **Effects of CSC-targeted treatments and conventional treatments.** It is believed that conventional treatments do not result in the elimination of CSCs that can repopulate the tumour and give rise to relapses. Conversely, CSCs-specific treatments allow for the eradication of the cells that sustain and promote the tumour growth, thereby resulting in the degeneration of the tumour mass.

Indeed it has been shown in cell lines and primary tumours that CSCs are relatively more resistant to radiation therapy and cytotoxic chemotherapy(Dave and Chang, 2009). Several mechanisms account for the resistance of CSCs to antitumoural therapies. It has been shown that human CSCs possess lower levels of pro-oxidants, thus rendering them resistant to radiation therapies(Dave and Chang, 2009). Furthermore, several molecular mechanisms that are active in CSCs have a protective role against chemotherapic agents: expression of cellular transporters, such as the MDR1 and ABC transporters (Jordan et al., 2006), high levels of anti-apoptotic proteins, such as those of the BCL-2 family (Al-Hajj et al., 2003; Reya et al., 2001), or increased efficiency of the DNA repair machinery and alterations in the cell cycle kinetics. Current therapies, though they may produce dramatic responses on the tumour mass, affect only the differentiated progenies of CSCs and do not allow for long-term remissions because they do not target the rare population of CSCs. This might explain why the tumour regression that results from conventional treatments does not necessarily correlate with patient survival(Huff et al., 2006). CSC-targeted therapies

that aim at the selective ablation of the these rare cells may therefore represent an attractive method to definitively eradicate the tumour mass.

Indeed, resistance of CSCs to conventional treatments requires for the establishment of new approaches that specifically target particular traits that are unique for these cells. One of the defining properties of CSCs is their increased self-renewing ability. Self-renewal is a complex mechanism governed by several pathways, including the Notch, Wnt and Hedgehog pathways. These pathways have been found to be aberrant in several human breast cancers and, if altered, they are sufficient to induce the formation of breast tumours in transgenic mouse models(Liu et al., 2005).

Currently, several evidences of a positive effect of CSC-based treatments have been produced in different tissues. Many of these rely on the targeting of self-renewing mechanisms that are specific for CSCs, and others induce differentiation of CSCs, disrupting their niche. For instance, targeting of the Hedgehog pathway in Chronic Myeloid Leukemia (CML) mouse and human cells with the molecule cyclopamine inhibited their growth *in vitro*(Zhao et al., 2009), and the same treatment was effective also on inhibiting the tumorigenicity of human gliomas in mice(Clement et al., 2007). Similarly, inhibition of the Notch pathway through blockage of the γ-secretases depleted CSCs in gliomas and medulloblastomas in transgenic mice and xenotransplants(Fan et al., 2006, 2010). Targeting of other molecules that are enriched or activated in CSCs has proven effective in preventing tumour growth *in vivo* and survival of mice models, and these include the tumour suppressor PML in Chronic Myeloid Leukemia (Ito et al., 2008), mTor with rapamycin in mouse models of leukemia (Yilmaz et al., 2006), the NF-ϰB pathway in human leukemic SCs (Guzman et al., 2002), IL-6 receptors (Wang et al., 2009), IL-3 receptor α(Jin et al., 2009), TGF-β and LIF(Penuelas et al., 2009; Ikushima et al., 2009). Other strategies that induce differentiation of CSCs, thus depleting their niche, include inhibition of the Wnt pathway in skin tumours which results in tumour regression and is accompanied by terminal differentiation of the cancer cells (Malanchi et al., 2008) and treatment of glioblastoma CSCs with bone morphogenetic proteins (BMP), which induces *in vitro* differentiation, thus abolishing their tumour-forming ability. Accordingly, *in vivo* administration of BMPs blocks the tumour growth and the mortality of mice transplanted with human glioblastoma cells (Piccirillo et al., 2006).

4.3 Stem Cells and Self-Renewal

A key question in cancer biology is whether CSCs possess different growth potential, life span or drug sensitivity compared to their normal counterparts and, more importantly, which are the relevant underlying molecular pathways. What is clear is the striking correlation between deregulated SC functions and tumourigenesis: many oncogenes are activated forms of genes that promote self-renewal and cell proliferation, and tumour suppressors are often genes that negatively regulate these processes.

CSCs share many properties with normal SCs, most notably their ability to self-renew and to give rise

to cells that differentiate. These tasks can be accomplished through two different strategies: *i)* a pool of SCs with equivalent developmental potential may divide symmetrically producing only identical SC in some divisions and only identical differentiated cells in others or *ii)* a single SC can divide asymmetrically through a single self-renewing mitotic division, in which one daughter cell retains the SC identity and the ability to replicate almost indefinitely, while the other undergoes limited rounds of mitotic division before entering a post-mitotic fully differentiated state (progenitor cells). The asymmetric cell division allows, with a single division, both for self-renewal and differentiation; however, it leaves SCs unable to expand in number. In order to expand their pool, SCs must adopt another type of self-renewing division, one that generates two daughter cells with the same SC fate (symmetric division) (Morrison and Kimble, 2006) (Fig. 4.6).

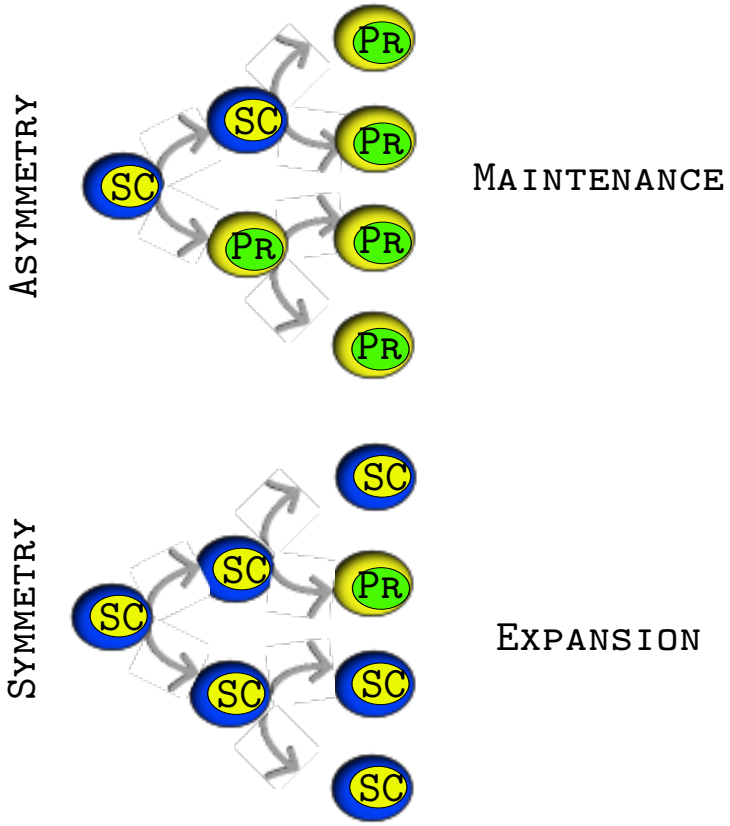

Figure 4.6: **Types of stem cell divisions.**
Different types of SC divisions have different effects on the SC pool.

4.3.1 Stem Cell Divisions

Asymmetric SC divisions have been initially observed in invertebrates such as the worm Caenorhabditis elegans and the fruit fly Drosophila melanogaster (Gonzalez, 2007; Januschke and Gonzalez, 2008; Morrison and Kimble, 2006). Asymmetry of cell division can be achieved through intrinsic mechanisms that involve the partitioning of cell fate determinants or through extrinsic mechanisms that rely on the cross-talk between the dividing SC and its niche. Intrinsic mechanisms require the regulated and polarized

assembly of cell polarity factors, such as the atypical protein kinase C (aPKC) and the partitioning factors (PAR-3 and PAR-6), and the controlled segregation of cell fate determinants such as Numb and partner of Numb (PON) or Brain tumour (Brat), Prospero (Pros) and their adaptor Miranda (Mira). Asymmetric localization of the PAR–aPKC complexes at the apical cortex initiates the asymmetric division and governs both asymmetric segregation of cell fate determinants, that accumulate to the opposite site of the plasma membrane (basal cortex), and the assembly of the mitotic spindle along an apical-basal axis. The regulated mitotic spindle orientation ensures the segregation of the cell polarity complex to one daughter, which will retain SC fate, and the cell fate determinants to the other cell that will differentiate. Classic examples of asymmetric divisions that are controlled by an intrinsic mechanism are provided by the C. elegans zygote (Morrison and Kimble, 2006) and the Drosophila larval neural SCs (Neuroblasts) (Gonzalez, 2007; Januschke and Gonzalez, 2008). The C. elegans zygote divides asymmetrically to produce one larger blastomere which will originate the ectoderm, and one smaller blastomere that will produce the mesoderm, endoderm and finally the germ line in a series of asymmetric divisions. The Drosophila neuroblast divides into a large daughter cell that will retain SC fate and continue to divide asymmetrically, and a small daughter cell that will become a ganglion mother cell (GMC) and divide once more, originating cells that will differentiate as neurons or glia. Extrinsically regulated asymmetric divisions rely on the asymmetric positioning of the two daughter cells in relation to the SC niche. This is achieved by the regulated orientation of the mitotic spindle that ensures that only one of the daughter cells remains in the niche (the SC), whereas the other cell is placed away from the niche and exposed to signals that induce differentiation(Morrison and Kimble, 2006). A classic example of an asymmetric division controlled by extrinsic mechanisms is provided by the male germline SCs of Drosophila. Male germline SCs are placed adjacent to a cluster of postmitotic cells (hub cells) that form their niche and provide the signals that are necessary for SC self-renewal. After the mitotic division, a male germline SC generates two daughter cells of equal size, one of which remains close to the hub and retains SC identity, and the other, the gonialblast, is placed away from the niche and enters a series of four mitotic divisions to produce the spermatocytes (Gonzalez, 2007). Indeed these two mechanisms are not mutually exclusive and in some cases may coexist to achieve asymmetry of SC division (Morrison and Kimble, 2006).

Some of the mechanisms of asymmetric division that have been described in invertebrates are conserved in mammalian SCs. During the development of the mouse cortex, undifferentiated neural progenitors asymmetrically distribute the fate determinant Numb to precursors destined for neurogenesis (Shen et al., 2002). Numb is also asymmetrically distributed to progeny of cultured satellite muscle cells, where it promotes myogenic differentiation of only one daughter cell (Shinin et al., 2006; Conboy and Rando, 2002). Thus, asymmetric segregation of Numb may be a conserved mechanism both in Drosophila and vertebrates. Furthermore, both mammalian basal epidermal progenitors (Lechler and Fuchs, 2005) and cortical ventricular zone neural progenitors (Chenn and McConnell, 1995) seem to regulate the orientation

of mitotic spindles. The spindle orientation relies on the cortical localization of the PAR– aPKC complex (Lechler and Fuchs, 2005), a mechanism that also controls the asymmetric division of Drosophila and C. elegans SCs (Morrison and Kimble, 2006).

Symmetric SC divisions result in an increase in the number of SCs. They are adopted by both vertebrates and invertebrates to form or regenerate tissues during development or after injury. Several examples of symmetric divisions during tissue development have been described. During larval development of C.elegans, symmetric divisions occur in the germ line SCs to develop the pool of undifferentiated germ cells and differentiated gametes (Morrison and Kimble, 2006). Mammalian SCs too undergo symmetric divisions during embryonic or early fetal development. Although direct imaging of these divisions is still lacking, researchers have shown that mouse haematopoietic SCs double in number every day in the fetal liver until 14,5 days post-coitus, suggesting that they undergo symmetric divisions (Morrison et al., 1995). In other systems like undifferentiated neural progenitors in the developing mouse cerebral cortex (Chenn and McConnell, 1995; Huttner and Kosodo, 2005; Noctor et al., 2004) or cells in the basal layer of the fetal epidermis (Lechler and Fuchs, 2005) direct imaging has confirmed symmetry of divisions. In both cases the expansion in the pool of undifferentiated progenitors was the result of divisions that generated two morphologically identical daughter cells that remained undifferentiated, although no proof was given to show that both were SCs. Symmetric divisions have been also observed in SCs in the adult Drosophila ovary, where SCs can be induced to divide symmetrically and to regenerate an additional SC after experimental removal of one SC from their niche (Morrison and Kimble, 2006). Mammalian adult SCs, that are supposed to divide asymmetrically under steady-state conditions (Morrison and Kimble, 2006; Januschke and Gonzalez, 2008), retain the capacity to divide symmetrically to repopulate the SC pool when depleted by injury or disease (Morrison and Kimble, 2006). Depletion of the SC pool in the sub-ventricular zone of the mouse forebrain after antimitotic drug infusion induces symmetric neural SC divisions that restore the SC number (Doetsch et al., 2002). Moreover, the death of rodent forebrain cells in adult rat subjected to strokes transiently increases the rate of symmetric division among sub-ventricular zone progenitors, leading to an increase in neurogenesis (Zhang et al., 2004). Finally, in the haematopoietic system, after chemotherapy-induced depletion of blood cells, SCs expand about ten-fold in number to replenish both the SC niche and the differentiated cell pools (Wright et al., 2001; Bodine et al., 1996; Morrison et al., 1997). All these observation suggest that the facultative use of symmetric or asymmetric divisions by SCs might represent a conserved mechanism, which allows production and maintenance of appropriate numbers of SCs and differentiated progeny in response to developmental or environmental signals. The balance between self-renewal and differentiation is therefore strictly regulated to maintain a relatively small population of long-lived SCs while producing large numbers of differentiated progeny.

4.3.2 Stem Cell Self-Renewal and Cancer

Recent genetic studies in flies have shown that aberrant regulation of self-renewal and differentiation in SCs can result in an increase in SC numbers and tissue overgrowth, leading to transplantable tumours which resemble mammalian cancer (Gonzalez, 2007; Januschke and Gonzalez, 2008; Wodarz and Gonzalez, 2006). The larval neuroblasts in Drosophila divide asymmetrically to generate one new neuroblast and a small basal GMC. Perturbations, usually loss-of-function, of any of the several proteins that control asymmetric self-renewing divisions in these cells, including proteins that regulate neuroblast polarity (lgl, dlg and scrib), asymmetric segregation of GMC-fate determinants (Mira, Numb), the GMC-fate determinants themselves (Pros, Brat) and mitotic spindle alignment (Pins, Mud) result in the development of breast tumours(Clarke and Fuller, 2006; Clevers, 2005; Gonzalez, 2007; Januschke and Gonzalez, 2008). Moreover, mis-segregation or gain of function mutations of the neuroblast fate determinant aPKC leads to an enormous increase in the number of larval neuroblasts (Lee et al., 2006). Finally, the larval mutants AurA and Polo also show increased numbers of neuroblasts that develop in malignant tumours after adult implantation (Januschke and Gonzalez, 2008). These observations convey the existence of a causal relationship between loss of polarity and/or asymmetric division in the neuroblast and tumourigenesis in the mutant neuronal tissue. Thus, asymmetric divisions might function as a mechanism of tumour suppression in the fly neuroblast, and impaired fate specification during SC division might be one of the initial events that drive these cells into malignancy. In higher organisms this correlation has not been demonstrated, although several evidences suggest that the intact function of regulatory mechanisms of self-renewal in SCs is necessary for the propagation of already established cancers in mouse models. The Polycomb group gene Bmi-1 is involved in the regulation of self-renewal of normal SCs (Lessard and Sauvageau, 2003; Molofsky et al., 2003; kyung Park et al., 2003; St-Jacques et al., 1998), but it is also required for the survival and proliferation of AML leukemic SCs (Lessard and Sauvageau, 2003). Similarly, the correct function of the Hedgehog pathway, which is involved in the regulation of SCs in various tissues (Ahn and Joyner, 2005; Beachy et al., 2004; Watkins et al., 2003), is also required for the transplantability of normal haematopoietic SCs and increases the number of leukemogenic SCs in a CML model (Zhao et al., 2009). Accordingly, inhibition of the Hedgehog pathway in cutaneous basal carcinoma induces regression of established lesions (Hutchin et al., 2005). Furthermore, it has been shown that the presence of tumour suppressor p53 is required for the maintenance of a quiescent state in haematopoietic SCs (Liu et al., 2009; Akala et al., 2008), and restoration of the p53 function in established p53 deficient tumours results in the regression of the malignancy (Xue et al., 2007; Ventura et al., 2007).

At present it is not clear whether there may be a direct causal relationship between the loss of SC polarity and/or asymmetric divisions and tumour initiation in humans. The machinery that drives asymmetry in adult tissue SCs in mammals is largely uncharacterized, and aberrant regulation of self-renewing

divisions in cancer SCs still needs to be confirmed. Nevertheless, the genes that control asymmetric cell divisions in flies have a conserved role in the regulation of cell polarity and in tumour suppression in mammals, suggesting that polarity loss may contribute causally to cancer also in higher organisms(Gonzalez, 2007; Januschke and Gonzalez, 2008). Some examples include HUGL-1, the human homologue of Lgl, which is frequently deleted in cancer and, if inactivated, leads to a loss of polarity and dysplasia in the central nervous system of mouse models(Grifoni et al., 2004; Klezovitch et al., 2004); Numb, a negative regulator of the cell-fate determinant Notch, which functions as a tumour suppressor in breast cancers (Colaluca et al., 2008); the LKB1, VHL and PTEN tumour suppressor proteins, which interact with components of the PAR–aPKC complex and are frequently mutated in tumours (Baas et al., 2004; Barry and Krek, 2004; von Stein et al., 2005); NuMA (Nuclear mitotic apparatus protein 1), the human orthologue of Mud, which is linked to leukemia (Sukhai et al., 2004) and breast cancer (Kammerer et al., 2005) susceptibility. An interesting correlation between the expansion of SC pools, cancer development and, possibly, regulation of SC divisions was recently described in familial adenomatous poliposis (FAP) colorectal tumours (Boman and Huang, 2008). Altogether, these observations imply that many genes that are involved in the regulation of SC self-renewal may act in fact as tumour suppressors or may become oncogenic if altered. Thus, deregulation of the machinery that controls and ensures the correct balance between symmetric and asymmetric SC divisions may lead to alteration of tissue homeostasis, increase of the SC pool and, finally, cancer.

Targeting of the machinery that regulates self-renewal in normal and cancer SCs inevitably raises the question of toxicity that can result from the inhibition of pathways that are shared between normal and tumour cells. A way to avoid this toxicity is to target mutations that are active only in CSCs. Some of these have already been identified and include the deletion of the PI-3 kinase pathway regulator Pten, which results in a mieloproliferative disease that quickly develops into a CSC based leukemia. Interestingly, deletion of Pten resulted also in the depletion of normal haematopoietic SCs in a cell-autonomous manner, most likely through mTOR. Rapamycin-mediated inhibition of mTOR induced the eradication of leukemic SCs and the restoration of the normal SC function (Yilmaz et al., 2006). Similarly, the Wnt/β-catenin pathway has been shown to sustain the growth of CSCs in chemically induced cutaneous squamous carcinomas but is not required for tissue homeostasis (Malanchi et al., 2008). These observations confirm that a good anticancer approach will be selectively targeting mechanisms of tumour propagation.

4.3.3 p53 and Self-Renewal

The tumour suppressor p53 is mutated in 50% of all human cancers; where it is present in its WT form, its function is often attenuated as a result of the alteration of its regulating pathways (Vousden and Prives, 2005). The activity of p53 in suppressing tumour formation through the induction of cell cycle arrest in stress situations has been long known, nevertheless, new roles for p53 in other processes like metabolism,

autophagy and oxidative stress are emerging. p53 is activated in response to cellular stress following DNA damage, telomere dysfunctions, replication stress, hypoxia, nutrient deprivation and in response to oncogene activation to limit the propagation of cells under adverse conditions (Kastan and Berkovich, 2007). The expression and activity of p53 is tightly regulated through numerous mechanisms involving several E3 ubiquitin ligases. In response to stress stimuli p53 is stabilized through the disruption of its interaction with of one of these ligases, Mdm2, thus preventing its ubiquitination and, consequently, its degradation(Momand et al., 2000). Once activated, p53 acts as transcription factor, up-regulating a series of target genes that are involved in various physiological and pathological processes as the inhibition of cell cycle, induction of apoptosis or senescence, control of genomic stability and inhibition of blood vessel formation, thus acting as an anti-tumorigenic agent (Vogelstein et al., 2000). In addition to its roles in tumour suppression, development and aging, newly identified functions for p53 have been described. Recent evidences suggest that p53 may be involved in the regulation of self-renewal and SC division. Rambhatla and colleagues have reported that p53 imposed an asymmetric proliferative fate on daughter cells both in mouse embryo fibroblasts and in one mammary epithelial cell line (Rambhatla et al., 2001) Accordingly, loss of p53 was found to increase self-renewal of neural SCs in a sphere-forming assay (Piltti et al., 2006; Meletis et al., 2006), suggesting that p53 can increase the frequency of neural SC symmetric divisions. In mammary cells, Colaluca and colleagues have shown that the cell fate determinant Numb mediates the increase in the levels and activity of p53 and the regulation of p53-dependent phenotypes, through the formation of a Numb-p53-HDM2 ternary complex (Colaluca et al., 2008). Finally, p53 was shown to negatively regulate the self-renewal of embryonic stem (ES) cells (Lin et al., 2005). Altogether these findings suggest that the tumour suppressor function of p53 may also require the regulation of self-renewing divisions. Indeed, recent findings that describe a beneficial effect of the reactivation of p53 in tumours make this protein a very promising target for anti-cancer interventions.

4.3.4 Myc and Self-Renewal

The Myc family of transcription factors undoubtedly plays an important role in tumorigenesis, as demonstrated by the fact that although mutations in these genes can be found with low frequency (one every five tumours), Myc proteins are found to be overexpressed by indirect mechanisms in the majority of cancers(Laurenti et al., 2009).

Myc genes are required in the developing organism but also play a critical role in adult tissues by regulating stem and progenitor cells. Extensive evidences show a role for Myc in SC self-renewal in Drosophila as well as in mammal adult and embryonic SCs. In Drosophila, Myc has been shown to inhibit differentiation and promote self-renewal in neuroblasts and ovarian germ line SCs(Betschinger et al., 2006).

Similar observations have also come from the study of mammalian SCs. By knocking down the endogenous c- and N-Myc, Varlakhanova et al. have recently shown that Myc is essential in ES cell

pluripotency and self-renewal, as well as being required during embryogenesis, as lack of Myc genes in mice embryos results in early lethality (Varlakhanova et al., 2010). These findings indeed confirm previous observations that state that Myc enhances iPS cell reprogramming, probably through regulation of proteins and miRNA that govern general metabolism, the pluripotency cell cycle machinery and self-renewal. Indeed, it has been described in murine ES cells that Myc is controlled by the LIF/STAT3 pathway, promoting self-renewal and pluripotency. Accordingly, exogenous expression of Myc is sufficient to sustain pluripotency independently of LIF (Cartwright et al., 2005).

A role for Myc in the regulation of adult SCs in mice models has been described for the epidermis, the haematopoietic system and neural precursors. Increased levels of c-Myc in the skin results in increased proliferation and arrests SC differentiation (Watt et al., 2008), and lack of Myc in the mouse epidermis results in severe skin defects and impaired wound healing, which are accompanied, from a cellular point of view, by the depletion of the proliferative compartment and premature differentiation (Zanet et al., 2005).

In the mouse haematopoietic system, Myc has been shown to induce self-renewing divisions in SCs, probably as an effector upon Notch or HOXB4-mediated growth induction (Satoh et al., 2004). Accordingly, the combined loss of c-Myc and N-Myc results in the depletion of the haematopoietic SC pool, impaired proliferation and differentiation(Laurenti et al., 2008).

Loss of N-Myc has a similar effect in neural precursors, as it induces increased differentiation (Knoepfler et al., 2002) . On the contrary, Myc overexpression is able to confer high self-renewing and neurogenic capacities to late-stage neural SCs. This activity is counteracted by the p19 pathway, as activation of p19 induces differentiation and loss of p19 increases self-renewal in neural SCs (Nagao et al., 2008). The activity of Myc in regulating neural SC self-renewal has been shown to act through the activation of its effector Miz-1 (Kerosuo et al., 2008) and more recently, the same group has identified CIP2A as a cooperator of Myc in the regulation of self-renewal of neural progenitor cells (Kerosuo et al., 2010).

Interestingly, inactivation of p53 and PTEN in neural SCs also results in increased self-renewing potential, and promotes maintenance of an undifferentiated state. This is accompanied by the overexpression of Myc which results in the regulation of numerous genes involved in cell cycle, apoptosis, as well as in SC self-renewal and differentiation (Zhang et al., 2008). These findings are consistent with previous observations that describe a role for p53 in the repression of Myc expression, which is achieved by direct binding of p53 to the Myc promoter (Ho et al., 2005). Furthermore Myc translation and degradation can be modulated by the downstream effectors of the PTEN/PI3K pathway (Gera et al., 2004; Sears et al., 2000).

These findings suggest that different regulators of SC fate and behaviour may converge onto the Myc signalling pathway, thereby modulating SC self-renewal and differentiation; accordingly, deregulation of these processes may induce the aberrant expression of Myc, thus priming the cells to a pre-transformed

phenotype. Not surprisingly, N-Myc has been shown to regulate the epigenetic state of 90-95% of the modifications of histone H3 in the human genome, suggesting that its role is not restricted to that of a canonical transcription factor (Cotterman et al., 2008).

4.4 Reprogramming of Adult Differentiated Cells

Reprogramming of adult cells into pluripotent cells can be achieved by the expression in adult mammalian cells of a few embryonic transcription factors. The first observations in this direction came from the very elegant work of Yamanata and Takahashi in 2003, when they expressed a set of 24 pluripotency-associated transcription factors in mouse fibroblasts, hoping that their activity would induce the expression of a dormant drug resistance allele integrated into the ESC-specific locus Fbxo15 (Tokuzawa et al., 2003). Indeed the expression of these transcription factors induced the formation of colonies with ESC properties, and the progressive elimination of individual factors taken from this pool led to the reprogramming of mouse fibroblasts with as little as four genes (c-Myc, Oct3/4, SOX2, Klf4) (Takahashi and Yamanaka, 2006). The expression of these four genes induced the formation of cells that if injected into nude mice, gave rise to teratomas that were composed by cells with the properties of all three germ layers. However, although these cells express several markers of pluripotency, some of the key markers of ESCs were only partially expressed. Subsequently, other works were published that described how the use of different genes in the reprogramming could yield the generation of iPS cells with closer resemblance to ESCs, and several groups were even able to generate cells with the ability to form a all-iPS cell mouse upon injection of these cells into tetraploid blastocysts (Stadtfeld et al., 2010).

In the last years, iPS cells have been also generated from human , rat and rhesus monkey fibroblasts, suggesting that the machinery of pluripotency is evolutionally conserved (reviewed in Stadtfeld and Hochedlinger, 2010). Furthermore, several groups have demonstrated that not only adult differentiated fibroblasts have the ability to return to their pluripotent state, but also keratinocytes, neural cells, stomach and liver cells, melanocytes, pancreatic β cells and terminally differentiated lymphocytes, showing that pluripotency can be universally induced (reviewed in Stadtfeld and Hochedlinger, 2010)

These very innovative findings opened new roads for cell-based treatment of several degenerative diseases as well as providing a very powerful tool for the study of development and differentiation. In fact, the possibility of reverting adult differentiated cells into embryonic-like cells that can transdifferentiate into any adult tissue has amazing clinical implications, boosting the bioengineering field and favouring the development of patient-specific cell-based therapies. Clinical applications of iPS cells concern not only their use in the therapy of degenerative diseases, but also their use as potent, patient-specific diagnostic tools. These cells, in fact, can be used for the tailored study of mechanisms of genetic diseases in the so called “disease modelling”, and to establish targeted therapeutic strategies (Lee et al., 2009; Raya et al., 2009). In the field of regenerative medicine, iPS cells represent a very promising tool as the use of

patient-derived functional cells to damaged tissues eliminates all the possible complications that derive from donor/host incompatibility. Furthermore, the potential to isolate the patients cells and to correct possible disease-causing mutations *ex vivo* by homologous recombination makes them a much stronger tool than the adult patient SCs, that are notoriously difficult to maintain in culture. Studies in this direction have been performed in mouse models for the treatment of haematological diseases such as sickle cell anaemia or hemophilia A. In the former, cells from the skin of adult mice affected by sickle cell anaemia were isolated and reprogrammed into iPS cells, and the disease-causing mutation was repaired in these cells by gene targeting. These cells, if transplanted back into the donor mice, were able to produce normal red blood cells, thus curing the disease(Hanna et al., 2007). Similarly, the transplantation of iPSC-derived endothelial progenitor cells into mice affected by hemophilia A, resulted in the phenotypic correction of the disease (Xu et al., 2009).

In the field of degenerative diseases, the study of the processes that are responsible for the disease progression is limited by the accessibility of the affected tissues and the inability to grow the cells in culture for the sufficient amount of time. The iPS cell technology has opened new lines of research as it allows for "disease modelling" *in vitro*, by deriving adult skin cells from affected patients, reprogramming them into iPS cells and then differentiating these cells into the cell type of the affected tissue. This method not only allows for the *in vitro* manipulation of cells that recapitulate the disease, but, by following the differentiation and development of mutated cells, it also gives the possibility to understand the early events that contribute to the progression of that particular disease. iPSC have been generated from patients affected by Hungtington's and Parkinson's disease, ALS, juvenile diabetes, muscolar dystrophy, Fanconi anaemia, Down syndrome and others, providing potent systems for the study of these diseases (reviewed in Stadtfeld and Hochedlinger, 2010). Such approaches are being undertaken also in the study of multigenic diseases like Alzheimer's disease type I diabetes, although the *in vitro* modelling of multigenic diseases may be more difficult than modelling of monogenic ones. Nevertheless, promising results *in vitro* have come from the treatment *ex vivo* of iPSCs derived from patients affected by SMA, familial dysautonomia (FD), and LEOPARD syndrome with experimental drugs that resulted in the attenuation of the symptoms (reviewed in Stadtfeld and Hochedlinger, 2010) (Fig. 4.7).

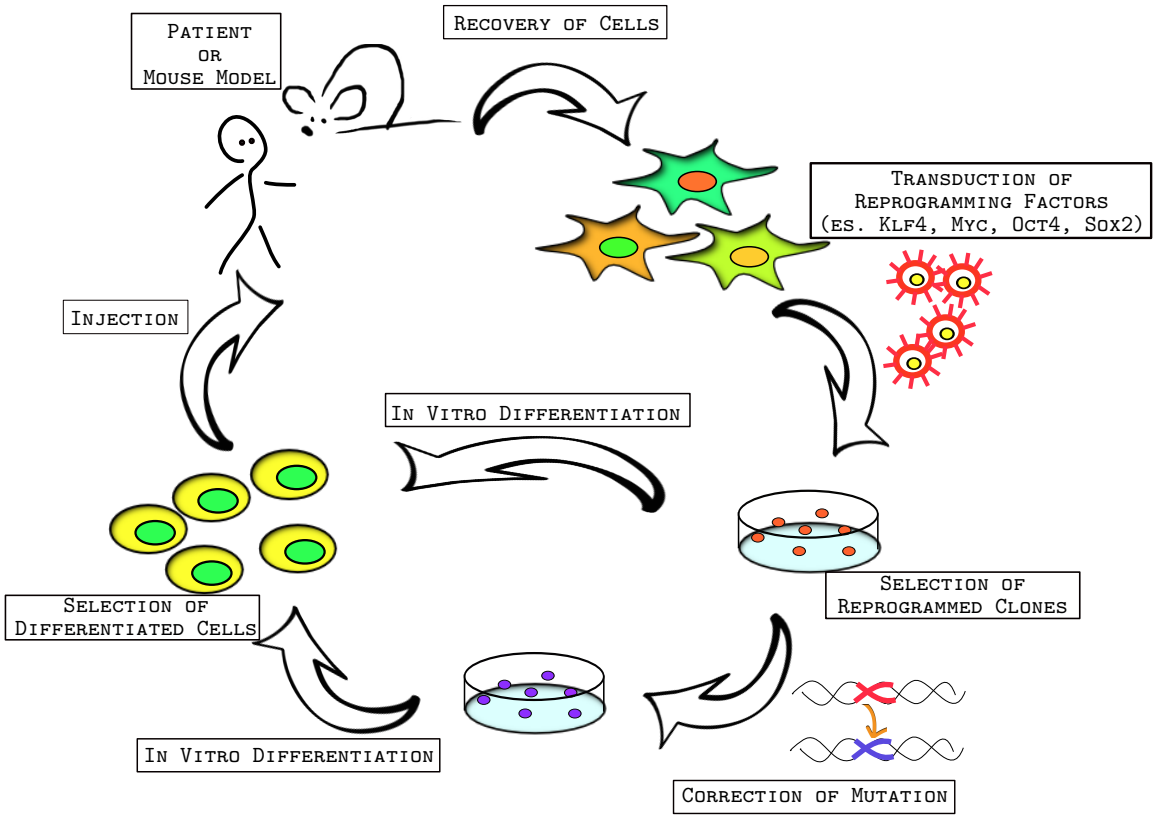

Figure 4.7: **iPS technology and applications.**
Cells from adult tissues from patients or mouse models are collected and reprogrammed according to published protocols. Reprogrammed clones are selected and used for developmental studies or corrected *in vitro* for their mutations. Cells are then induced to differentiate into specific adult cells and used for *in vitro* studies or to repair the lesions in patients or mouse models.

The iPSC technology has been subject to a very rapid development, but the application of this technique in the clinic is still far from imminent. Several concerns are slowing the translational process, and these all revolve around safety issues. In fact, iPSCs are prone to form teratomas, like ESCs, and the differentiation protocols still do not ensure 100% differentiation efficiency. Furthermore, the generation of iPSCs proceeds through the integration of vectors that may disrupt endogenous genes, therefore rendering it necessary to improve the iPSC generation techniques, with as little alteration of the target cells as possible. Finally, it has been shown that reprogrammed cells are subject to the accumulation of genomic alterations that involve the epigenetic imprinting and often result in the maintenance in the reprogrammed cells of the epigenetic memory of the cell of origin. Indeed, all these fall backs challenge the application of this technique in human patients, and has led many research groups to analyse in depth the process of reprogramming from a genetic and an epigenetic point of view, to be able to achieve the creation of cells with minimal or no genomic alteration.

The discovery of iPSCs has undoubtedly widened the knowledge of the processes of development and differentiation, and has promising implications in regenerative medicine. In fact it has shown that few

transcription factors are in charge of maintaining the SC fate and that epigenetic signatures accompany the differentiation process. Because these mechanisms are often deregulated in cancer, the study of iPSCs will possibly also help in elucidating the alterations that take place during tumorigenesis.

5 MATERIAL AND METHODS

5.1 Animal Manipulation

5.1.1 Animal Models

MMTV-ErbB2-transgenic mice were in the FVB background (Muller et al., 1988). P53KO mice were in the C57/BL6J background (back-crossed in our group starting from a 129sv background). As controls for these mice we used corresponding WT strains (FVB or C57/BL6J respectively, purchased from Harlan) . Transgenic mice expressing the green fluorescent protein (GFP) (Okabe et al., 1997) or the Red fluorescent protein (RFP) (Vintersten et al., 2004) that were used for the mammosphere clonality assay are in the C57/BL6J background. For serial transplantation experiments we used GFP transgenic mice in a FVB background. All the experiments with WT mammospheres were carried out in samples derived from FVB WT mice.

5.1.2 Transplantation Experiments

The sample material to be injected (primary mammary cells, dissociated mammospheres, PKH cell subsets or intact mammospheres) was collected into sterile Eppendorf tubes and gently pelleted in a benchtop microfuge. Cell or mammosphere pellets were resuspended in fresh PBS, counted, and resuspended in PBS at the appropriate cell density (injection volume= 20-30 µl). 3 week-old female singenic mice were anaesthetised with 2.5% Avertin in PBS (100% avertin: 10 g of tribromoethanol, Sigma, in 10 ml of tertamyl alcohol, Sigma) and the fat-pad of their 4th mammary gland was depleted of the endogenous epithelium. At 3 weeks of age the epithelial tree has not undergone the puberty-driven development that results in the penetration of the fat pad, and can easily be removed by surgical asportation of the area spanning from the nipple to the lymph node, leaving the fat-pad clear for the injection of exogenous cells (Fig. 5.1).

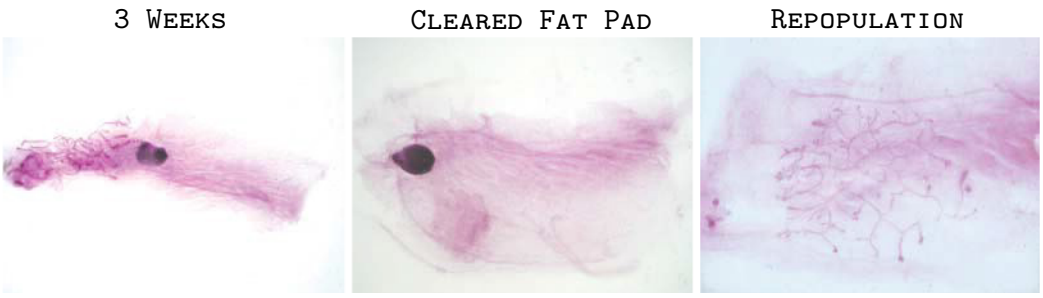

Figure 5.1: **Fat pad whole mounts.**
Whole mounts of 3-week-old fat pad (left panel), cleared fat pad (central panel) and cleared fat pad 8 weeks after transplantation of primary mammary epithelial cells (right panel). Modified from Smalley and Ashworth, 2003 (Smalley and Ashworth, 2003).

For the evaluation of positive outgrowths, the fat pads were collected (8 to 10 weeks after transplantation), stained with Carmine Alum and analysed as described ((DEOME et al., 1959; Sleeman et al., 2006). Briefly, fat pads were scored as negative for outgrowths if "no epithelial structures could be observed or if an epithelial ductal network could be seen, in which the majority of ductal branching had the same direction and had grown in from one edge of the fat pad". They were instead scored as positive if "outgrowths could be seen to have originated from a central region of the cleared fad pad and the directionality of the ductal branching was different in different parts of the fat pad". The presence of TEBs in the outgrowths was also a hallmark of exogenous epithelial growth. For each outgrowth, we calculated the extent of host fat pad filling, expressed as percentage of penetration. Values of fat filling were heterogeneous among different outgrowths, and ranged from 25 to 80%.

5.1.3 Statistical Analysis of Positive Transplants

Limiting dilution data and SC frequencies were analysed using generalised linear models, as implemented in the limdil function of the 'statmod' package (http://cran.r-project.org/web/packages/statmod/index.html) for the R computing environment (http://www.r-project.org/). The single hit Poisson model underling limiting dilution was estimated by a complementary log-log generalised linear model. A confidence interval was obtained for the SC frequency by computing two-sided 95% Wald confidence intervals. In cases of zero outgrowths, exact binomial confidence intervals (one-sided 95% Clopper-Pearson) were computed. Goodness of fit of the single-hit model was estimated by testing, using the likelihood ratio test, the null hypothesis that the angular coefficient equals to 1 in the linear model fitted with two two-parameters. The null hypothesis was not rejected ($p > 0.05$) for any dilution series (Bonnefoix et al., 1996).

5.1.4 Carmine Alum Whole Mount Method

Transplanted mammary glands were stretched out onto slides and fixed overnight in a 1:3 solution of acetic acid/ethanol. Slides were washed twice in distilled water for 10 minutes and then stained overnight at room temperature with Carmine Alum solution (0.2% carmine, 0.5% aluminium potassium sulfate in water, Sigma). Destaining was performed in 70% ethanol for 30 minutes, followed by two 30 minutes washes in 95% and 100% ethanol. Finally, samples were soaked in a 1:2 solution of benzylalcohol/benzylbenzoate (Sigma) until the fat pads clarified.

5.1.5 Nutlin-3 Treatment *in vivo*

Nutlin3 was either purchased from Cayman Chemicals or supplied by M.Varasi (Dept. of Chemistry, DAC s.r.l., Milan, Italy). Two month old MMTV-ErbB2 mice were treated with Nutlin-3 or DMSO for two weeks (i.p. injection once every two days). Mice were sacrificed either immediately after treatment to

evaluate the effect o Nutlin-3 on SCs by limiting dilution transplantation, or after two months to evaluate tumour formation after Nutlin-3 treatment.

5.1.6 Preparation of Paraffin Sections

For the preparation of paraffin-embedded sections: breast tissues freshly collected from mice, or whole-mounted tissues were fixed overnight with 10% formalin. Matrigel cultures were embedded in 1% low melting point agarose. The prepared samples were sequentially treated for 1 hour at room temperature with 70%, 80%, 95% ethanol, three times with 100% ethanol, twice with xylene and twice for two hours at 58°C with paraffin. The specimens were then embedded in paraffin and sectioned with a microtome at 2 µm thickness. Slides were stained with haematoxylin-eosin for histological analysis or stained by immunohistochemistry.

5.1.7 Immunohistochemistry

Paraffin sections were twice deparaffinized with histolemon (Carlo Erba) for 10 minutes and hydrated through graded alcohol series (100%, 95%, 70%, 50%, 30% ethanol and water) for 5 minutes. Antigen unmasking was performed with 0.1 mM citrate buffer (pH=6) under microwave irradiation for 10 minutes at 750W followed by incubation with 3% hydrogen peroxide in distilled water for 5 minutes at room temperature. Slides were subsequently pre-incubated with an antibody mixture (2% BSA, 2% normal goat serum, 0.02% Tween20 in TBS) for 20 minutes at room temperature and then stained with primary antibody overnight at 4C. After two washes with TBS slides were incubated with a secondary antibody (DAKO Envision system HRP rabbit or mouse) for 30 minutes at room temperature and washed twice again in TBS. The sections were subsequently incubated in peroxidase substrate solution (DAB DAKO) for 2 to 5 minutes, rinsed in water, counterstained with haematoxylin for 30 seconds, dehydrated through graded alcohol series (water and 30%, 50%, 70%, 95%, 100% ethanol) for 5 minutes each and finally mounted with Eukitt (Kindler GmbH). Primary antibodies used in this work were: rabbit anti-K5 (Covance), mouse anti-K8 (Progen Biotechnik), rabbit anti-Ki-67 (Novocastra Laboratories), rabbit anti-cleaved caspase-3 (D175, Cell Signalling).

5.2 Cell Culture and Manipulation

5.2.1 Isolation of Mouse Mammary Epithelial Cells

The 2nd, 3rd and 4th mammary glands were collected from 4-12 week-old virgin WT, ErbB2-transgenic or p53 KO mice. Mammary tissues were mechanically dissected into small pieces with scissors, and enzymatically digested with the following digestion mixture: Dulbecco's modified Eagle's medium (DMEM, BioWhittaker), 5% fetal bovine serum (FBS), 2 mM glutamine, 100 U/ml penicillin and 100 µg/ml strep-

tomycin, supplemented with 200 U/ml collagenase (Sigma) and 100 U/ml hyaluronidase (Sigma) for 5 hours at 37°C in a humid atmosphere containing 5% CO2. Every 30 minutes, the samples were mixed by pipetting to facilitate the tissue dissociation. When the digestion was complete, the cell suspensions were centrifuged at 80xG for 5 minutes to allow precipitation of epithelial cells but not of fibroblasts and adipose cells(Stingl et al., 1998).The cell suspension was washed in PBS and filtered through 100, 70, 40 and 20 µm meshes to eliminate cell aggregates. The cells were then subjected to osmotic shock with 0.2% NaCl for 2 minutes, followed by a neutralisation step with 1,6% NaCl to lysate red blood cells. The remaining epithelial cells were plated to obtain mammospheres, stained with the PKH26 fluorescent dye or used in transplantation assays.

5.2.2 Mammosphere Culture

Primary mammary cells were plated onto ultralow attachment plates (Falcon) at a density of 100,000 viable cell/ml (to obtain primary mammospheres) in a serum-free mammary epithelial basal medium (MEBM, BioWhittaker), supplemented with 2 mM glutamine, 100 U/ml penicillin and 100 µg/ml streptomycin, 5 µg/ml insulin, 0.5 µg/ml hydrocortisone, 2% B27 (Invitrogen), 20 ng/ml EGF and bFGF (BD Biosciences), and 4 µg/ml heparin (Sigma) and cultured at 37° C in a humid atmosphere containing 5% CO2 (standard culture). In these conditions mammary epithelial cells grow as spherical clonal colonies called mammospheres(Dontu et al., 2003; Liao et al., 2007) that reach their maximum size in 5-6 days. After 7 days of culture, primary mammospheres (obtained from freshly isolated mammary cells) were dissociated mechanically using a fired-polished pipette and re-plated to obtain secondary mammospheres at a density of 20,000 cells/ml in 6-well low-adhesion plates. The same procedure was repeated at each passage.

5.2.3 Mammosphere Growth Curves

For the measurement of mammosphere growth curves, 5,000 cells from primary dissociated mammospheres were plated in quadruplicate onto ultralow attachment plates (24 multiwell) at each passage. After 6 days, the newly formed mammospheres were counted and subsequently collected and manually dissociated by pipetting. At each passage, the number of retrieved mammospheres reflects the number of mammosphere-initiating cells present in the original culture and the number of cells counted after dissociation allows for the evaluation of the number of cells per sphere that were formed. The average number of cells that compose a sphere (sphere size) was calculated as the ratio between the number of cells and the number of spheres at each passage. Cumulative sphere and cell curves were calculated based on the ratio between plated spheres and obtained spheres and cells respectively. Since the mammosphere size was constant over the several passages (Cicalese et al., 2009), the number of plated mammospheres was calculated as 5,000 divided by the average size of the mammospheres over the passages. The cumulative curves plotted in a semi-logarithmic graph appear as straight lines, thus suggesting they approximate an exponential curve,

as expected for a cell population that grow or die with a constant rate during the time. Growth rates (G.R.) were evaluated as the slope of the trendline of the exponential curves. To verify the exponential correlation between the cumulative numbers and time of culture, exponential regression of the data was performed. The coefficients of determination (R^2) showed values near to 1 in each of the measured curve, thus indicating the goodness of the fitting model.

5.2.4 PKH26 Assay

The PKH26 staining was performed with a slight modification to the described protocol (Sigma, PKH26-GL). Primary mammary cells were washed and resuspended in PBS at the concentration of 10 million cells/ml, and stained for 5 minutes at room temperature by adding an equal volume of a 2x PKH26 mix (1:250 PKH-26 dye in PBS). The reaction was blocked for 1 minute by adding an equal volume of 1% bovine serum albumin (BSA) in PBS. The cells were then washed twice with culture medium and plated to obtain primary mammospheres. FACS sorting was performed on single cell suspensions from secondary mammospheres using a FACS Vantage SE flow cytometer (Becton&Dickinson) equipped with a 488 nm laser (Enterprise Coherent) and with a band pass 575/26 nm optical filter for PKH-26 fluorescence detection. An average sorting rate of 1,000 events per second at a sorting pressure of 20 PSI was maintained. Cells were first sorted to separate PKH^{high} and $PKH^{low+neg}$ cells. The PKH^{high} region was defined according to the estimated percentage of SCs in mammospheres. A second round of cell sorting was then performed to separate PKH^{low} from PKH^{neg} cells. The PKH^{neg} gate was selected according to the basal fluorescence of unstained cells. The boundary regions were excluded to minimise potential cross contamination due to Gaussian spreading of intensity curves. The obtained PKH-subsets were cultured as mammospheres, plated in methylcellulose for time-lapse experiments or used in transplantation assays.

5.2.5 Time-Lapse Analysis

Methylcellulose (MethoCult® SF M3236) was reconstituted with 20% mammosphere medium containing 5x concentrated supplements. 500-1,000 PKHhigh cells were re-suspended in Methyl Cellulose in complete medium, plated in glass bottom dishes (MatTek Corporation, US) and incubated in a humid atmosphere containing 5% CO2 at 37°C over night to allow the cells to sediment. Time-lapse video microscopy was performed with a Scan^R screening station (Olympus-SIS, Munich, Germany) equipped with a microscope incubation chamber (Evotec, Germany). Cells were observed through a 10x 0.4 NA objective. Both DIC (differential interference contrast) and PKH red fluorescence images were collected with auto focusing procedures and compensated for focal shift. Different focal planes were recorded to prevent loss of image contrast due to axial cell movement inside the well. Images were captured every hour for 7 days, starting 14 hours after plating, and reconstructed using the ImageJ software.

5.2.6 Matrigel Culture

Single cells deriving from dissociated primary mammospheres were matrigel-embedded. About 1,000 cells were re-suspended in 500 µl of Matrigel Matrix (BD Bioscience) and plated in a 12 well plate. After 30 minutes at 37 °C, 1 ml of differentiation medium (DMEM: F12 1:1, 2% FBS, 10 ng/ml EGF, 5 µg/ml insulin, 100 U/ml penicillin and 100 µg/ml streptomycin) was layered on the Matrigel and then changed every three days. After 3 weeks the formed structures were analysed under an inverted microscope and embedded in paraffin.

5.2.7 Lentiviral Infection

293-T packaging cells, an immortalised cell line from human fetal kidney fibroblast, were cultured in a humid atmosphere containing 5% CO2 in DMEM supplemented with 10% FBS, 2 mM glutamine, 100 U/ml penicillin and 100 µg/ml streptomycin. For lentiviral production 293-T cells were transfected with the calcium-phosphate procedure with a mixture of 4 DNAs: 2,5 µg of pRSV (Rev), 5 µg of pMDL (gag&pol), 3 µg of pENV (VSV-G), and 10 µg of the lentiviral vector per plate. 62.5 µl of 2M CaCl2 were added to the DNA mix and brought to a total volume of 500 µl with water. The mix was added drop-wise to 500 µl of 2X HBS (HEPES buffered saline: 250mM HEPES pH 7.0, 250mM NaCl and 150mM Na2HPO4). After 15 minutes of incubation, the precipitate was distributed on 60-70% confluent exponentially growing cells. The medium was replaced 12 hours later with fresh medium and 36 hours later with mammosphere medium. Viral supernatant was collected after 24 hours and filtered through a 0.45 µm syringe-filter. Cells from dissociated primary mammospheres were resuspended in viral supernatants to a final concentration of 50,000 cell/ml and subjected to three cycles of infection in suspension (6h, o/n, 6h). After the third infection cycle, the cells were resuspended in fresh mammosphere medium to obtain secondary mammospheres.

For this study we utilised the following lentiviral vectors:

- pLKO-Numb (and its control pLKO): a vector expressing short hairpin RNAs directed against Numb and the cassette for the puromycin resistance.
- pSico-p53sh (and its control pSICO): a vector expressing short hairpin RNAs directed against p53.
- pWPI-p53 (and its control pWPI): a vector carrying the human p53 cDNA under the control of the CMV promoter.
- pWPI-MycER (and its control pWPI): created from the pWPI backbone and the insertion of the MycER sequence Littlewood et al. (1995).
- pRDI-Myc (and its control pRDI): a vector carrying the human c-Myc sequence under the control of the CMV promoter

- pTWEEN-Omomyc (and its control pTWEEN): a vector carrying the Omomyc sequence under the control of the CMV promoter
- pLL3.7-mMyc (and its control pLL3.7): a vector expressing short hairpin RNAs directed against mouse c-Myc and the cassette for the puromycin resistance.

5.2.8 Human Mammary Epithelial Cell Isolation

Human samples of normal mammary glands were retrieved from reduction mammoplasties performed at IEO, Milan, Italy. Tissues were processed as described (Dontu et al., 2003; Pece et al., 2010) to isolate mammary epithelial cells. Human mammospheres were infected with lentiviral vectors using the same protocol previously set up for murine mammospheres.

5.3 Protein Expression Analysis

5.3.1 RT-PCR and PCR

Total RNA from mammospheres was isolated using the PicoPureRNeasy isolation Kit (Arcturus) and reverse transcribed using random hexamers (Roche Diagnostics), according to the manufacturer protocols. Real-time RT-PCR analyses were done in triplicate on the Applied Biosystems 7500 Fast Real-Time PCR System with the SYBR Green PCR kit as instructed by the manufacturer (Applied Biosystems). The amount of c-Myc mRNA was normalised to the amount of 18S rRNA.

5.3.2 Immunofluorescence

Cells from dissociated mammospheres were fixed in suspension with 4% paraformaldehyde for 10 minutes, washed three times in PBS and plated onto polilysinated coverslips. Cells were then permeabilized 5 minutes with 0.1% Triton-X100 in PBS at room temperature, washed three times in PBS and blocked with 3% BSA in PBS (blocking solution) for 20 minutes. Staining with primary antibodies was performed in a humid chamber for 1 hour at room temperature and followed by three washes in PBS. Coverslips were then stained with secondary antibodies for 30 minutes at room temperature, washed three times in PBS, counterstained with DAPI and mounted in mowiol. Samples were analysed under an AX-70 Provis (Olympus) fluorescence microscope equipped with a b/w cooled CCD camera (Hamamatsu c5985). In this work we used a rabbit monoclonal c-Myc antibody (1:800 in blocking solution, D84C12 Cell Signalling) followed by an anti-rabbit Cy5 antibody (1:100 in blocking solution, Jackson Laboratories).

5.3.3 Intracellular Localisation of Numb

To detect endogenous Numb, FACS-sorted PKH^{high} cells were cultured in suspension for 36 hours in the presence of 25 µM Blebbistatin. Immunofluorescence was performed as described in section 2.5 using an

anti-Numb antibody (Colaluca et al., 2008) followed by an anti-mouse Alexa 647 antibody (30 minutes at room temperature, 1:100 in blocking solution, Jackson Laboratories) . Confocal analysis was performed with a Leica TCS SP2 AOBS confocal microscope. For each cells 15-20 adjacent 0.5µm optical sections were collected.

5.3.4 Western Blot Analysis

10,000 to 20,000 cells from dissociated mammosphere were collected, washed in PBS and lysed in 50 µl of Laemmli sample buffer (62.5 mM Tris-HCl pH 6.8%, 2% SDS, 5% 2-mercaptoethanol and 10% glycerol). SDS-PAGE was performed in a BIORAD apparatus using a SDS running buffer (0.025 M tris-base pH 8.8; 0.192 M glycine; 0.1% SDS). Following SDS-PAGE electrophoresis, proteins were transferred to nitrocellulose membranes (Protan; Schleicher & Schuell) by electroblotting for 16 hours at 30V. Membranes were stained with Ponceau S to verify the efficiency of the transfer. Membranes were blocked in blocking solution (5% low fat milk in TBS-T: Tris Buffered Saline, 0.1% Tween 20) for 1 hour and then incubated with the primary antibody in blocking solution for 1 hour at room temperature or 12 hours at 4°C. The membranes were washed three times in TBS-T (10 minutes each) and incubated with a secondary antibody linked to horse-radish peroxidase for 1 hour at room temperature. After three 15-minute washes in TBS-T, the proteins were visualised using enhanced chemiluminescence (ECL, Amersham), according to manufacturer's instructions, followed by autoradiography. The following antibodies were used in this work: mouse monoclonal anti-vinculin (1:1000 in blocking solution, Sigma), rabbit polyclonal anti-ph18p53 (1:1000 in blocking solution, calbiochem), mouse monoclonal anti-p53 (1:1000 in blocking solution, clone AI25, gift from K. Helin), mouse monoclonal anti-p21 (1:300 in blocking solution, clone F5, Santa Cruz), rabbit polyclonal anti-cleaved caspase3 (1:500 in blocking solution, clone D175, Cell Signalling), rabbit polyclonal anti-p16 (M156 Santa Cruz).

For Myc immunoprecipitation, lysates from 4 million cells for each sample were incubated with protein A resin and mouse monoclonal antibody against c-Myc (C-33, Santa Cruz) for 4 hours. Immunoprecipitated material was loaded onto an SDS-PAGE gel and subsequently blotted onto a nitrocellulose membrane. Myc was visualised with a rabbit polyclonal anti c-Myc antibody (1:1000 in blocking solution, gift of S. Hann, Vanderbilt University School of Medicine, Nashville, TN). Normalisation was evaluated by the expression of vinculin.

5.4 Comparative Genomic Hybridisation Analysis

Genomic DNA was prepared using the Qiagen Genomic DNA kit (Genomic tip 100/G), according to the instructions supplied by the manufacturer. DNA from non-infected cells was labeled with Cy5, whereas DNA from the reprogrammed clones was labeled with Cy3. Equal amounts of Cy5- and Cy3-labeled DNA were hybridised against high- density tiling microarrays containing probes mapping to mouse chromosomes

9-14 (Roche Nimblegen array MM8 WG CGH3; Build 36). The median probe density on the arrays was 1,388 bp. The data were analysed using the software provided by the manufacturer.

6 RESULTS

6.1 Characterisation of Normal and Tumor Mouse Mammary Stem Cells

The cancer stem cell hypothesis is constantly being supported by new emerging data, and it is gaining more and more consent with time. In light of this, the need to study the mechanisms that regulate the behaviour of normal and tumour SCs requires these cells to be isolated, cultured and maintained *in vitro* in their multipotent state. This is why, in recent years, there have been several attempts at the isolation and culture of normal and tumour SCs and these have conveyed to the establishment of culturing conditions for SCs of various organs including bone marrow, brain, breast, gut and skin and of several tumour tissues. Based on recently published protocols (Dontu et al., 2003; Liao et al., 2007), we set-up culturing conditions for the *in vitro* propagation of mouse mammary SCs and CSCs. These protocols rely on the ability of these cells to grow in suspension, in a serum-free medium supplemented with EGF and FGF, as spheroids called mammospheres (Fig. 6.1).

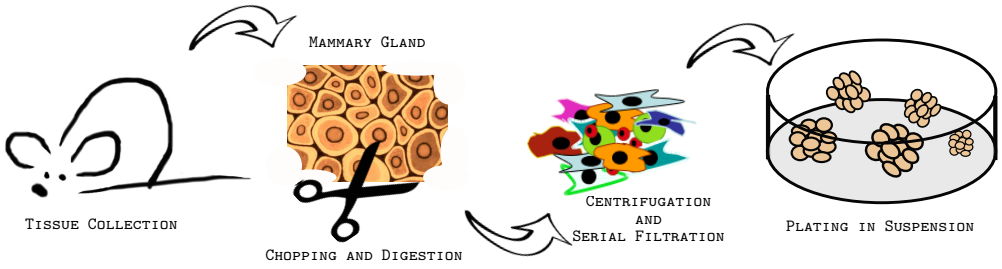

Figure 6.1: **Schematic representation of the isolation and characterisation of mouse mammary SCs.**
Tissues are collected from the mice, mechanically dissected and subjected to enzymatic digestion. The samples are then centrifuged to remove the stroma and run through serial passages of filtration to eliminate undigested clusters. The purified cell suspension that is obtained is then plated in suspension, in the absence of serum and in the presence of growth factors, to allow epithelial SCs to form mammospheres.

As tumour model, we have used a transgenic mouse carrying a constitutively active form of the ErbB2 oncogene (with the activating mutation Val^{664} to Glu^{664}) under the control of the Mouse Mammary Tumour Virus (MMTV) promoter (Muller et al., 1988). ErbB2 is mutated or overexpressed in 20-30% of breast cancer cases, and it has been recently demonstrated that the tumours that are formed in the MMTV-ErbB2 mouse follow a CSC model (Grange et al., 2008).

We have characterised the mammospheres that are formed by culturing epithelial cells isolated from normal mammary glands or tumour biopsies and we have shown that these mammospheres *i)* are clonal in origin (Fig. 6.2), *ii)* they can be serially passaged (Fig. 6.3) , *iii)* they are able to form complex threedimensional structures if cultured in semisolid media *in vitro* (Fig. 6.4), and *iv)* they can reform tissues with the same complexity of their tissue of origin if transplanted into the cleared fat-pad of

singenic recipient mice (Fig. 6.5). The transplantation of mammary epithelial cells into the fat-pad of a recipient mouse is a standard technique to study the regenerative potential of cells. At 3 weeks the mammary epithelium of the inguinal mammary gland is still concentrated in the nipple area and has not penetrated the fat pad. After surgical removal of the endogenous epithelium, the cells are inoculated in their physiological environment and allowed to develop (DEOME et al., 1959).

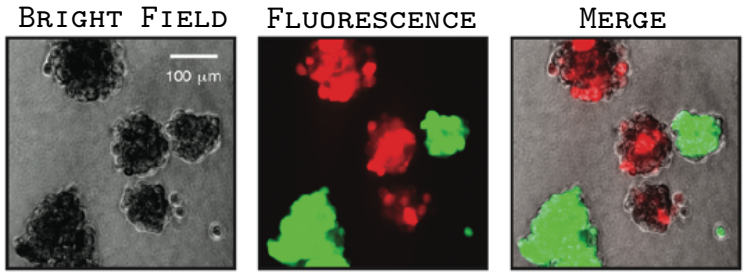

Figure 6.2: **Mammospheres are clonal in origin.**
Mammary epithelial cells were isolated from transgenic mice carrying either the GFP or the RFP proteins, mixed in equal amounts and plated to form mammospheres. After one week in culture, the clonality of the formed spheres was assessed by evaluating under a fluorescence microscope the content of GFP- or RFP-expressing cells in each mammosphere. All the observed mammospheres were composed entirely by GFP- or RFP-positive cells, confirming that they were clonal and derived from the division of a single cell. Scale bars as reported.

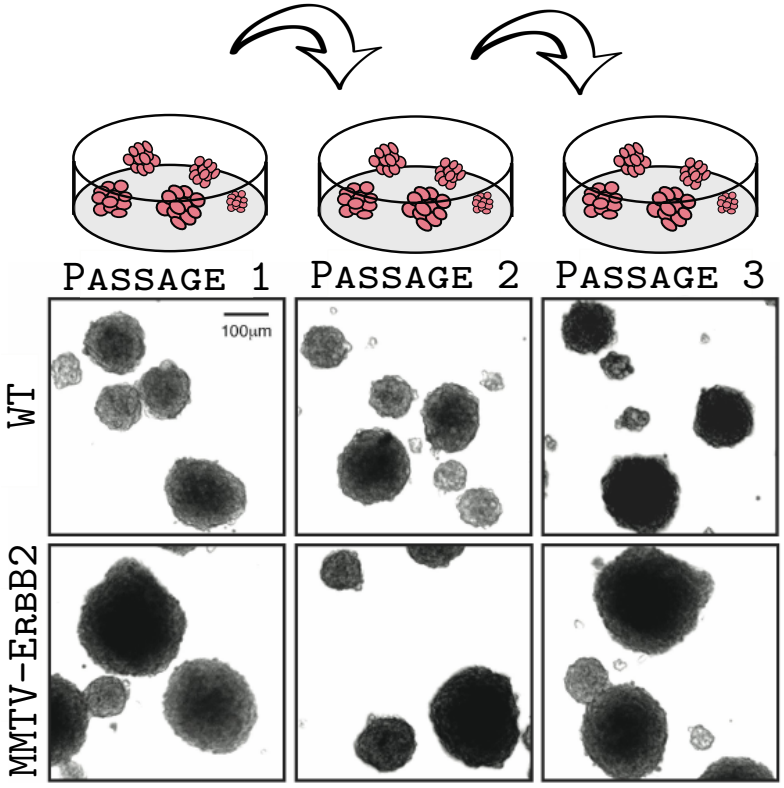

Figure 6.3: **Mammospheres can be serially passaged.**
WT and tumour primary mammospheres can be collected and mechanically disaggregated by pipetting. If the resulting cell suspensions are replated, secondary mammospheres are formed and the process can be repeated for several passages, showing that they contain cells endowed with self-renewing abilities. Figures show representative images of mammospheres formed by WT mammary epithelial cells or tumour cells. Scales as reported.

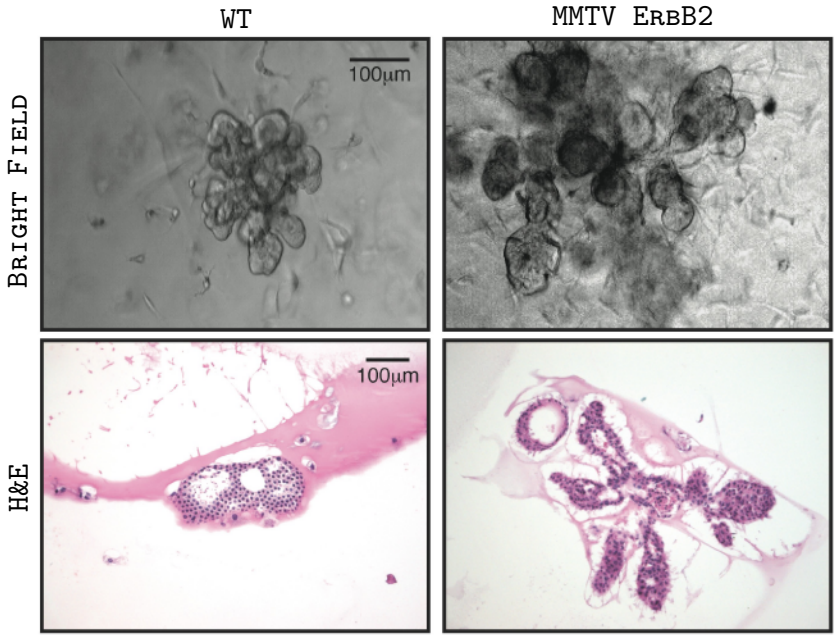

Figure 6.4: **WT and tumour mammospheres differentiate and form threedimentional structures in Matrigel.**
Primary WT and tumour mammospheres were disaggregated and plated at clonogenic densities in 3D Matrigel cultures. Under these conditions, WT cells formed acinus-like structures and occasionally (<1%) branched/ductal-acinar structures. Single cells from dissociated tumour mammospheres formed branched/ductal-acinar structures, which were disorganised and frequently lacked lumens, as has been reported for human primary mammary cancer samples (Farnie et al., 2007). Images show transmitted light (Bright Field) and Hematoxilin/Eosin staining of sections of the paraffin-embedded structures (H&E). Scale bars as reported.

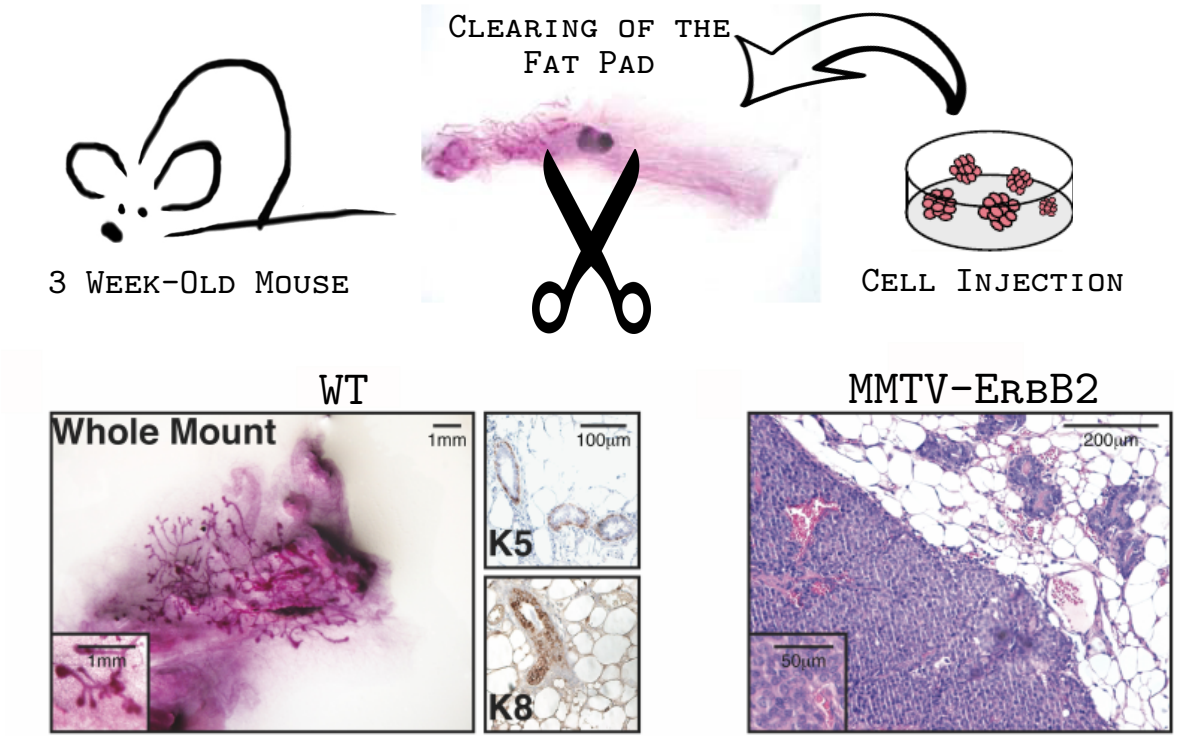

Figure 6.5: **Mammospheres form tissues upon transplantation *in vivo*.**
Cells from primary normal or tumour mammospheres were transplanted into the cleared fat-pad of 3-week old recipient mice as reported (DEOME et al., 1959). The resulting outgrowths were evaluated after 8-10 weeks by whole mount staining for normal mammary glands, and paraffin-embedding and sectioning for tumours. Images show: *i)* Left panel: whole mount staining of a positive outgrowth resulting from the injection of cells deriving from WT mammospheres; immunohistochemical analysis of basal epithelial marker K5 and luminal epithelial marker K8 in the same positive epithelial outgrowth. *ii)* Right panel: Hematoxylin&Eosin staining of a paraffin-embedded and sectioned tumour arising from the injection of tumour mammospheres in a recipient mouse. Scale bars as reported.

Altogether, these observations suggest that mammospheres derive from the clonal expansion of cells endowed with self-renewing and differentiating potential, two properties that define SCs. Serial transplantation experiments confirmed that these cells are indeed true SCs (Fig. 6.6).

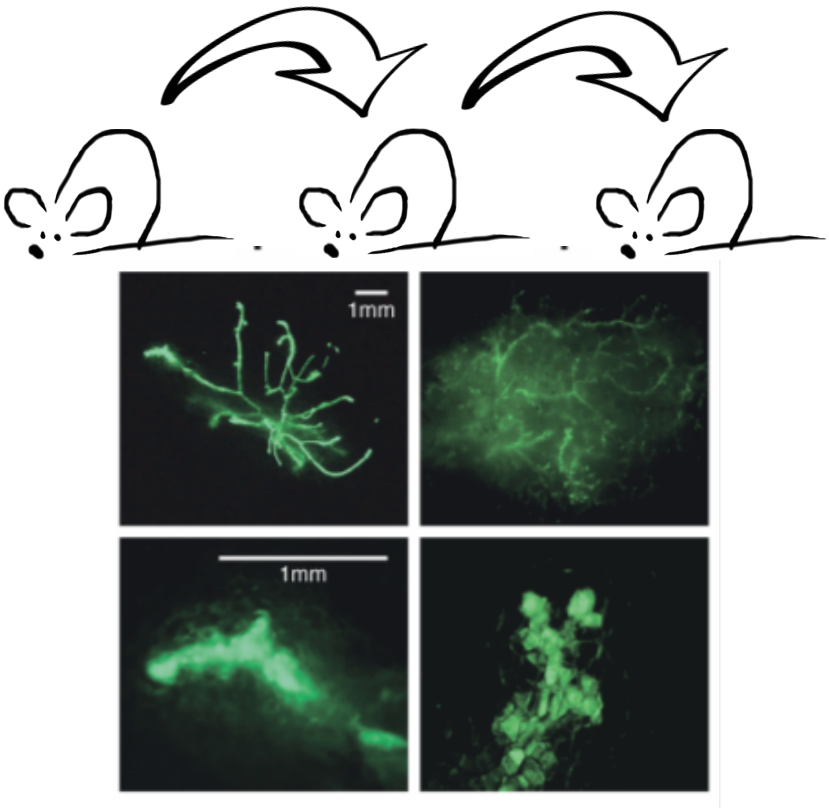

Figure 6.6: **Serial transplantation of positive outgrowths**
Serial transplantation of mammary epithelial cells derived from a transgenic GFP mouse. Primary transplant (left panels) and secondary transplants (right panels) are shown. Scale bars as reported.

Not all cells that form mammospheres possess stem-like properties, suggesting that these structures have an intrinsic hierarchic organisation. To investigate the content in SCs of normal and tumour mammospheres, we performed limiting dilution transplantations of cell suspensions derived from disaggregated normal or tumour mammospheres, into the cleared fat-pads of singeneic mice. The results of these experiments are summarised in Table 6.1 and show that whereas WT cell suspensions contain approximately 1 SC every 300 cells, in tumour cell suspensions, the frequency is increased by three-fold (1 CSC every 100 cells). We calculated the mammosphere sizes to be around 360 cells (362±14; n=15) in normal mammospheres and 520 (522±14; n=13) cells in tumour mammospheres, which predict that each WT mammosphere contains 1 SC, whereas tumour mammospheres contain approximately 5 CSCs per sphere. These assumptions were also confirmed for WT samples by limiting dilution transplantation of whole mammospheres, that yielded a frequency of one positive transplantation every single mammosphere injected (Table 6.1).

Cell Injection

		WT	ErbB2
Cell Number:	10^5	7/7	6/6
	10^4	11/11	2/2
	10^3	6/6	6/6
	500	6/8	2/2
	100	5/7	4/6
	50	1/8	
	25	0/6	
	10	0/6	0/2
SC frequency	Estimate	**1:322**	**1:95**
	upper - lower limits	1:191 – 1:542	1:36 – 1:251
p-Value	Fit	0.58	0.50
	Difference	0.03	

WT Mammosphere Injection

Sphere Number:	10	6/6
	5	11/11
	1	6/6
SC frequency	Estimate	**1:1.1**
	upper - lower limits	1:0.6 - 1:2.0
p-Value (Fit)		0.82

Table 6.1: **Summary of limiting dilution transplantation experiments performed with single cell suspensions or whole mammospheres.**
Upper table: cell suspensions from WT or tumour secondary mammospheres were inoculated in recipient mice in limiting dilution conditions (from 10,000 to 10 cells). Results show the number of positive outgrowths evaluated as normal mammary epithelium (WT samples) or tumours (tumour samples) that arose 8-10 weeks after injection. SC frequencies (Estimates and upper/lower limits) were calculated by limiting dilution analysis, as described in Material and Methods. Fitting to single hit model is indicated by p-values $> 0{,}05$ (Fit). The significance of the difference in SC frequencies is indicated by p-values $< 0{,}05$ (Difference).
Lower table: intact WT mammospheres were injected into recipient mice. Results show positive outgrowths. SC frequencies (Estimates and upper/lower limits) were calculated by limiting dilution analysis, fitting to single hit model is indicated by p-values $> 0{,}05$ (Fit).

Interestingly, the limiting dilution transplantation of freshly isolated cells from normal mammary tissues or ErbB2-driven tumours showed that in primary uncultured tissues as well, the number of SCs is increased in tumours compared to normal samples (Table 6.2).

Freshly Isolated Cells Injection

		WT	ErbB2
Cell Number:	10^5	2/2	2/2
	$5x10^4$	4/4	2/2
	10^4	1/8	4/4
	$5x10^3$	1/8	3/4
	10^3	0/4	2/8
	500	0/4	0/8
	100		0/8
	50	0/5	0/4
	10		0/4
SC frequency	Estimate	1:30,775	1:3,914
	upper - lower limits	1:14,709 – 1:64,390	1:1,935 – 1:7,919
p-Value	Fit	0.11	0.22
	Difference	$3x10^{-4}$	

Table 6.2: **Limiting dilution transplantation of freshly isolated cells from normal and tumour tissues.**
Freshly isolated cell suspensions from WT or tumour tissues were inoculated in recipient mice in limiting dilution conditions (from 10,000 to 10 cells). Results show the number of positive outgrowths evaluated as normal mammary epithelium (WT samples) or tumours (tumour samples) that arose 8-10 weeks after injection. SC frequencies (Estimates and upper/lower limits) were calculated by limiting dilution analysis, as described in Material and Methods. Fitting to single hit model is indicated by p-values $> 0{,}05$ (Fit). The significance of the difference in SC frequencies is indicated by p-values $< 0{,}05$ (Difference).

The calculated frequencies of SCs in normal and tumour tissues were around 1:30,000 and 1:4,000 respectively. Altogether these experiments show that in tumour mammospheres and tumour tissues, the number of SCs is markedly increased compared to the WT counterparts.

6.1.1 Analysis of the Growth Properties of Normal and Cancer SCs

The observation that the number of SCs that can be found in tumour samples is increased compared to normal samples both *in vivo* and *in vitro*, suggested that these cells may possess increased self-renewing potential. However, the mammosphere system does not allow for a conventional characterisation of the proliferative potential of SCs, due to their low representation in the bulk of cells that are found in mammosphere cultures. To circumvent this problem, we analysed the replicative history of normal and tumour SCs by staining them with a vital fluorescent membrane dye (PKH26) that is equally distributed between the two daughter cells at each cell division, thus enabling the correlation between the intensity of the staining and the replicative history of each cell (Lanzkron et al., 1999). Freshly isolated cells were stained with the PKH26 dye and cultured as mammosphere for two passages. Tertiary mammospheres were then disaggregated and cell suspensions were separated by FACS sorting into a subpopulation of

intensely-stained PKH^{high} cells (slowly dividing), an intermediate PKH^{low} subpopulation of cells (rapidly dividing) and a subpopulation of unstained PKH^{neg} (very rapidly dividing) cells (Fig. 6.7).

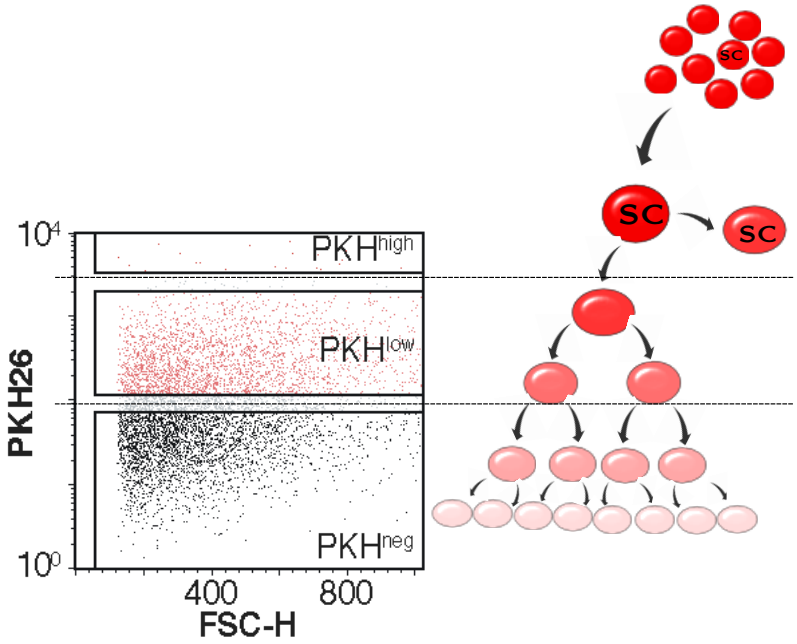

Figure 6.7: **FACS analysis of cell suspensions deriving from disaggregated tertiary WT mammospheres stained with the PKH26 dye.**
FACS plot of the distribution of cells from WT mammospheres according to the intensity of their staining with the PKH26 dye. In a first round of sorting, the PKH^{high}population is isolated from the bulk. Subsequently, an intermediate and negative populations are separated. On the right, a graphic representation of the PKH26 dye dilution according to the proliferative history of the cells.

The PKH^{high}cells were defined as the 0.5-1 % of the total population, based on the estimated fraction of SCs in the mammosphere cell cultures (0.3% in WT mammospheres and 1% in tumour mammospheres). The gating for the sorting of PKH^{neg}cells was defined based on the fluorescence intensity of unstained cells.

Replating of the three PKH populations in normal and tumour samples revealed that only the PKH^{high}population in normal samples was able to form mammospheres *in vitro*, whereas cells with the ability to form mammospheres could be found in all three PKH populations in tumour samples, suggesting that, as expected, CSCs are actively proliferating and normal SCs remain quiescent (Fig. 6.8).

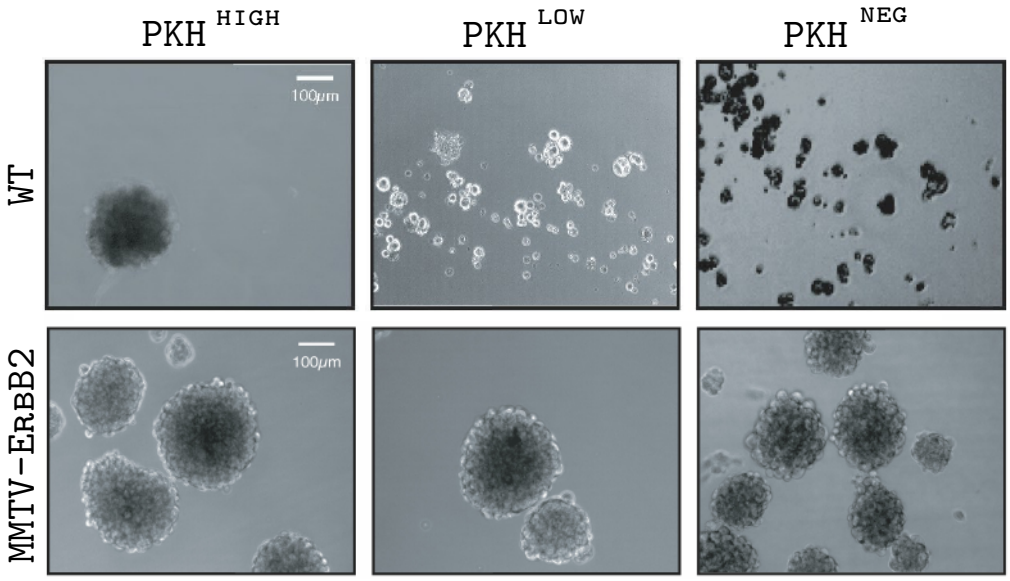

Figure 6.8: **Replating of the 3 PKH populations.**
Only PKH^{high}cells from WT samples are able to form mammospheres *in vitro*, whereas the intermediate populations ony form small aggregates that cannot be passaged further. On the contrary, tumour mammospheres can arise from all three PKH populations, suggesting that CSCs are actively proliferating. Figures show representative images of mammospheres formed after the replating of sorted PKH-populations. Scale bar as represented.

Accordingly, the injection of the WT populations in the cleared fat-pad of singeneic mice resulted in the formation of positive outgrowths only with the PKH^{high}population, with as little as a single cell in 10 out of 26 cases. Indeed, this population was highly enriched in SCs, and we could estimate the frequency of SCs to be approximately 1:3. On the contrary, the injection of the PKH^{low}and PKH^{neg}populations did not result in the formation of a mammary tissue even at high numbers (up to 100,000 cells).

In line with the data generated *in vitro*, all three the tumour PKH populations were able to generate mammary tumours if injected *in vivo*, although the frequency of tumour initiating cells was progressively lower in the intermediate- and negatively-stained populations compared to the brightly stained cell fraction (Table 6.3).

WT

		PKH^{high}	PKH^{low}	PKH^{neg}	PKH$^{low+neg}$
Cell Number:	10^5		0/1	0/1	0/10
	$5x10^4$		0/2	0/2	0/6
	10^4		0/3	0/2	
	$5x10^3$		0/2	0/2	
	10^3	2/2	0/2		
	500	4/4			
	100	5/5			
	10	13/15			
	1	10/26			
SC frequency	Estimate	1:3.4	< 1:80,782	< 1:76,766	< 1:433,951
	upper - lower limits	1:0.7 - 1:5.7			
p-Value	Fit	0.06			
	Difference		$1x10^{-160}$	$1x10^{-112}$	$2x10^{-258}$

MMTV-ErbB2

		PKH^{high}	PKH^{low}	PKH^{neg}
Cell Number:	10^5		4/4	4/4
	$5x10^4$		2/2	2/2
	10^4		2/2	2/2
	$5x10^3$		2/2	2/2
	10^3	4/4	4/4	4/4
	500	2/2		
	100	4/4	2/2	0/2
	10	12/12	0/4	0/4
	1	7/14	0/4	0/6
SC frequency	Estimate	1:1.4	1:60	1:351
	upper - lower limits	1:0.7 - 1:5.7	1:15 - 1:238	1:105 - 1:1179
p-Value	Fit	0.88	0.12	0.17
	Difference		$3x10^{-7}$	$1x10^{-18}$

Table 6.3: **Limiting dilution transplantation of PKH-sorted cells.**
PKH26 subpopulations from WT (upper table) or tumour (lower table) mammospheres were injected into the cleared fat pads of syngeneic mice (number of injected cells as indicated). Results are shown as number of outgrowths or tumours per number of injections. SC frequencies (estimates and upper - lower limits) were calculated by limiting dilution analysis, as described in Material and Methods. Fitting to single hit model is indicated by p-values >0.05 (Fit). Differences in SC frequencies are calculated for each sample against the PKH high cell subset. Their significance is indicated by p-values <0.05 (Difference).

Altogether, these data show that in WT samples SCs undergo limited self-renewing divisions and can be isolated to near purity based on their replicative history. Contrarily, CSCs possess increased proliferative potential and undergo several rounds of self-renewing divisions *in vitro*.

6.1.2 Tumour SCs Divide Mainly Symmetrically

The increased self-renewing potential in CSCs cannot necessarily be correlated with the observed expansion in the number of CSCs in tumour mammospheres and tumour tissues compared to WT samples. In normal conditions SCs are maintained in a constant number by self-renewing divisions that result in the formation of one SC and one progenitor cell that will continue to proliferate and differentiate; in this scenario, several rounds of divisions result in the maintenance of the SC pool. However, it has been shown that, during development and injury, SCs can undergo a symmetric type of division that generates two identical daughter cells endowed with SC properties, thus expanding the SC pool (Noctor et al., 2004; Wright et al., 2001; Zhang et al., 2004; Lechler and Fuchs, 2005; Morrison et al., 1995)(Fig. 6.9)

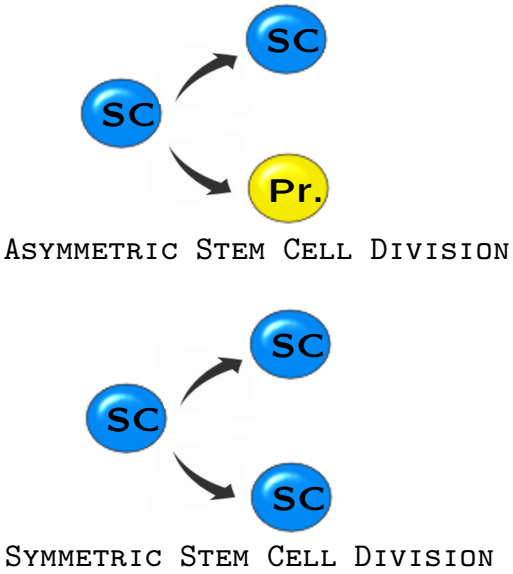

Figure 6.9: **Schematic representation of the two types of SC division.**
Asymmetric SC divisions result in the formation of two daughter cells of which one remains quiescent (SC) and one carries on proliferating (Progenitor). Symmetric SC divisions expand the SC pool by generating two functionally identical cells endowed with stem properties.

To investigate whether this process could explain the observed increase in the number of CSCs compared to WT samples, we performed live time-lapse imaging of the first SC divisions during mammosphere formation, with a protocol that has been already described for the hematopoietic system (Huang et al., 1999). Briefly, purified PKH^{high}populations from WT and tumour mammospheres were plated in metil-cellulose media, monitored every hour over a period of 4 days and images were collected at each timepoint. The reconstruction of the image sequence for each dividing cell allowed us to discriminate symmetrically

or asymmetrically dividing cells depending on the replicative fate of the two daughter cells. Cell divisions that yielded two daughter cells with the same replicative fate were defined symmetric; cell divisions that yielded two daughter cells of which one remained quiescent and the other carried on dividing were considered asymmetric.

Following this approach we were able to determine that 80% of SCs in WT samples adopts an asymmetric mode of division (n=103) and in much lower frequencies, a symmetric mode of division (7.8%). In tumour samples CSCs mainly divided symmetrically (80%, n=156), while only 10% of cells divided asymmetrically (Fig. 6.10).

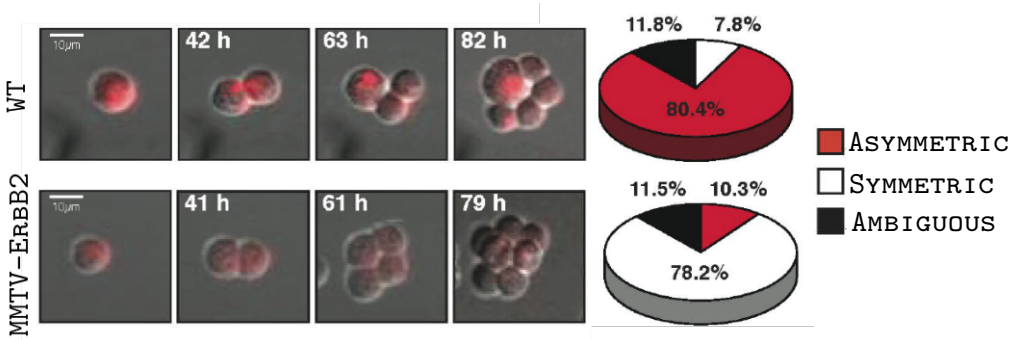

Figure 6.10: **Time-lapse imaging of the first cell divisions of a forming mammosphere.** Time-lapse microscopy images of the cell divisions during mammosphere formation. Elapsed time after seeding is shown at each division event. Pie charts show the frequencies of different types of divisions. Scale bars are reported.

To corroborate these observations from a molecular point of view, we decided to analyse the pattern of expression of the fate determinant Numb in dividing SCs by immunofluorescence staining. It's been shown that Numb is required for asymmetric cell divisions in Drosophila neuroblasts (Knoblich, 1997; Caussinus and Gonzalez, 2005) and its asymmetric distribution is critical for mouse cerebral cortical SC and neuroblast asymmetric divisions (Shen et al., 2002). Similarly, asymmetric segregation of Numb in cultured satellite muscle cells promotes myogenic differentiation of one of the daughter cells (Shinin et al., 2006; Conboy and Rando, 2002). The specificity of the anti-Numb antibody was verified by immunofluorescence staining for Numb in cells infected with puromycin-selectable control (pLKO) or Numb-RNAi (pLKO-Numb) vectors (Fig. 6.11).

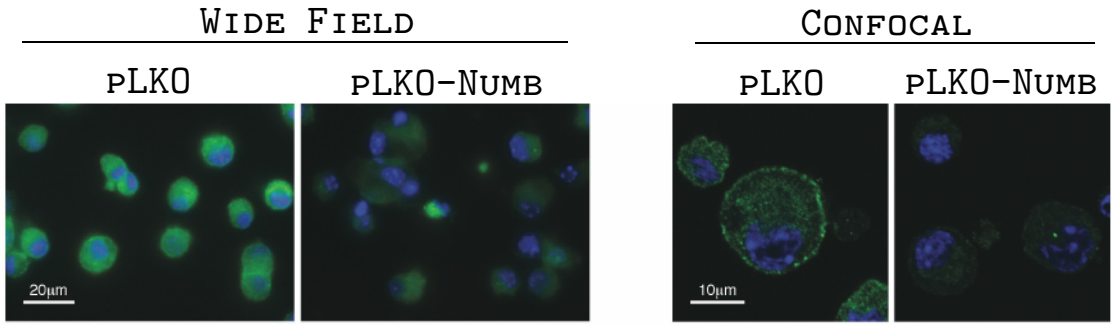

Figure 6.11: **Numb RNAi in WT cells.**
The specificity of the anti-Numb antibody (a monoclonal antibody, Ab21, generated against amino acids 537–551 of human Numb) was verified by staining RNA-interfered cells and control cells. Wide-field and confocal microscopy analysis of the infected cells showed punctuate staining of the anti-Numb antibody at both the cell membrane and the cytosol of all cells, consistently with previously reported localisation of Numb in mammalian cells at the cortical membrane and within intracellular vesicles (Dho et al., 2006; Nishimura et al., 2003; Santolini et al., 2000; Smith et al., 2004). In the short hairpin RNA-infected cells, the anti-Numb staining was markedly reduced in intensity and only detectable in the cytosol, confirming that the observed anti-Numb membrane staining reflects a specific localisation pattern of Numb in mammosphere cell suspensions.

To visualise the partitioning of Numb during the first division of normal and tumour SCs, we isolated the PKH^{high}population of cells from WT and tumour mammospheres and plated them for 36 hours in the presence of 25 µM Blebbistatin, a small molecule that blocks the cell division by arresting the furrow ingression, without interfering with mitosis (Straight et al., 2003). The cells were then fixed and stained by immunofluorescence for Numb and analysed in confocal microscopy.

The confocal analysis of the distribution of Numb in dividing SCs from WT and tumour mammospheres supported our previous observations from the time-lapse experiments, and showed an asymmetric localisation of Numb along the membrane of the majority of WT SCs, and a symmetric distribution on the membrane of dividing CSCs (Fig. 6.12).

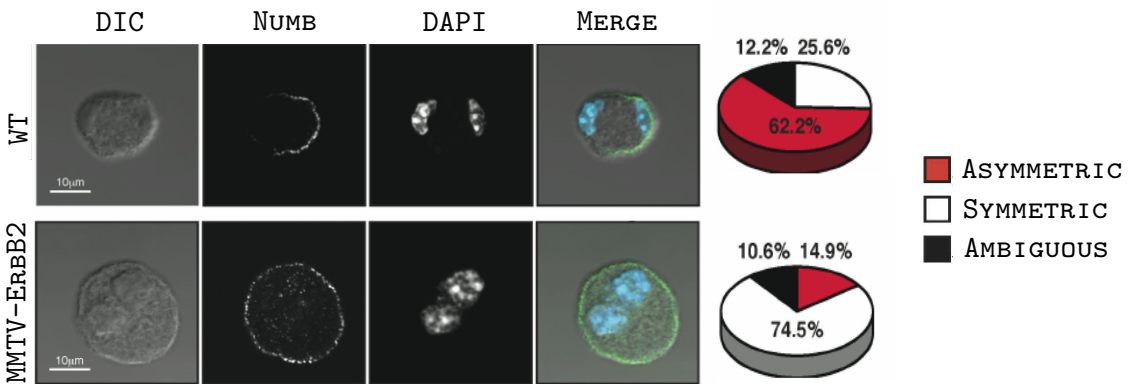

Figure 6.12: **Distribution of fate-determinant Numb in WT and tumour SCs.**
Confocal analysis of the distribution of Numb on the cell membrane of dividing SCs from WT or tumour samples. DIC, Numb and DAPI staining and merged channels (Merge) of a representative cell are shown for each sample. In ~60% (n=82) of WT PKH^{high} cells, the anti-Numb staining was weakly cytoplasmic and formed a clear crescent at the cell membrane, while in ~25% of the cases Numb was uniformly localised around the cell cortex. In the remaining cells, the distribution of Numb was ambiguous. Confocal immunofluorescence analysis of Numb localisation in blebbistatin-treated ErbB2 PKH^{high} cells revealed a uniform distribution of Numb around the cortex in the majority of the analysed cells (74.5%; n=47), with only 14.9% of cells showing polarised localisation.
Relative frequencies of asymmetric and symmetric divisions are shown in the pie charts. Ambiguous: Numb distribution not consistent among different confocal sections. Scale bar as reported.

Altogether these findings suggest that symmetric and asymmetric divisions coexist in both WT and tumour SCs, but with opposite relative proportions: WT SCs mainly divide asymmetrically, while tumour SCs divide symmetrically.

6.1.3 CSCs Possess Increased Self-renewing Properties

To investigate the replicative potential (measured as self-renewing ability and lifespan *in vitro*) of CSCs compared to WT SCs, we cultured these cells as mammospheres for several passages. As the behaviour of SCs in culture is reflected in their ability to form mammospheres, we set up a method to measure a growth curve that would take into account the fluctuation of both the number of cells and the number of spheres over passage. At each passage, 5000 cells were plated in quadruplicate in 24-well plates to form mammospheres, and after one week in culture, the number of formed spheres was counted. These spheres were then collected and disaggregated, and the number of cells was counted to estimate the mammosphere size. The data was then arranged into cumulative growth curves that show the variation in the number of mammospheres and cells during passages. As shown in Fig. 6.13, WT mammospheres progressively decrease in number and exhaust in culture after 6-7 passages and can not be further cultured, suggesting that WT SCs have limited lifespan and self-renewing potential. Interestingly, normal tissues can be serially transplanted only up to 6-7 times (Daniel et al., 1968), confirming our *in vitro* observations. On the contrary and in line with the observation that CSCs divide symmetrically, tumour mammospheres expanded in number over the passages, and showed a near immortal behaviour (up to 36 passages in selected experiments).

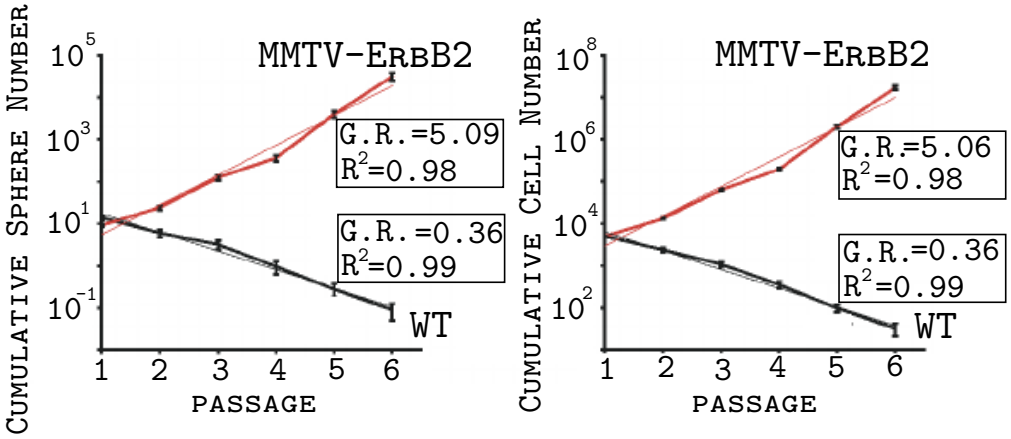

Figure 6.13: **Growth curves of WT and MMTV-ErbB2 mammospheres.** Semi-logarithmic plotting of Cumulative Sphere (left panel) and Cumulative Cell (right panel) Numbers were obtained from serial replating of WT (black lines) and tumour (red lines, MMTV-ErbB2) mammospheres. Regression analysis of the data set was performed to obtain trend lines (light lines) that best approximate the curves. The growth rates (GR) and the coefficients of determination (R^2) for each trend line are reported inside the graph.

Both in the case of WT and ErbB2-tumour mammospheres the cumulative mammosphere number approximated an exponential curve (R^2= 0.99 and 0.98 respectively, Fig. 6.13) indicating that the growth rate was constant at each passage. However, WT mammosphere growth curve showed a slope of ~0.3, indicating that SCs decrease by 70% at each passage, whereas the slope of the tumour exponential curve was ~5, indicating a constant expansion of the number of mammospheres of ~5-fold at every passage.

Together, these findings demonstrate that WT SCs rapidly lose self-renewal potential in culture, while tumour SCs are nearly immortal, and suggest that these different behaviours reflect intrinsic properties of WT and tumour SCs, which are not influenced by the time in culture. Furthermore, these data suggest that the two observed properties of tumour SCs, i.e. extended replicative-potential and increased frequency of symmetric self-renewing divisions, are at the basis of the ability of tumour SCs to grow indefinitely and to expand geometrically in culture.

6.2 Mechanisms That Regulate SC Self-renewal

6.2.1 p53 Regulates SC Divisions

One of the key tasks of the current research is to identify critical processes that are altered in CSCs and account for the acquired properties that could be used as targets for specific anticancer therapies against CSCs, that may escape conventional anticancer therapies.

In recent years it has become more and more clear that p53 is involved in the regulation of SC self-renewal, and this has been shown in neural stem cells (Armesilla-Diaz et al., 2009; Meletis et al.,

2006; Nagao et al., 2008)and in hematopoietic SCs (Herrera-Merchan et al., 2010; Zhao et al., 2010). Interestingly, the loss of p53 has been shown to induce the upregulation of CD44 and consequently the expansion of tumour initiating cells in luminal breast epithelial cells (Godar et al., 2008). Finally, p53 has been reported to impose an asymmetric cell fate in MEFs and in a mammary epithelial cell line (Rambhatla et al., 2001).

To understand the role of p53 in regulating mammary SC self-renewal, we took advantage of a knockout mouse model where the endogenous alleles for p53 have been deleted. The pre-malignant mammary tissue was collected from these mice and the mammary epithelial cells were purified and cultured as mammospheres for *in vitro* and *in vivo* analyses. Indeed, p53 KO mammospheres showed increased self-renewing potential and lifespan of SCs compared to control mammospheres (Fig 6.14), and prevalence of symmetric SC divisions (74.9% of symmetric divisions and 14.4% of asymmetric divisions, n=190) visualised both via time-lapse imaging (Fig. 6.15) and Numb distribution of dividing cells (Numb was weakly cytoplasmic and uniform around the cortex in 74.4% of the p53 KO PKH^{high} cells, with only 9.3% of cells showing a membrane crescent on the membrane, n=43) (Fig. 6.16).

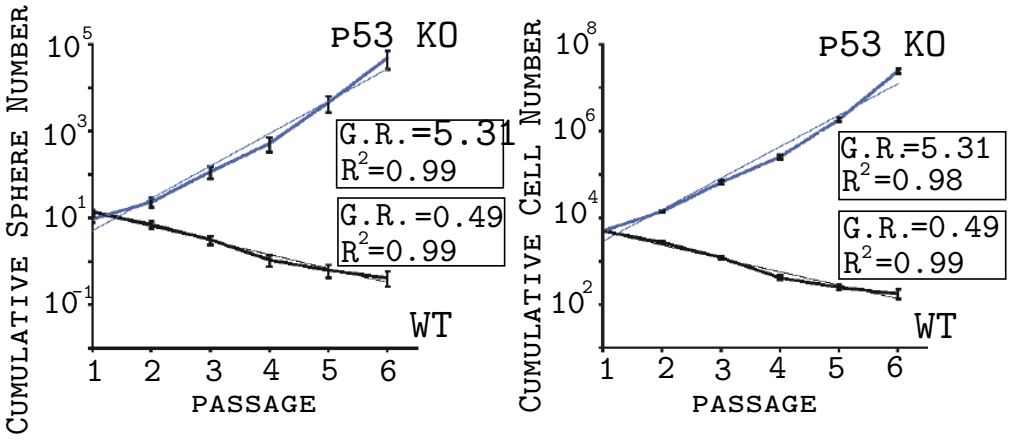

Figure 6.14: **Growth curve of control or p53 KO mammospheres.**
Semi-logarithmic plotting of Cumulative Sphere (left panel) and Cumulative Cell (right panel) Numbers were obtained from serial replating of WT (black lines) and p53 KO (blue lines) mammospheres. Regression analysis of the data set was performed to obtain trend lines (light lines) that best approximate the curves. The growth rates (GR) and the coefficients of determination (R^2) for each trend line are reported inside the graph.

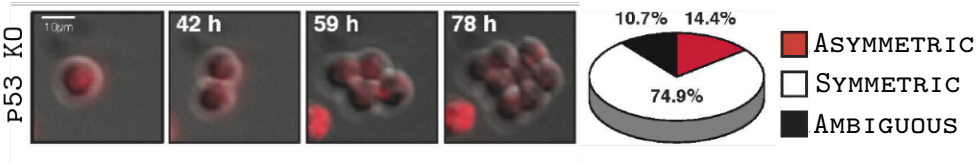

Figure 6.15: **Time-lapse imaging of a forming p53 KO mammosphere.**
Time-lapse microscopy images of the cell divisions during p53 KO mammosphere formation. PKH^{high} cells were purified from p53 KO mammospheres and visualised by time-lapse imaging as described. Elapsed time after seeding is shown at each division event. Pie charts show the frequencies of different types of divisions. Scale bars are reported.

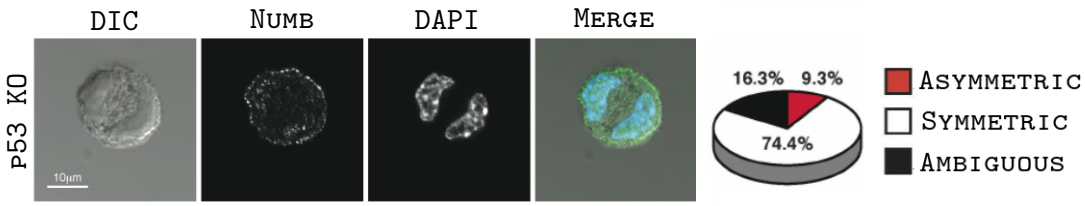

Figure 6.16: **Numb localisation in p53 KO dividing SCs.**
Confocal analysis of the distribution of Numb on the cell membrane of dividing SCs from WT or p53 KO samples. DIC, Numb and DAPI staining and merged channels (Merge) of a representative cell are shown. Relative frequencies of asymmetric and symmetric divisions are shown in the pie charts. Ambiguous: Numb distribution not consistent among different confocal sections. Scale bar as reported.

These data suggest that like tumour SCs, p53 KO mammary SCs are near immortal and can be unlimitedly propagated, their growth curve showing similar growth rates to the ones that we had observed in tumour mammospheres (Fig. 6.13). Furthermore, they undergo increased numbers of self-renewing divisions, mainly of symmetric type, during mammosphere expansion, suggesting that p53 regulates polarity of SC division in mammary SCs.

To investigate whether the increased self-renewal potential of p53 KO SCs is due to other secondary genetic abnormalities that might accumulate in the absence of p53, we silenced its expression in WT cells by infecting them with a lentiviral vector expressing a short hairpin RNA against p53 (pSICO-p53sh). Indeed, the downregulation of p53 levels induced the expansion of the mammosphere culture, and increased self-renewing potential in the interfered SCs (Fig. 6.17).

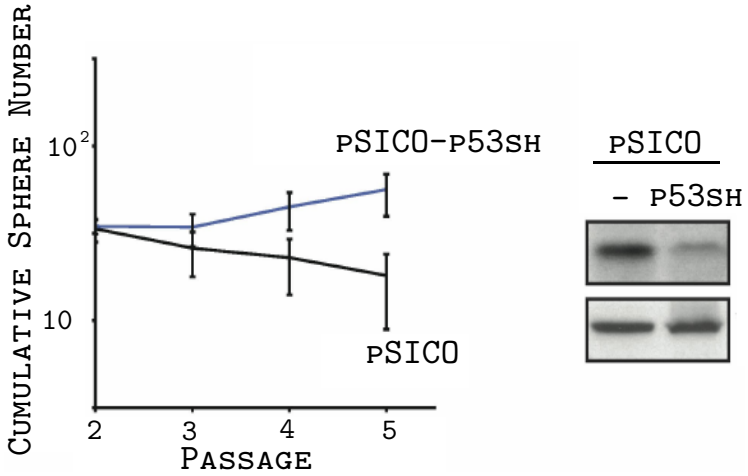

Figure 6.17: **RNAi silencing of p53 in WT SCs.**
WT mammospheres were infected with lentiviral vectors expressing short hairpin RNAs directed against p53 (pSico-p53sh), or with the control empty-vector (pSICO), and cultured in non-adherent conditions for 6 days. 5,000 cells from secondary mammospheres were re-plated in quadruplicate in a serial replating experiment (left graph; mean ± SD), and analysed by Western Blotting for the expression of p53 (right panel). Western blots were normalised against the levels of vinculin expression.

This confirmed that the increase in self-renewal of p53 KO SCs is the direct consequence of the loss of p53.

In vivo analysis of the behaviour of SCs in the absence of p53 confirmed that their increased self-renewal and their ability to divide symmetrically results in the expansion of the SC pool *in vitro*. Indeed, limiting dilution transplantation of cell suspensions deriving from the dissociation of WT and p53 KO mammospheres revealed that, as for tumour mammospheres, the number of SCs in p53 KO mammospheres was approximately three-fold higher (1:118 cells; 0.85%) than in control mammospheres (Table 6.4). The average size of p53 KO mammospheres was ~600 cells (595±17; n=12), thus predicting a frequency of ~5 SCs per mammosphere, as that of tumour mammospheres.

CELL INJECTION

		WT	p53-/-
Cell Number:	10^5	7/7	2/2
	10^4	11/11	2/2
	10^3	6/6	2/2
	500	6/8	6/6
	100	5/7	6/10
	50	1/8	5/10
	25	0/6	0/8
	10	0/6	0/12
	1		0/6
SC frequency	Estimate	1:322	1:118
	upper - lower limits	1:191 – 1:542	1:69 – 1:205
p-Value	Fit	0.58	0.12
	Difference	0.01	

Table 6.4: **Limiting dilution transplantation of cells from WT or p53 KO mammospheres.**
Cell suspensions from WT or p53 KO secondary mammospheres were inoculated in recipient mice in limiting dilution conditions (from 10,000 to 1 cell). Results show positive outgrowths as normal mammary epithelium that arose 8-10 weeks after injection. SC frequencies (Estimates and upper/lower limits) were calculated by limiting dilution analysis, as described in Material and Methods. Fitting to single hit model is indicated by p-values $> 0{,}05$ (Fit). The significance of the difference in SC frequencies is indicated by p-values $< 0{,}05$ (Difference).

Altogether, these data demonstrate that p53 regulates self-renewal of mammary SCs and that loss of p53 favours the continuous expansion of mammary SCs through subsequent rounds of symmetric divisions.

6.2.2 Impaired Function of p53 in CSCs

To determine whether p53 is responsible for the behaviour of CSCs in our tumour model, we evaluated the mutational status of p53 in 10 samples of MMTV-ErbB2 derived tumours by exon sequencing and could not find any mutation. Nevertheless, the analysis of the p53-mediated response to DNA damage (induced by treatment with UV or Adriamycin) revealed that, compared to WT mammospheres, tumour mammospheres show a lesser extent of p53 activation in response to stress. The levels of p53 were low or undetectable in untreated WT or ErbB2 cells, and accumulated between 4 and 8 hours after treatment, when its phosphorylation was also evident. The extent of adriamycin- or UV-induced p53 stabilisation and phosphorylation was, however, significantly reduced in the tumour samples compared to controls (Fig. 6.18).

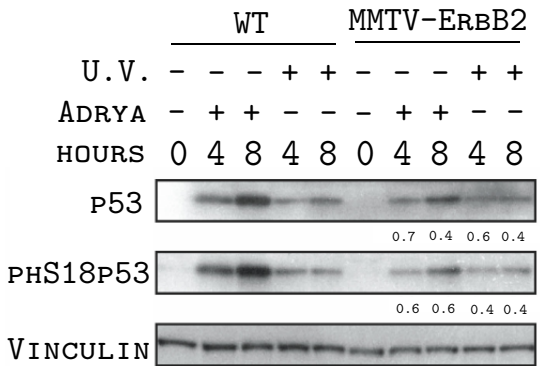

Figure 6.18: **p53-mediated response to DNA damage in WT and tumour mammospheres.** Cells from primary mammospheres were treated with adriamycin (2 μg/ml) or UV rays (50 J/m^2) 2 days after re-plating and collected at the indicated time points. Levels of p53 and extent of p53 serine-18 phosphorylation were analysed by Western Blot using specific antibodies (p53 and phS18p53 respectively). Values below the blots refer to the densitometric analysis of the anti-p53 and anti-phS18p53 signals normalised against the corresponding anti-vinculin values and expressed (at each time-point) as tumour/WT ratio.

This observation is consistent with published data that show that p53 can be attenuated in tumours due to the deregulation of other genes that control its activation (Miller et al., 2005).

To verify that indeed p53 is responsible for the increased self-renewing abilities of CSCs, we increased the levels of p53 expression in tumour mammosphere by infecting them with a lentiviral vector for the over-expression of p53 (pWPI-p53) or with an empty vector (pWPI). Analysis of the growth curve revealed that indeed the overexpression of p53 had a moderate, yet significant, effect in decreasing the replicative potential of CSCs (Fig. 6.19).

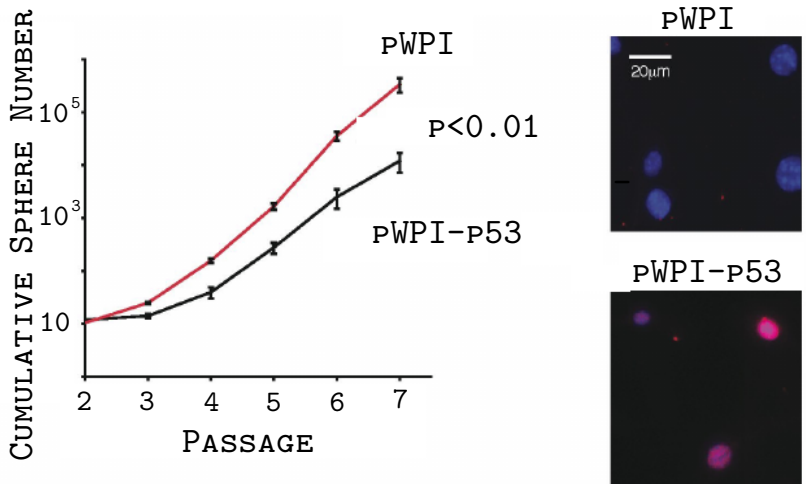

Figure 6.19: **p53 overexpression in tumour mammospheres.**
Serial re-plating of tumour mammospheres after p53 over-expression. The graph shows the serial replating of mammospheres infected with pWPI (red line) or pWPI-p53 (black line). Individual panels on the right show immuno-fluorescence analysis of p53 levels in mammospheres infected with pWPI or pWPI-p53; nuclei are counterstained with DAPI. Significance of differences between pWPI and pWPI-p53 infected cells at passage 7 was assessed using the T-test. Scale bars as reported.

The partial effect of p53 restoration on the growth curve of tumour mammospheres may be due to presence in these cells of other mechanisms that actively inhibit its function. It has been shown, in fact, that the expression of ErbB2 in mammary epithelial cells induces a the downregulation of p53 by acting on the localisation of MDM2, a ubiquitine E3-ligase that targets p53 for degradation(Zheng et al., 2004). To circumvent this, we decided to increase the levels of p53 in tumour mammospheres by inhibiting the activity of MDM2 with Nutlin-3, a small molecule that binds to MDM2 and impairs its function in degrading p53(Vassilev et al., 2004). To this end, we collected, disaggregated and replated tumour and WT primary mammospheres to form secondary mammospheres in the presence of increasing concentrations of Nutlin-3. Indeed, we could observe by Western Blot that upon treatment with Nutlin-3 the levels of p53 in secondary mammospheres were increased in WT and tumour samples, with slightly higher levels and a more evident dose-dependent response in the tumour mammospheres (Fig. 6.20)

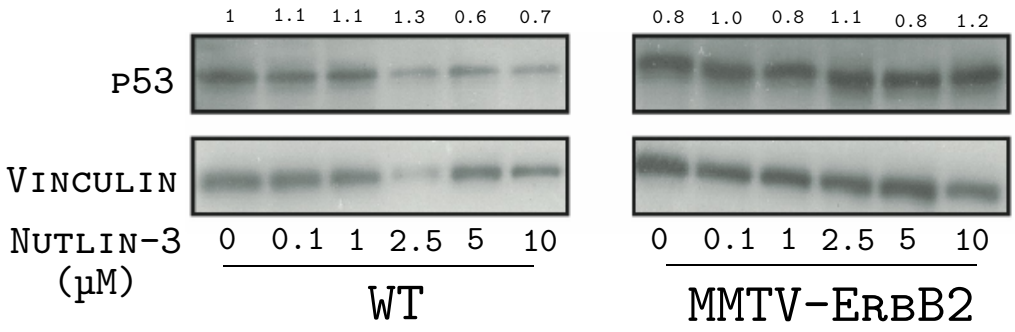

Figure 6.20: **WB analysis of p53 expression following Nutlin-3 treatment.** Western Blot analysis of p53 expression in WT or tumour secondary mammospheres after treatment with Nutlin3. Values above the blots were obtained by densitometric analysis of the anti-p53 signal normalised against the corresponding anti-vinculin values and expressed as arbitrary units relative to the signal (=1) of WT untreated samples.

To study the effect of Nutlin-3 on WT and tumour SCs self-renewal we measured the number of SCs in WT and tumour mammospheres at each passage after treatment. Interestingly, while Nutlin-3 had no effect on the number of secondary WT mammospheres, and only marginally decreased the number of ErbB2-tumour mammospheres, disaggregation and replating of secondary mammospheres generated tertiary mammospheres with decreasing efficiency in tumour samples (up to ~7 and ~14-folds with the maximal drug doses of 5 and 10 μM, respectively), but still did not affect the growth WT mammospheres. Notably, the absolute numbers of tertiary tumour mammospheres were comparable, at the highest concentrations of Nutlin3 (2.5, 5, and 10 μM), to those of untreated WT tertiary mammospheres(Fig. 6.21).

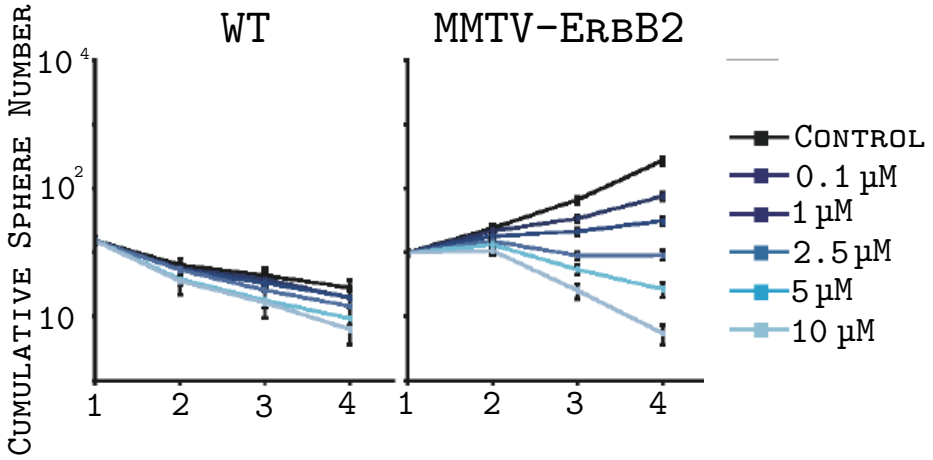

Figure 6.21: **Serial replating of WT and tumour mammospheres after Nutlin-3 treatment.** Cumulative Sphere Number (± SD, three independent experiments). Growth curves were obtained by serial re-plating of WT and tumour (ErbB2) mammospheres treated with increasing concentrations of Nutlin3 (as indicated) or DMSO (control).

Together, these results demonstrate that Nutlin-3 induces p53 stabilisation in both WT and tumour mammospheres, but that it reduces the frequency of self-renewing divisions only in the latter. This is consistent with the observation that p53 directs asymmetric divisions in mammary SCs, and suggests that Nutlin-3 reduces the frequency of self-renewing divisions selectively in tumour SCs by switching their mode of division from symmetric to asymmetric. To provide a direct demonstration of this, we performed time-lapse imaging of tumour PKH^{high}cells in the presence of Nutlin-3. Results show that the majority of CSCs, after treatment with Nutlin-3, divided asymmetrically (75.9%, n=54). Of the remaining cells, 18.5% divided symmetrically, a proportion that is comparable to that observed in WT samples (Fig. 6.22).

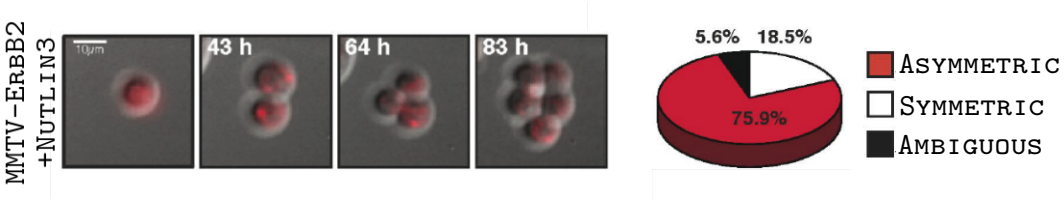

Figure 6.22: **Time-Lapse analysis of Nutlin-3 treated CSCs.**
Time-lapse microscopy images of the first divisions of a tumour PKH^{high} cell treated with 2.5 µM Nutlin-3. Elapsed time (from seeding) is reported inside each panel. Relative frequencies of asymmetric and symmetric divisions are shown in the pie charts. Ambiguous: divisions that could not be interpreted as symmetric or asymmetric. Scale bars as reported.

To exclude that Nutlin-3 acts through a p53-independent mechanism, we treated p53 KO SCs and evaluated the effect of the treatment on their growth curve. Indeed we confirmed that Nutlin-3 had no off-target effect as we could not appreciate any effect on the sphere-forming efficiency of p3 KO SCs (Fig. 6.23).

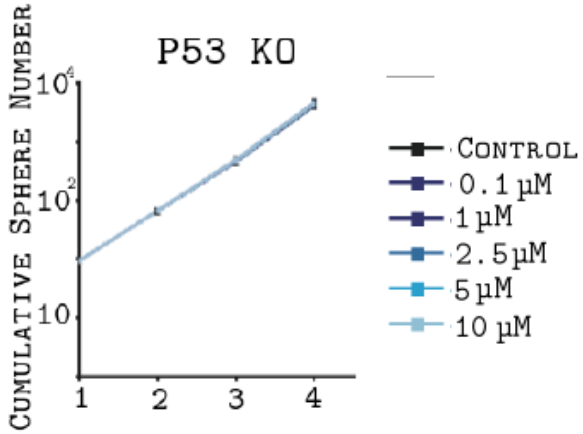

Figure 6.23: **Effect of Nutlin-3 on p53 KO mammospheres.**
Cumulative Sphere Number (± SD, three independent experiments) obtained by serial re-plating of p53 KO mammospheres treated with increasing concentrations of Nutlin3 (as indicated) or DMSO (control).

To evaluate the biological significance of the effect of Nutlin-3 treatment on tumour SCs, we analysed their ability to form tumours *in vivo* after transplantation. Secondary tumour mammospheres treated with DMSO (control) or 2.5 μM and 10 μM Nutlin-3 were injected into recipient mice. Strikingly, after 8 weeks, CSCs that had been subjected to the treatment had formed tumours with a reduced volume of about eight-fold compared to the untreated tumour mammospheres (Fig.6.24); however, histological analysis of tumour sections revealed no difference in their proliferation (by Ki67 staining) or in the tissue histology (Fig. 6.25).

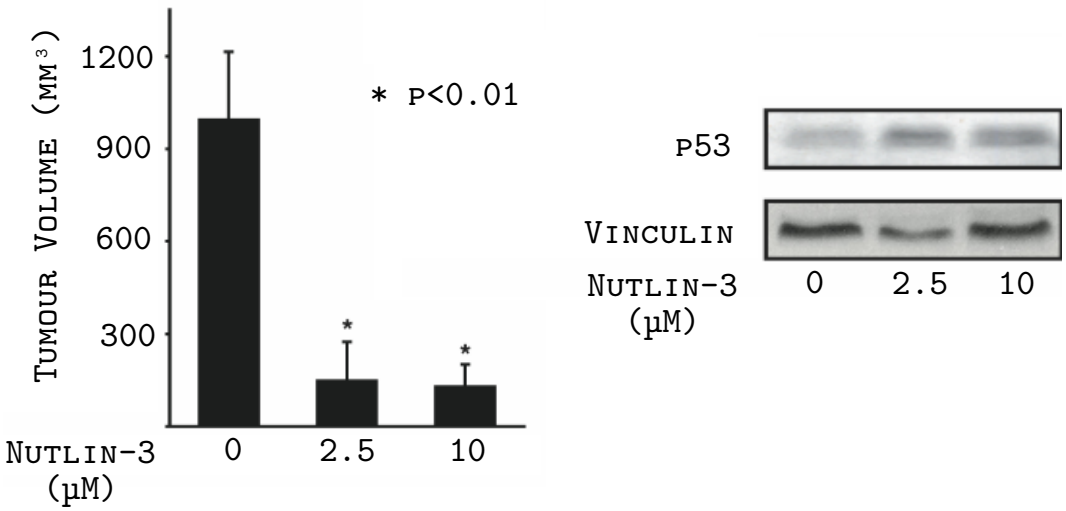

Figure 6.24: **Injection of DMSO and Nutlin-3 treated mammospheres into recipient mice.** Primary tumour mammospheres were disaggregated and plated in the presence of Nutlin-3 at the indicated concentrations. After 48 hours, the forming mammospheres were analysed for the re-expression of p53 by WB (right panel) and injected (10,000 live cells) into the mammary glands of syngeneic mice (8 injections per each concentration). After 2 months, the mice were sacrificed and inspected for tumour growth. All injections gave rise to tumours. The graph (left panel) shows the measurements of tumour volumes (mean ± SD).

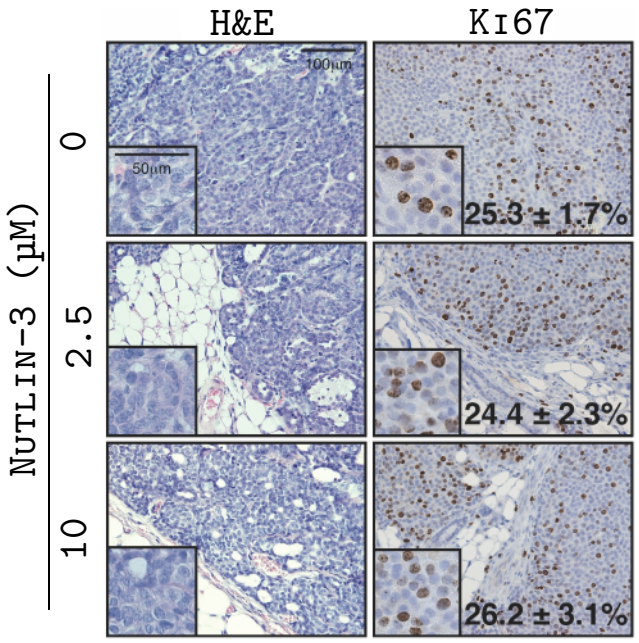

Figure 6.25: **Analysis of histology and proliferation in tumours deriving from the injection of Nutlin-3 treated mammospheres.**
Representative images of haematoxylin-eosin and anti- Ki67 stained sections from paraffin-embedded tumours that arose from the injection of control or Nutlin-3-treated tumour mammospheres. Percentage (± SD) of Ki67 positive cells is reported inside each panel (a minimum of 1,000 cells counted). Scale bars as reported.

We then investigated the effect of Nutlin-3 on spontaneous tumours *in vivo*. Two month-old MMTV-ErbB2 mice were treated with DMSO or Nutlin-3 for two weeks (one i.p. injection every two days). At the end of the treatment, a fraction of the animals was sacrificed to evaluate the effect of the treatment on CSCs. To this end, tumour tissues were collected, cells were purified as described and injected in limiting dilution into recipient mice. The remaining animals were kept under observation for further two months to evaluate the tumour growth *in vivo*. Indeed, treatment with Nutlin-3 resulted in the formation of tumours with reduced volumes compared to control-treated mice (Fig. 6.26).

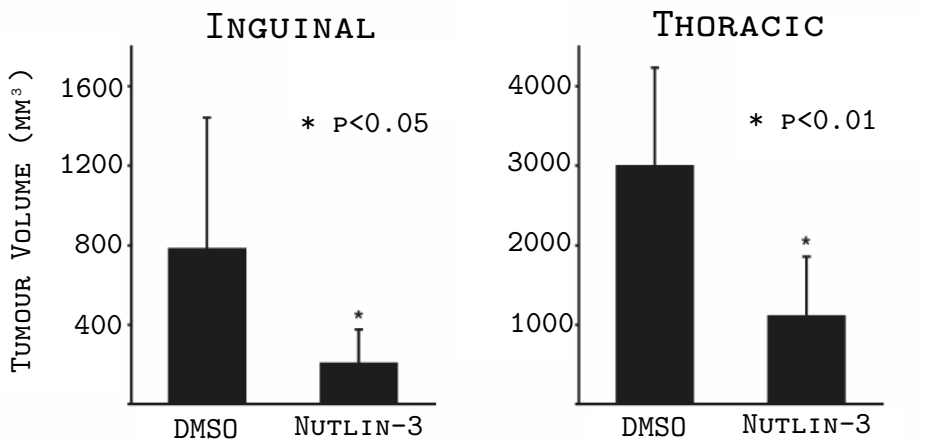

Figure 6.26: **Effect of Nutlin-3 treatment on spontaneous ErbB2-driven mammary tumours.** Two-month old WT or ErbB2 transgenic mice were treated i.p. with DMSO or 20 mg/kg or Nutlin-3 every 2 days for 2 weeks. Four mice per treatment group were sacrificed two months later for inspection of tumour growth. Tumour volume (mean (± SD) for inguinal (left) and thoracic (right) mammary tumours is shown in the graphs. All tested mice developed tumours. Measurement of the volume of thoracic and inguinal mammary tumours showed a ~3 and ~4 fold decrease respectively in Nutlin-treated animals compared to controls. P-values as indicated.

As assessed by limiting dilution transplantation of the tissues collected after the 2-week treatment, Nutlin-3 reduced the content in CSCs in spontaneous tumours (Table 6.5).

CELL INJECTION

		WT		ErbB2	
		DMSO	Nutlin3	DMSO	Nutlin3
Cell Number:	10^5	2/2	2/2	2/2	1/2
	$5x10^4$	3/4	3/4	4/4	
	10^4	1/6	2/8	8/8	3/6
	$5x10^3$	0/4	0/4	2/6	0/6
	10^3	0/2	0/2	1/4	0/8
	100	0/2	0/2	0/2	0/2
SC frequency	Estimate	1:41,841	1:37,172	1:5,038	1:54,563
	upper - lower limits	1:17996 - 1:97156	1:16745 - 1:82521	1:2647 - 1:9588	1:17448 - 1:170635
p-Value	Fit	0..31	0.51	0.41	0.36
	Difference		0.84		$3x10^{-5}$

Table 6.5: **Limiting dilution transplantation of Nutlin-3 treated mammary tumours.** Primary mammary cells from control or Nutlin-3-treated mice were injected into the cleared fat pads (WT samples) or the mammary gland (tumour samples; ErbB2) of syngeneic mice (number of injected cells as indicated). Results are shown as number of outgrowths or tumours per number of injections. SC frequencies (estimates and upper - lower limits) were calculated by limiting dilution analysis, as described in Material and Methods. Fitting to single hit model is indicated by p- values>0.05 (Fit). Differences in SC frequencies are calculated for each sample against the DMSO-treated samples. Their significance is indicated by p-values <0.05 (Difference). As expected, SCs frequency in the DMSO-treated ErbB2-tumours was 9-10 fold higher than in the WT mammary gland. Nutlin3 treatment, however, markedly reduced the frequency of SCs in the ErbB2-tumours, to an extent that was comparable to that of the WT tissue.

Interestingly, analysis of tumour sections from DMSO and Nutlin-3 treated MMTV-ErbB2 mice revealed no difference in the frequency of proliferating or apoptotic cells in the Nutlin-3 treated tumours compared to controls, suggesting that the effect of Nutlin-3 on spontaneous tumours is solely due to the effect that the restoration of the levels of p53 has on CSC division (Fig. 6.27).

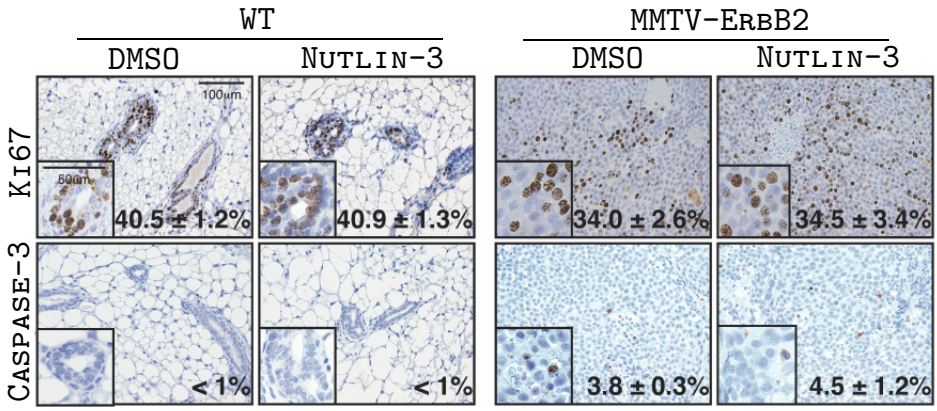

Figure 6.27: **Effect of Nutlin-3 treatment on proliferation and apoptosis in tumour tissues.** Two-month old WT or ErbB2 transgenic mice were treated i.p. with DMSO or 20 mg/kg of Nutlin3 every 2 days for 2 weeks. Three mice per treatment group were sacrificed immediately after the treatment to evaluate apoptosis (by anti-activated caspase3 staining) and proliferation (by anti-Ki67 staining) on paraffin embedded mammary tissue sections. Percentage (± SD) of positive cells is reported inside the panels (at least 1,000 cells counted). Scale bars as reported.

Together, these data demonstrate that two weeks of Nutlin-3 treatment reduced the frequency of CSCs and delayed tumour growth, in the absence, however, of significant anti-proliferative effects on cancer cells. These observations suggest that the increased self-renewal of tumour SCs contributes to tumour growth *in vivo*, and that Nutlin-3 is able to reduce tumour development by inhibiting symmetric divisions in CSCs.

6.2.3 Myc is the Effector of p53 in Regulating Stem Cell Division

The role of p53 in regulating SC self-renewal has been described in several systems and we have provided further data that confirm this function also in mammary epithelial cells. Nevertheless, p53 is involved in a plethora of pathways involving responses to stress (DNA damage or oncogene activation). Therefore, the role of p53 in the regulation of SC divisions requires further analyses to understand the mechanisms with which this function is carried out.

It has been shown that Myc regulates self-renewal in different systems: in Drosophila the cell fate determinant Brat, that is asymmetrically segregated in neuroblast division, downregulates Myc thereby inhibiting self-renewal (Betschinger et al., 2006). In human neural stem or progenitor cells, Myc has been shown to act through Miz-1 in regulating self-renewal (Kerosuo et al., 2008) and to cooperate with the p53-p19 pathway (Nagao et al., 2008) and with Pten (Zheng et al., 2008) in controlling self-renewal and differentiation in these cells.

Furthermore, there are several evidences showing that Myc is transcriptionally repressed by p53 in an *in vitro* system (Ragimov et al., 1993)and in human and mouse cell lines (Ho et al., 2005). More recently, a putative mechanism for this regulation has been described, involving the expression of the miR-145 micro RNA (miRNAs) (Sachdeva et al., 2009), that is able to posttranscriptionally regulate Myc expression.

These observations led us to hypothesise that Myc could act downstream to p53 as a general regulator of self-renewing signals also in our models. To test this hypothesis we evaluated the expression of Myc in p53 KO mammospheres and MMTV-ErbB2 derived tumour mammospheres. To this end we cultured p53 KO and tumour cells and collected secondary mammospheres for protein or total mRNA extraction. Because with our antibody endogenous levels of Myc were undetectable in WT samples, we immunoprecipitated the protein and evaluated its expression by WB. Analysis of Myc at the protein level revealed a marked upregulation in p53 KO and tumour mammospheres compared to the WT control (Fig. 6.28). This data was confirmed by the analysis of Myc mRNA expression by qPCR (Fig. 6.29).

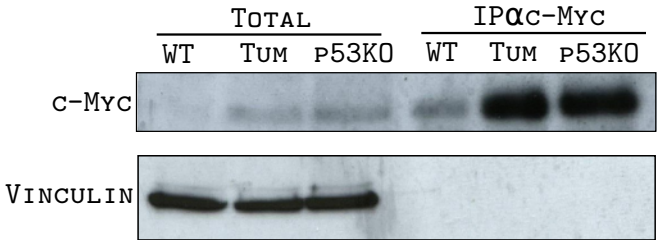

Figure 6.28: **Immuno Precipitation analysis of Myc expression in p53 KO and tumour mammospheres.**
Cell lysates from 4 million WT, p53 KO or tumour cells were incubated with a mouse monoclonal anti-Myc antibody and protein A beads. Immunoprecipitated material was loaded onto a SDS-PAGE gel and blotted onto a nitrocellulose membrane. Loading control was performed by visualising vinculin expression in total lysate controls.

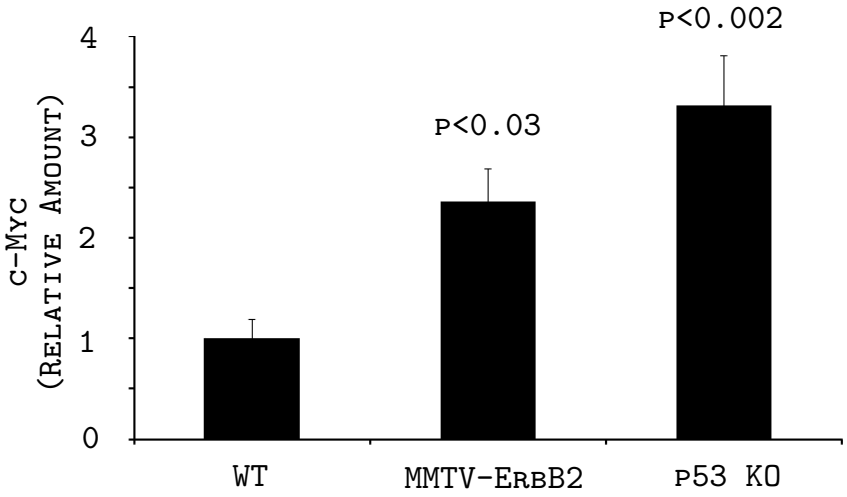

Figure 6.29: **Myc expression in WT, p53 KO and tumour mammospheres.**
Myc expression in WT, p53 KO and tumour mammospheres was evaluated by Q-PCR analysis of Myc mRNA in secondary mammospheres (means ± SD of three biological replicates). Values are expressed as arbitrary units relative to WT samples (assigned equal to 1). Myc expression was normalised against the rRNA 18S subunit. Significance of differences between indicated samples was assessed using the T-test.

Analysis of Myc expression in p53 KO and tumour mammospheres revealed increased expression levels compared to WT controls, suggesting a role for Myc in the regulation of self-renewal in p53 KO and tumour SCs, as we had hypothesised. To confirm this idea, we used two different approaches to decrease the levels of Myc expression in p53 KO and tumour mammospheres. First, we tried silencing Myc expression in p53 KO and tumour mammospheres by infecting the cells with a lentiviral vector for specific Myc RNA interference (pLKO-c-Myc-shRNA) or a control vector (pLKO). However, probably due to the fact that Myc is essential for cell survival (Davis et al., 1993), the silencing resulted in the arrest in cell growth and infected cells could not be passaged further (Fig 6.30).

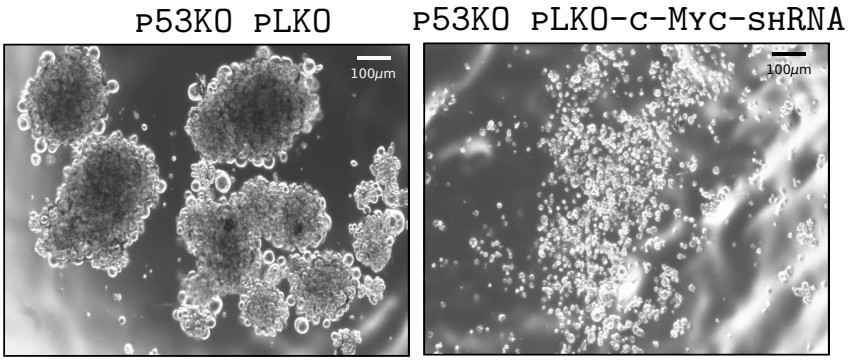

Figure 6.30: **Myc RNAi in p53 KO mammospheres.**
Representative images of tertiary p53 KO mammospheres infected with an empty vector (pLKO) or a vector carrying short hairpin RNA against Myc (pLKO-c-Myc-shRNA). Interference of Myc in secondary mammospheres resulted in cell growth arrest and prevented the formation of tertiary mammospheres. Scale bars as represented.

As an alternative approach, we expressed in p53 KO mammospheres a mutant form of Myc (Omomyc), that acts as a dominant negative protein that is able to bind and sequester the endogenous Myc, thus preventing its activity as transcription factor(Soucek et al., 1998). Once again, the inhibition of Myc function with the Omomyc mutant turned out to be incompatible with cell growth and we could not observe the formation of mammospheres (Fig. 6.31).

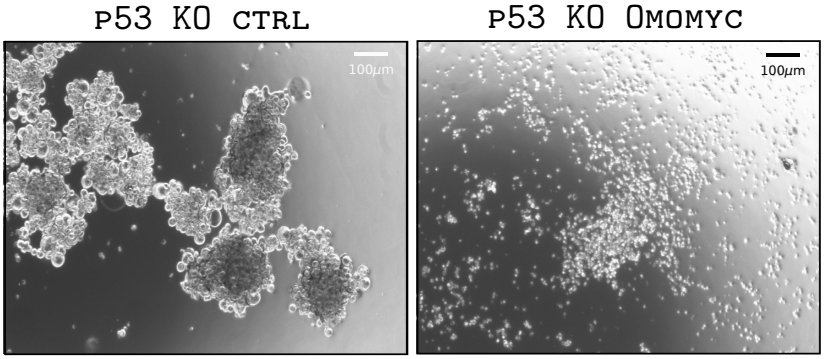

Figure 6.31: **Omomyc expression in p53 KO mammospheres.**
Representative images of tertiary p53 KO mammospheres infected with an empty vector (Ctrl) or a vector carrying the dominant negative Myc (Omomyc). Expression of Omomyc in secondary mammospheres resulted in cell growth arrest and prevented the formation of tertiary mammospheres. Scale bars as represented.

In light of these observations, we decided to adopt an indirect approach to verify that Myc is responsible for the increased self-renewing properties of CSCs and that it acts in the same pathway as p53. We have shown that p53 imposes an asymmetric mode of division onto SCs and that if absent or impaired, SCs divide symmetrically thus expanding in number. Interestingly, we have noted that in those systems where SCs divide prevalently symmetrically, Myc is expressed at higher levels. Taken together, these observations lead to the postulation of a model where the absence of p53 results in symmetric SC division through the (direct) regulation of Myc expression. Given that the restoration of the levels of p53 expression in tumours leads to a switch in the SC mode of division from symmetric to asymmetric, we expect that this effect is carried out through downregulation of Myc. To uncouple the p53 and Myc pathways, we enforced the expression of Myc in tumour mammospheres by infecting them with a lentiviral construct carrying the sequence for human Myc fused with a modified estrogen receptor (MycER), conditionally tunable by treatment with 4-HydroxiTamoxifen (4-OHT) (Littlewood et al., 1995). In this scenario, and according to our model, modulation of p53 expression would not have any effect on an exogenously regulated Myc. We then restored the levels of p53 in MycER-expressing tumour mammospheres by treating them with Nutlin-3 as previously described. If, as hypothesised, Myc is negatively regulated by p53 to control self-renewing divisions in SCs, the restoration of p53 levels in tumour mammospheres that would determine a switch in self-renewing divisions from a symmetric to an asymmetric mode, would not have any effect in the context of exogenously expressed MycER (see schematic representation in Figg. 7.3, 7.4 and 7.5 of the Discussion section).

Indeed, expression of MycER in Nutlin-treated tumour mammospheres rendered the treatment ineffective, and disaggregation and replating of treated secondary mammospheres resulted in the formation of tertiary spheres with a high frequency as compared to control tumour cells treated with Nutlin-3. Thus, in the context of enforced expression of Myc, the restoration of p53 levels in tumour mammospheres is not sufficient to decrease CSCs self-renewing properties, suggesting that indeed Myc acts downstream to p53 in this pathway (Fig. 6.32).

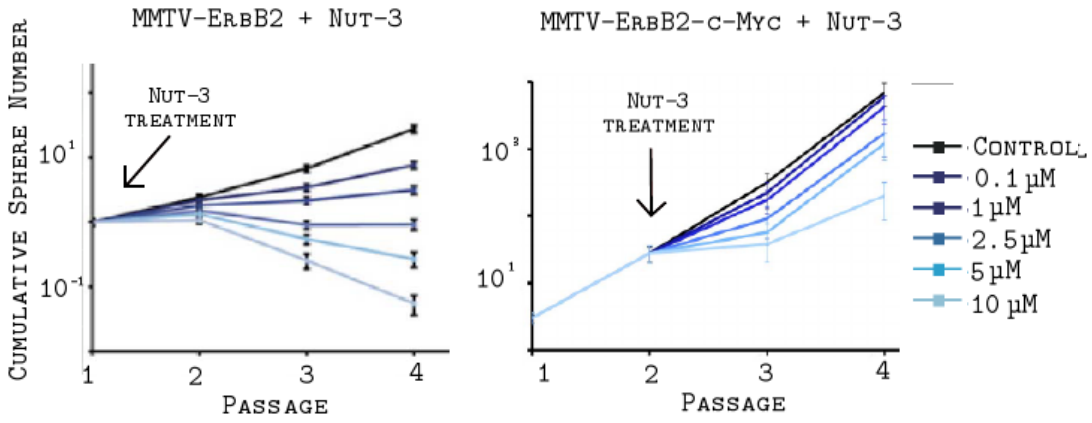

Figure 6.32: **Serial replating of control or MycER-expressing tumour mammospheres after Nutlin-3 treatment.**
Cumulative Sphere Number (± SD, one representative experiment of three independent experiments that have given similar results). Growth curves were obtained by serial re-plating of control tumour mammospheres (MMTV-ErbB2) or tumour mammospheres expressing MycER (MMTV-ErbB2-c-Myc) treated with increasing concentrations of Nutlin3 (as indicated) or DMSO (control). Arrows indicate moment of Nutlin-3 treatment.

6.3 Enforced Expression of Myc in Mammary Stem Cells

We have shown that CSCs mainly divide symmetrically, and that this is due to an impaired function of p53, as demonstrated by the fact that restoration of its levels in CSCs induces a switch in the mode of SC division from symmetric to asymmetric. Furthermore we have shown that the absence of p53 results in an upregulation of Myc, a known regulator of self-renewal in several systems. We show evidences that Myc acts downstream to p53 in this pathway and in particular, that it is negatively regulated by p53, as the restoration of p53 levels in CSCs that exogenously expressed a MycER protein did not result in a switch in the mode of SC division from symmetric to asymmetric.

We wondered whether Myc alone could be responsible for an increase in the self-renewing abilities of SCs or if in our tumour and p53 KO systems it cooperates with other factors to achieve this effect. To address this point we expressed Myc in WT SCs to verify how its upregulation would modulate their self-renewing properties.

6.3.1 High Levels of Myc Expression Induce a p53-Dependent Checkpoint

To express Myc in WT SCs, we infected primary WT mammospheres with a lentiviral vector expressing MycER, sorted infected cells by GFP reporter gene expression, and cultured the cells as mammospheres in the presence of 500 nM 4-OHT. As already described, at each passage we plated 5,000 control or MycER-infected cells in 24-well low adhesion plates, monitored the formation of mammospheres and measured their growth curve. Interestingly, the induction of MycER prevented the formation of secondary mammospheres; the few cells surviving the treatment could not be passaged further (Fig. 6.33).

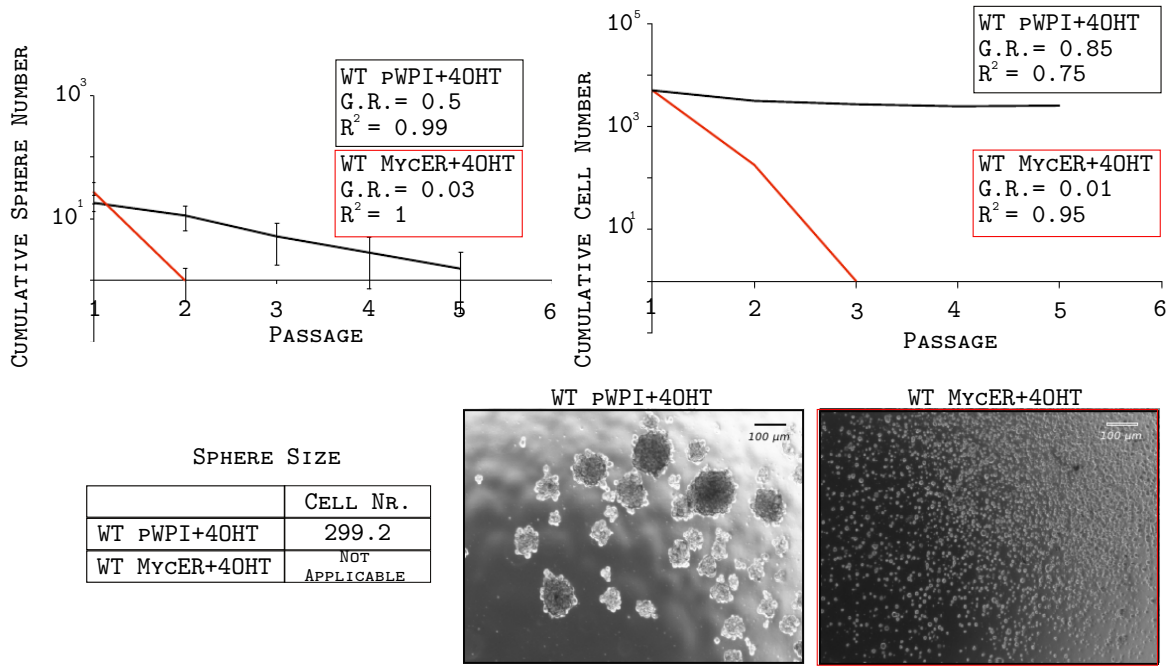

Sphere Size

	Cell Nr.
WT pWPI+4OHT	299.2
WT MycER+4OHT	Not Applicable

Figure 6.33: **Behaviour of mock and MycER infected cells after 4-OHT treatment.**
Upper panel: Semi-logarithmic plotting of Cumulative Sphere (left panel) and Cumulative Cell (right panel) Numbers were obtained from serial replating of WT mock-infected (black lines, WT pWPI) and MycER-infected (red lines, WT MycER) mammospheres after 4-OHT treatment. Regression analysis of the data set was performed to obtain trend lines (light lines) that best approximate the curves. The growth rates (GR) and the coefficients of determination (R^2) for each trend line are reported inside the graph.
Table: average mammosphere size between the different passages. We have demonstrated that mammosphere size remains constant at every passage (Cicalese et al., 2009). Mock-infected and Tamoxifen-treated mammospheres were composed of approximately 300 cells, as previously reported (Section 6.1). MycER-expressing cells did not form mammospheres upon 4-OHT treatment.
Lower panel: representative images of mock-infected secondary mammospheres or MycER-infected cells after 6 days of exposure to 4-OHT. Scale bars as represented.

To exclude any off-target for the treatment with 4-OHT, we cultured mock-infected cells in the absence or in the presence of 500 nM 4-OHT. We could not notice any significant alteration of the growth curve or the mammosphere size of the treated cells compared to the untreated sample (Fig. 6.34).

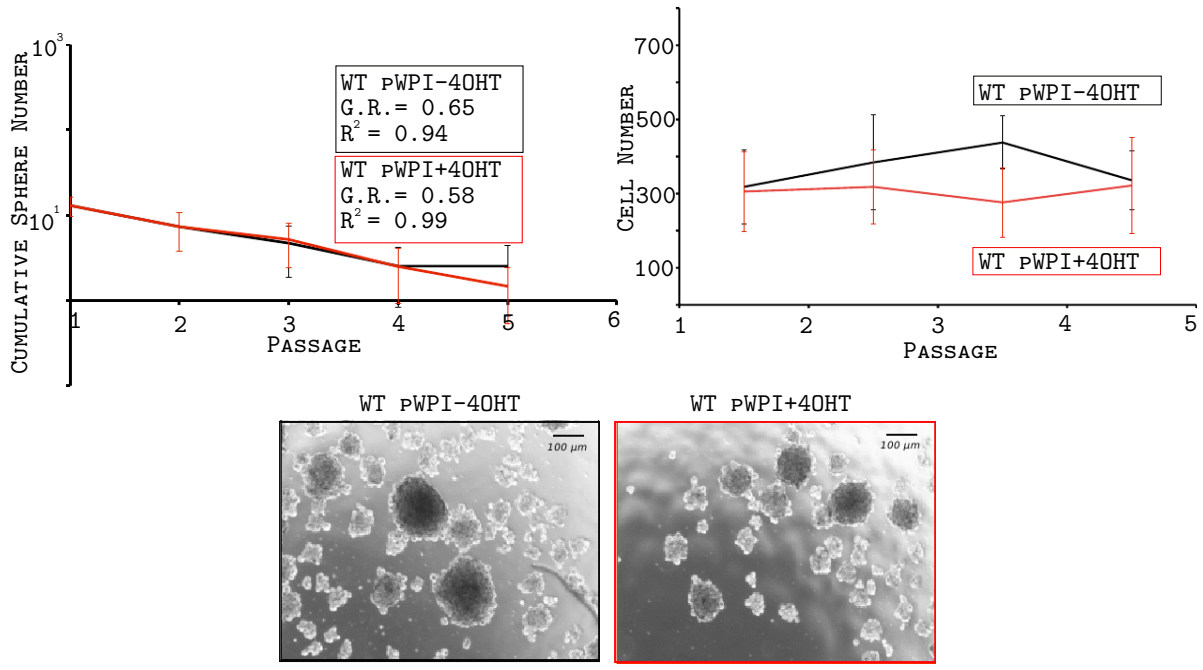

Figure 6.34: **Effect of Tamoxifen treatment on mock-infected cells.**
Upper panel: Semi-logarithmic plotting of Cumulative Sphere Numbers (left panel) were obtained from serial replating of WT mock-infected mammospheres in the absence (black lines, WT pWPI-4-OHT) and in the presence (red lines, WT pWPI+4OHT) of 500 nM 4OHT. Regression analysis of the data set was performed to obtain trend lines (light lines) that best approximate the curves. The growth rates (GR) and the coefficients of determination (R^2) for each trend line are reported inside the graph. Right panel: WT mock-infected mammosphere size over passages in the absence (black line) or in the presence of 4-OHT (red line).
Lower panel: representative images of mock-infected secondary mammospheres in the presence of the absence of 4-OHT. Scale bars as represented.

We evaluated the expression and localisation of MycER in infected cells by immunofluorescence staining. Whereas in the mock-infected cells the endogenous Myc was undetectable, in the MycER-infected cells, treatment with 4-OHT induced an overexpression of Myc and indeed it could be found localised at the nuclei (Fig. 6.35).

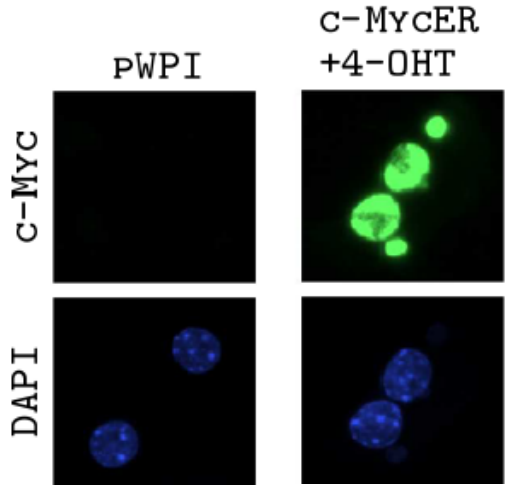

Figure 6.35: **Myc expression and localisation in control or MycER-expressing cells.** Single-cell suspensions from secondary mammospheres were fixed with 4% paraformaldehyde, permeabilised with 0.1% Triton-X100 and blocked in 3% BSA in PBS. Staining was performed with a Myc-specific antibody, followed by an anti-rabbit Cy5 antibody. Nuclei were counter-stained with DAPI. The cells were then analysed under an AX-70 Provis (Olympus) fluorescence microscope to evaluate Myc expression.

We reasoned that the growth arrest that we observed in response to MycER activation could be due to an apoptotic response, and to address this we evaluated the expression of cleaved caspase-3 by Western Blot (WB) analysis. We infected primary mammospheres with the empty vector or with MycER and allowed for secondary mammospheres to form. We then disaggregated, sorted for GFP expression and replated secondary mammospheres in the presence or in the absence of 4-OHT. Treatment was carried out either once on the day of replating (+s), or every day during mammosphere formation (+d). Both in the single-treated and the daily-treated mammospheres we observed a significant increase in the levels of cleaved caspase-3, suggesting that these cells undergo apoptosis upon overexpression of Myc (Fig. 6.36).

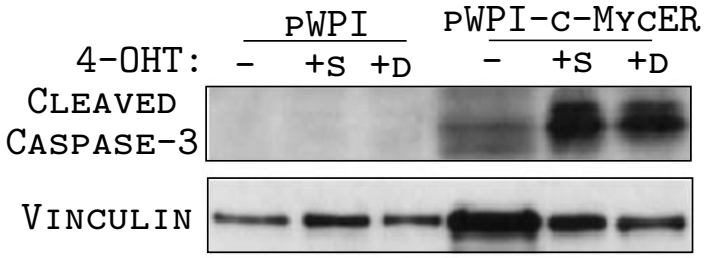

Figure 6.36: **WB analysis of cleaved caspase-3 expression.** Western Blot analysis of cleaved caspase-3 expression in WT mammospheres infected with control vector (pWPI) or MycER (pWPI-MycER) and exposed to no treatment (-), single treatment on the day of replating (+s) or daily treatment during mammosphere formation (+d). Western blots were normalised against the levels of vinculin expression.

To characterise the checkpoint that was triggered in response to the overexpression of MycER, the same cells were analysed by WB for the activation of the p53 pathway and the p21 pathway, two key regulators of oncogene-induced checkpoints (Bartkova et al., 2006). Strikingly, we could observe massive activation of the p53, p21 and p16 proteins in 4-OHT treated cells compared to mock-infected cells (Fig. 6.37).

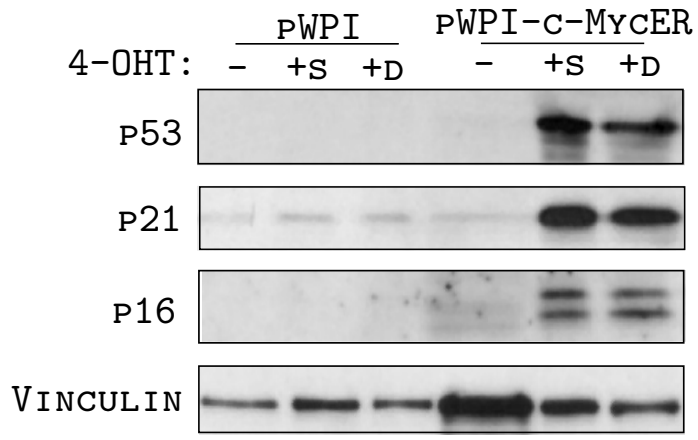

Figure 6.37: **WB analysis of the checkpoint activation in response to Myc overexpression.** Western Blot analysis of the expression of p53, p21 and p16 in WT mammospheres infected with control vector (pWPI) or MycER (pWPI-MycER) and exposed to no treatment (-), single treatment on the day of replating (+s) or daily treatment during mammosphere formation (+d). Western blots were normalised against the levels of vinculin expression.

To confirm that indeed the checkpoint that is triggered upon Myc activation is dependent on p53, we infected p53 KO mammospheres with the MycER construct and treated the cells with 500 nM 4-OHT. As expected, treatment of infected p53 KO mammospheres with 4-OHT did not affect their growth, suggesting that p53 is required for the activation of the checkpoint and the growth arrest in response to Myc activation (Fig. 6.38).

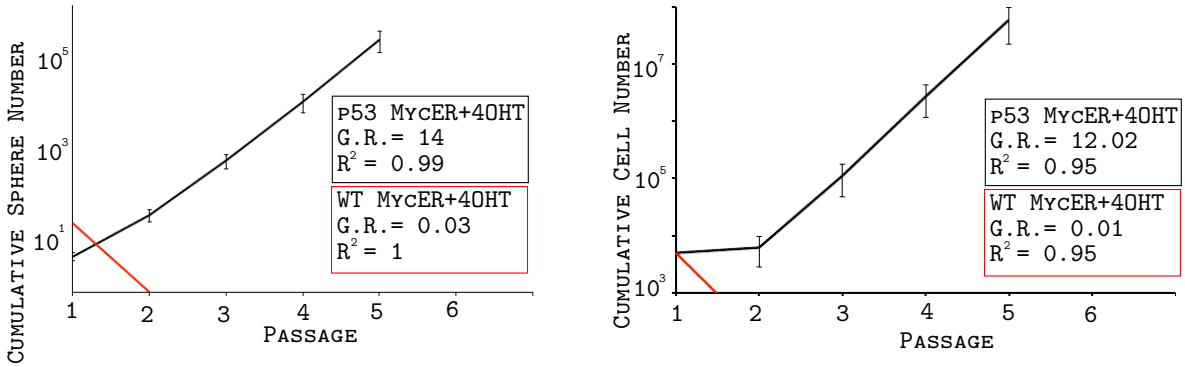

Figure 6.38: **Growth curve of p53 KO or WT MycER-infected mammospheres upon 4-OHT treatment.**
Semi-logarithmic plotting of Cumulative Sphere (left panel) and Cumulative Cell (right panel) Numbers were obtained from serial replating of p53 KO (black lines, p53 MycER) and WT (red lines, WT MycER) mammospheres upon treatment with 500 nM 4-OHT. Regression analysis of the data set was performed to obtain trend lines (light lines) that best approximate the curves. The growth rates (GR) and the coefficients of determination (R^2) for each trend line are reported inside the graph.

These data suggest that upon Myc overexpression, mammary SCs activate a p53-dependent pro-apoptotic checkpoint that induces growth arrest.

6.3.2 Low Levels of Myc Expression Increase SC Self-Renewal Without Inducing Transformation

The activation of an apoptotic checkpoint in response to the expression of Myc in our system did not help us in elucidating the role of this protein in the regulation of self-renewal of mammary SCs. However, quite unexpectedly, the same MycER-infected cells showed a striking phenotype in the absence of 4-OHT treatment. In fact, if cultured as mammospheres without being exposed to 4-OHT, these cells showed a remarkable increase in their self-renewing potential and could be passaged indefinitely in a manner similar to tumour or p53 KO SCs. Furthermore, the absence of 4-OHT induction resulted also in a dramatic increase of mammosphere size compared to controls, suggesting that they possessed increased replicative potential (Fig. 6.39).

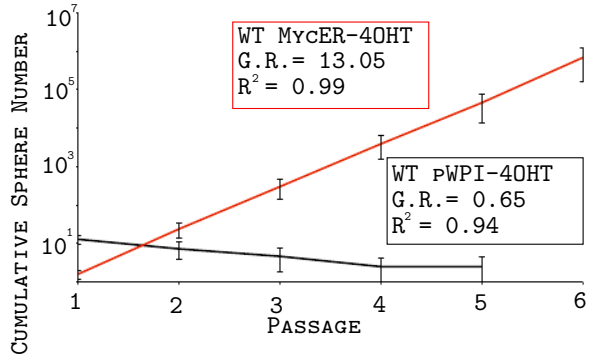

Sphere Size

	Cell Nr
WT pWPI-4OHT	384.5
WT MycER-4OHT	3085.7

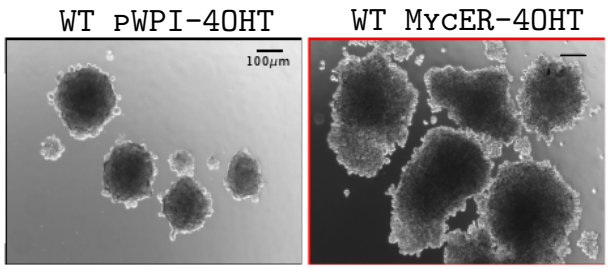

Figure 6.39: **Growth curve of control or MycER infected cells in the absence of 4-OHT treatment.**
Upper panel: Semi-logarithmic plotting of Cumulative Sphere (left panel) and Cumulative Cell (right panel) Numbers were obtained from serial replating of WT mock-infected (black lines, WT pWPI) and MycER-infected (red lines, WT MycER) mammospheres. Regression analysis of the data set was performed to obtain trend lines (light lines) that best approximate the curves. The growth rates (GR) and the coefficients of determination (R^2) for each trend line are reported inside the graph.
Table: average mammosphere size between the different passages. We have demonstrated that mammosphere size remains constant at every passage (Cicalese et al., 2009). Mock-infected mammospheres were composed of approximately 350 cells, as previously reported (Section 6.1). MycER-expressing mammospheres showed drastic increase in size (~3,000 cells).
Lower panel: representative images of mock-infected secondary mammospheres or MycER-expressing mammospheres after 6 days of culture. Scale bars as represented.

We reasoned that the remarkable phenotype that we observed upon infection of MycER without the 4-OHT-mediated induction, could be due to a leakage in the ER conditional system and to investigate this issue we evaluated the expression of Myc in these cells by immunofluorescence. As hypothesised, the levels of Myc expression in the nuclei of 4-OHT untreated cells were lower compared to the ones observed in induced cells, but higher than the mock-infected control, where the endogenous Myc could not be detected (Fig. 6.40).

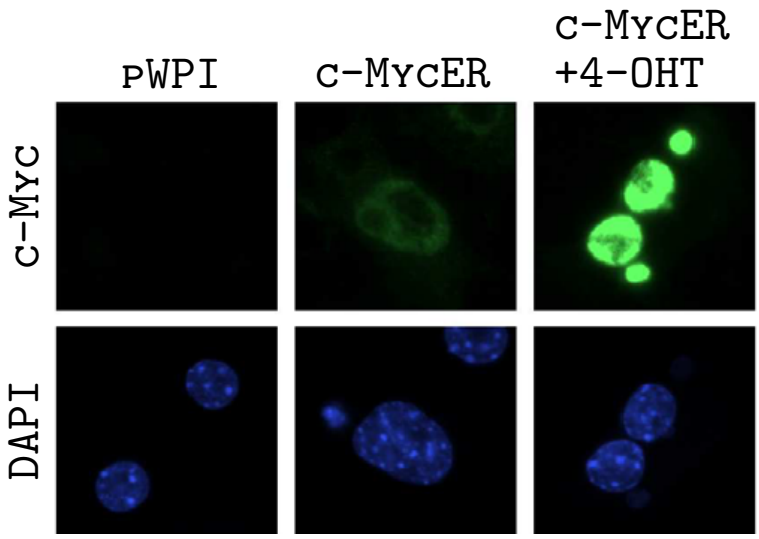

Figure 6.40: **Immunofluorescence staining for Myc expression in control or 4-OHT treated or untreated MycER-infected cells.**
Staining of single-cell suspension from secondary WT mammospheres infected with control vector (left panels) or MycER in the absence (middle panels) or in the presence (right panel) of 4-OHT treatment with a Myc-specific antibody. Single-cell suspensions from secondary mammospheres were fixed with 4% paraformaldehyde, permeabilised with 0.1% Triton-X100 and blocked in 3% BSA in PBS. Staining was performed with a Myc-specific antibody, followed by an anti-rabbit Cy5 antibody. Nuclei were counter-stained with DAPI. The cells were then analysed under an AX-70 Provis (Olympus) fluorescence microscope to evaluate Myc expression.

These data suggest that whereas high levels of Myc expression (such as the ones resulting from the induction of the ER system) induce a p53-dependent pro-apoptotic checkpoint, low levels of Myc expression

(such as the ones that result from the leakage of the ER system) are able to confer increased regenerative potential (mammosphere size) and lifespan (extended serial replating efficiency) to mammary epithelial SCs.

To confirm that the acquired self-renewing properties of mammary SCs in the presence of the MycER protein at low levels were not an effect of the ER system, we expressed a constitutive form of Myc in WT mammospheres by lentiviral infection. Unfortunately, probably due to the fact that the Myc gene was expressed under the control of a strong promoter (CMV), the high levels of Myc expression that resulted from the infection did not induce an increase in the self-renewing abilities of WT SCs (Fig. 6.41).

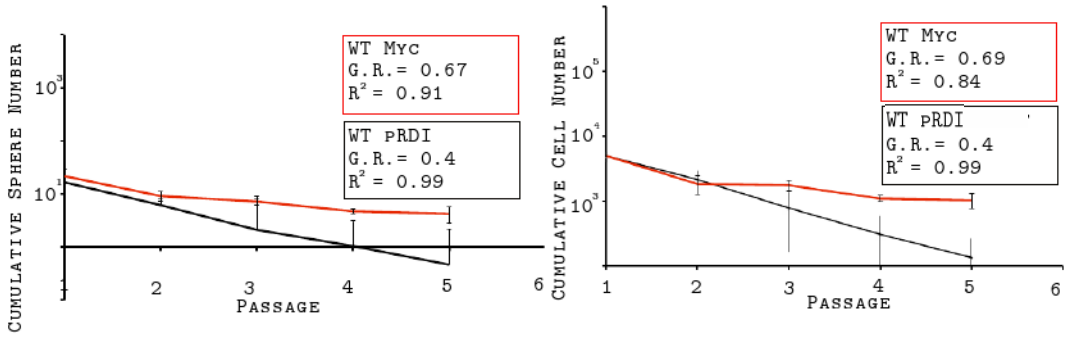

Figure 6.41: **Infection of WT mammospheres with a constitutive Myc.** Semi-logarithmic plotting of Cumulative Sphere (left panel) and Cumulative Cell (right panel) Numbers were obtained from serial replating of mock-infected (black lines, WT pRDI) and Myc-expressing (red lines, WT Myc) mammospheres. Regression analysis of the data set was performed to obtain trend lines (light lines) that best approximate the curves. The growth rates (GR) and the coefficients of determination (R^2) for each trend line are reported inside the graph.

To circumvent this problem, we expressed the constitutive Myc vector in WT mammospheres at lower levels by infecting the cells with decreasing concentrations of lentiviral supernatant, in such a way that different integration efficiencies could be achieved. In this way, we hoped to obtain the formation of clones that expressed sufficient amounts of the Myc protein to induce proliferation without activating a pro-apoptotic checkpoint. We cultured the infected cells to verify the emergence of an immortal clone in these mammosphere cultures. Indeed, at low virus titers, we could observe the emergence of immortal clones that possessed increased self-renewing abilities (Fig. 6.42).

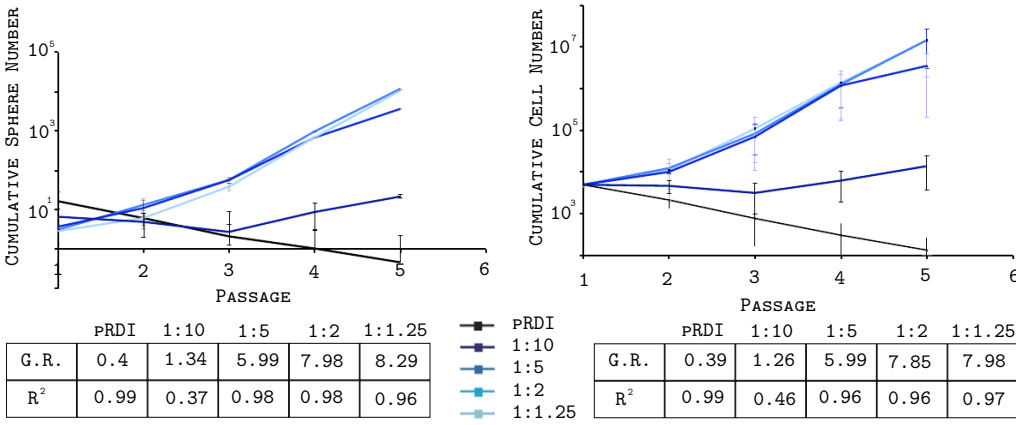

	pRDI	1:10	1:5	1:2	1:1.25
G.R.	0.4	1.34	5.99	7.98	8.29
R^2	0.99	0.37	0.98	0.98	0.96

	pRDI	1:10	1:5	1:2	1:1.25
G.R.	0.39	1.26	5.99	7.85	7.98
R^2	0.99	0.46	0.96	0.96	0.97

Figure 6.42: **Infection of WT mammospheres with a constitutive Myc at different virus titers.** Semi-logarithmic plotting of Cumulative Sphere (left panel) and Cumulative Cell (right panel) Numbers were obtained from serial replating of cells infected with a control vector (pRDI) or with the constitutive Myc vector (pRDI-Myc) at different viral titers (numbers indicate the dilution factors of the viral supernatant). One representative experiment of two that gave similar results. Regression analysis of the data set was performed to obtain trend lines that best approximate the curves (not shown). The growth rates (GR) and the coefficients of determination (R^2) for each trend line are reported in the tables below the curves.

The increase in the replicative potential of WT SCs expressing low levels of a constitutive Myc also correlated with an increase in the mammosphere size and in the estimated number of SCs per sphere, calculated as the mean of the number of sphere-forming cells per dissociated sphere at every passage (Fig. 6.43).

	pRDI	c-Myc 1:10	c-Myc 1:5	c-Myc 1:2	c-Myc 1:1.25
Mammosphere size (Cell Number)	297.6	744.3	1331.9	1590.8	1713.1
SC/Sphere	0.4	1.7	7.6	11.0	11.9

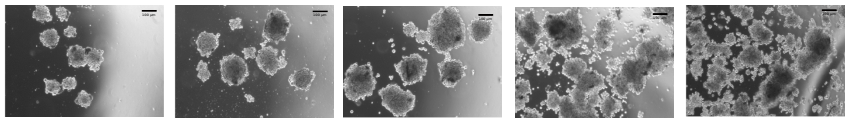

Figure 6.43: **Sphere dimension and estimated SC number after Myc infection at different titers.**
Mean sphere dimension and mean number of SC per sphere over passages in mammosphere cultures from mock-infected (pRDI) or constitutive Myc-expressing mammospheres (c-Myc) infected with different concentrations of viral supernatant. At each passage 5,000 cells were plated in 24-well low adhesion plates. After 6 days the number of formed spheres was counted and the spheres were collected and disaggregated to count the number of total cells. Sphere dimensions were calculated at each passage as the ratio between the total number of cells and the number of spheres that were counted. The number of SCs per sphere was estimated as ratio between the number of counted spheres and the number of plated spheres (equivalent to 5,000 cells, as estimated by the calculated sphere dimension). Figures show representative images of mammospheres that were formed after infection with the empty vector or the constitutive Myc at different titers. Scale bars as represented (100 μm).

To exclude that the effect of low expression of Myc on SCs was limited to the mouse system, we cultured as mammospheres normal human mammary epithelial cells purified from reductive mammoplasties, following published protocols (Dontu et al., 2003; Pece et al., 2010). We then infected the human mammospheres with the MycER construct and could observe that, compared to the normal counterpart that exhausted in culture after few passages, the MycER-expressing spheres had acquired an immortal phenotype, and showed increased sizes, thus confirming that the effect of low levels of Myc is not restricted to mouse SCs (Fig. 6.44).

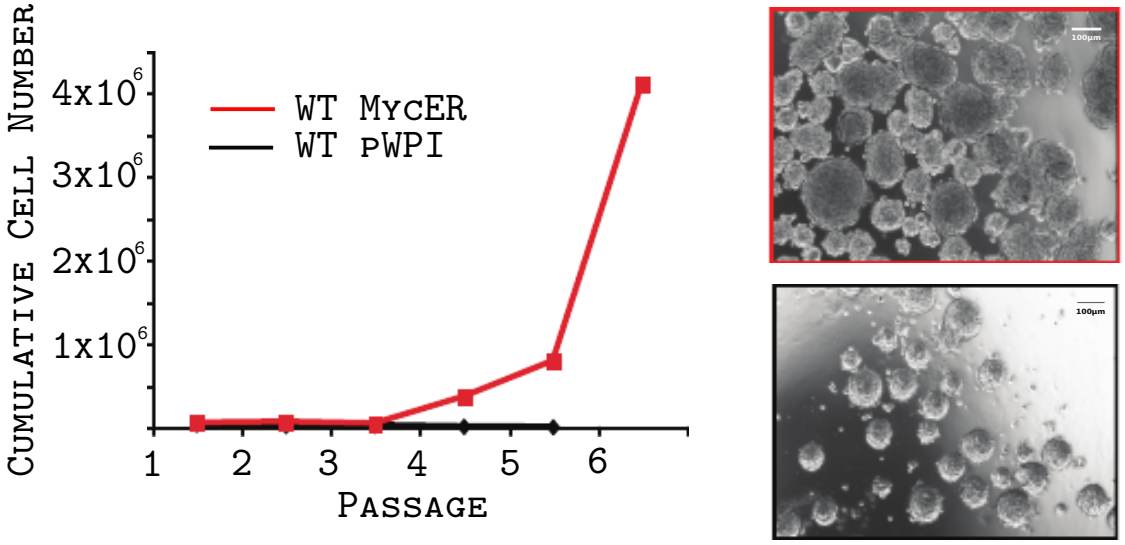

Figure 6.44: **Infection of human mammospheres with MycER.**
Plotting of Cumulative Cell Numbers were obtained from serial replating of human mammary epithelial cells infected with a control vector (pWPI, black line) or with the MycER vector (MycER, red line). Figures show representative images of human mammospheres infected with the control vector or with MycER. Scale bars as represented.

As high levels of Myc expression resulted in the activation of a p53-mediated apoptotic checkpoint in mammary SCs, we investigated if a similar response could be triggered by low levels of Myc . Interestingly, the expression of Myc at low levels had no effect on the activation of p53, p21, or p16 (Fig. 6.37).

To confirm that indeed low levels of Myc expression had no effect on the function of p53, we evaluated the extent of the p53-mediated response to stress in low Myc-expressing mammospheres. To this end, we treated low Myc-expressing and control mammospheres with 2 µg/ml adriamycin and measured the levels of activation of p53 by immunoblotting its phosphorilated form in Ser18. Both in control-infected and MycER-expressing mammospheres the treatment with the the DNA-damaging agent resulted in the stabilisation of the p53 protein and in its phosphorilation on Ser18. This showed that activation of p53 in response to stress was not impaired in the presence of low levels of Myc, thus confirming that low Myc does not activate a p53-mediated response nor does it act on its function, supporting the idea that Myc is regulated by p53 in controlling SC self-renewal (Fig. 6.45).

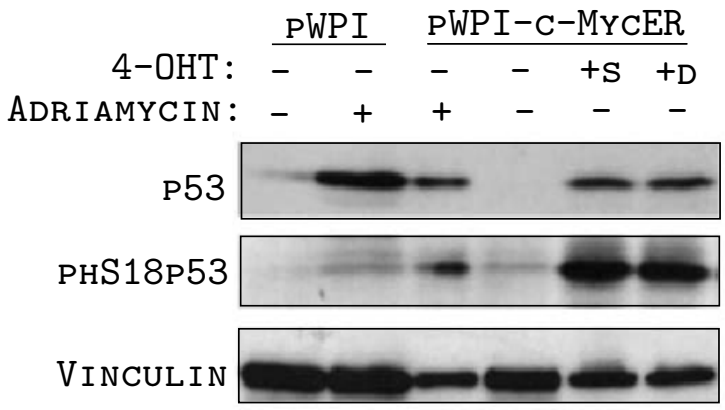

Figure 6.45: **WB analysis of p53 activation in response to stress in the context of low Myc expression.**
Western Blot analysis of the stabilisation of p53 and its phosphorilation in response to DNA-damage. Western blots were normalised against the levels of vinculin expression. Control mammospheres (pWPI) and low Myc-expressing mammospheres (pWPI-c-MycER) were cultured in the presence or in the absence of adriamycin. As positive control for the activation of p53, we induced the expression of high levels of Myc by treating MycER-infected cells with 4-OHT once (+s) or daily during mammosphere formation (+d). Western blots were normalised against the level of vinculin expression.

In line with these observations, the expression of low levels of Myc in p53 KO mammospheres did not have any increasing effect on their growth rate, and low Myc expression had identical effects (in terms of replicative potential and lifespan) on WT or p53 KO mammospheres (Fig. 6.46).

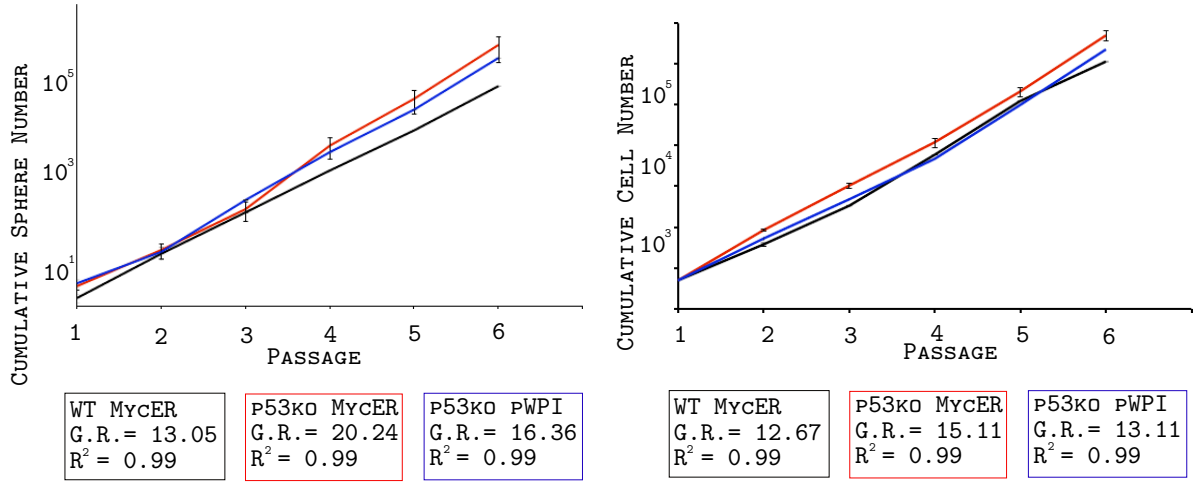

Figure 6.46: **Growth curves of WT or p53 KO mammospheres expressing low levels of Myc**
Semi-logarithmic plotting of Cumulative Sphere (left panel) and Cumulative Cell (right panel) Numbers were obtained from serial replating of WT mammospheres infected with MycER or p53 KO mammospheres infected with a control vector (pWPI) or MycER. Regression analysis of the data set was performed to obtain trend lines that best approximate the curves (not shown). The growth rates (GR) and the coefficients of determination (R^2) for each trend line are reported for each curve under the graphs. The effect of low levels of Myc is similar in WT and p53 KO mammospheres and also similar to the effect of the absence of p53 alone.

These data altogether show that low levels of Myc expression increase the self-renewing properties of SCs, albeit not triggering the activation of any p53-mediated response. This observation suggests that low levels of Myc do not create a selective pressure to lose the p53-mediated checkpoint response.

We then wondered how Myc biologically influences the behaviour of mammary SCs, as we had demonstrated that low levels of Myc expression are able to *i)* increase the number of SCs (evaluated as the number of SCs per mammosphere, *ii)* confer extended self-renewing abilities to SCs (which results in unlimited serial replating of the mammospheres), *iii)* increase the regenerative and proliferative potential of SCs (that are able to form mammospheres with increased size). We therefore investigated whether low Myc-expressing SCs are transformed and to answer this question we performed transplantation experiments in which we injected cell suspensions deriving from the dissociation of low Myc-expressing mammospheres into the cleared fat-pad of syngeneic mice. Two months after the injection, the transplanted mice were sacrificed and the mammary gland collected for whole mount staining to evaluate the presence of positive outgrowths. Indeed, after two months, we were able to find positive outgrowths deriving from the injection of low Myc-expressing cells, and, interestingly, the morphology of the epithelial tree that was generated showed no alteration, suggesting that low Myc-expressing SCs did not have a transformed phenotype (Fig. 6.47).

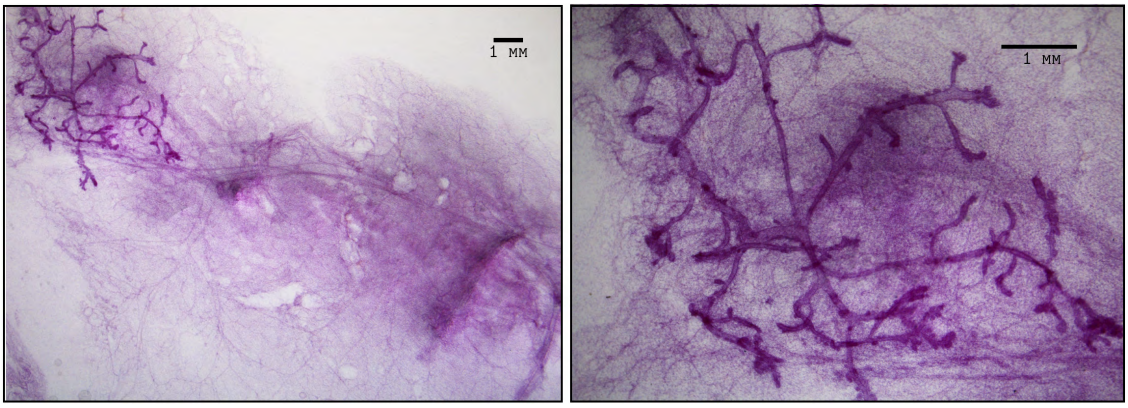

Figure 6.47: **Whole mount staining of a positive outgrowth resulting from the injection of low Myc expressing cells in the cleared fat-pad of recipient mice.**
Carmine-stained whole mount of typical outgrowths after injection of cell suspension from low Myc-expressing secondary mammospheres. Scale bars as indicated.

Prolonged observation of injected mice revealed no formation of palpable masses up to 7 months after the injection (20 animals under observation), suggesting that low Myc-expressing mammospheres are immortalised but do not show a transformed phenotype.

These data show that the biological effect of low levels of Myc on SCs is not the result of a transforming process, as low Myc-expressing SCs behave like normal SCs if injected into recipient mice.

6.4 The Consequence of Low Myc Expression on Mammosphere Cultures Can Be Explained by a Dual Effect on SCs and Progenitors

We have shown that low levels of Myc result in an increase in the number of SCs, and they are able to confer extended self-renewing properties and increased regenerative (proliferative) potential. Biologically, this effect could be explained by two different mechanisms depending on whether Myc targets the SC or the progenitor cell. In fact, we have shown that Myc is regulated by p53 and that in turn it has an effect in controlling SCs self-renewal, as shown for tumour mammospheres. This results in the expansion of the number of SCs, nevertheless, we can not rule out the possibility that the effect of low Myc on mammosphere cultures is due to an effect on progenitor cells, where it could induce reprogramming into cells with stem-like properties, thus increasing their number.

To address this issue we took advantage of the PKH protocol that we had set up and validated for the isolation of SCs from the bulk of the mammospheres and that led us to the characterisation of their self-renewing properties, and analysed the effect of low levels of Myc on separate populations of stem or progenitor cells.

6.4.1 Low Levels of Myc Induce SC Symmetric Division

To investigate whether low levels of Myc have an effect on SC divisions, we analysed the symmetry of SC division by isolating the PKH^{high}quiescent population from low Myc-expressing or mock-infected mammospheres and visualising the first rounds of cell divisions during mammosphere formation by time-lapse imaging. Indeed, as we had previously observed in CSCs or p53 KO SCs, the majority of low Myc-expressing SCs divided symmetrically, giving rise to two daughter cells endowed with the same replicative potential (Fig. 6.48).

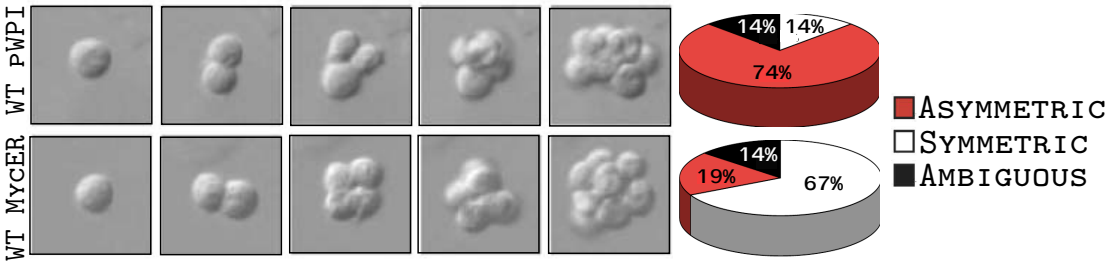

Figure 6.48: **Time-lapse analysis of low Myc-expressing SCs.**
Time-lapse microscopy images of the first divisions of mock-infected of low Myc-expressing PKH^{high} cell. Relative frequencies of asymmetric and symmetric divisions are shown in the pie charts. Ambiguous: divisions that could not be interpreted as symmetric or asymmetric.

These data were confirmed also by staining control or low Myc-expressing SCs with an anti-Numb antibody as previously described, to evaluate by confocal microscopy the symmetry of distribution of

Numb on the cell membrane. Indeed, our previous observations were confirmed, as the majority of low Myc-expressing SCs showed symmetric distribution of Numb on the cell membrane during cell division (Fig. 6.49).

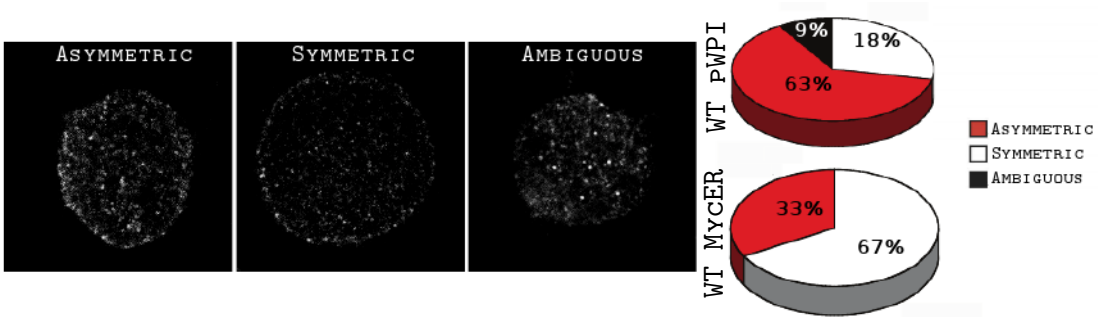

Figure 6.49: **Numb localisation in dividing low Myc-expressing SCs.** Confocal analysis of the distribution of Numb on the cell membrane of dividing SCs from control or low Myc-expressing samples. Representative images of the different modes of division are shown. Relative frequencies of asymmetric and symmetric divisions of control (pWPI) or low Myc expressing (WT MycER) cells are shown in the pie charts. Ambiguous: Numb distribution not consistent among different confocal sections.

These results show how low levels of Myc expression alone endow mammary SCs with increased proliferative potential by determining a switch in the mode of SC division from an asymmetric to a symmetric one, thus expanding the SC pool.

6.4.2 Low Levels of Myc Expression Induce Reprogramming of Progenitor Cells Into Cells With Stem Properties

Reprogramming of adult differentiated cells into pluripotent SCs has been achieved in recent years by expressing the embryonic-specific factors Myc, Klf, Oct4 and Sox2(Wernig et al., 2007; Takahashi and Yamanaka, 2006; Okita et al., 2007) . In particular, Myc has been shown to enhance the efficiency of somatic cell reprogramming into pluripotent cells by a thousand-fold (Nakagawa et al., 2008). Furthermore, if expressed by itself in human fibroblast, it has shown to give a strong embryonal stem-like transcription pattern (Sridharan et al., 2009). It is therefore reasonable to hypothesise that Myc alone could be able to reprogramme mammary progenitors into cells with tissue-specific adult SC properties. To address this issue, we separated mammary progenitor cells from SCs by means of the PKH26 labelling system we had previously set up. We have shown that the rapidly dividing populations of cells (identified as $PKH^{low}$and PKH^{neg}) do not contain cells capable to form mammospheres *in vitro* nor to repopulate the cleared fat-pad of recipient mice if injected *in vivo*. To test the effect of low levels of Myc on progenitor cells we focused on the PKH^{neg}population, to limit as much as possible the probability of cross-contamination between the PKH subpopulations. PKH^{neg}cells were infected with the MycER construct or the empty vector and cultured in suspension. Strikingly, whereas the mock-infected progenitor cells, as expected, were not able

to form mammospheres even at the first passage, the low Myc-expressing progenitors were able to grow in culture and form mammospheres. These mammospheres could be propagated *in vitro* unlimitedly and expanded in culture at each passage (Fig. 6.50).

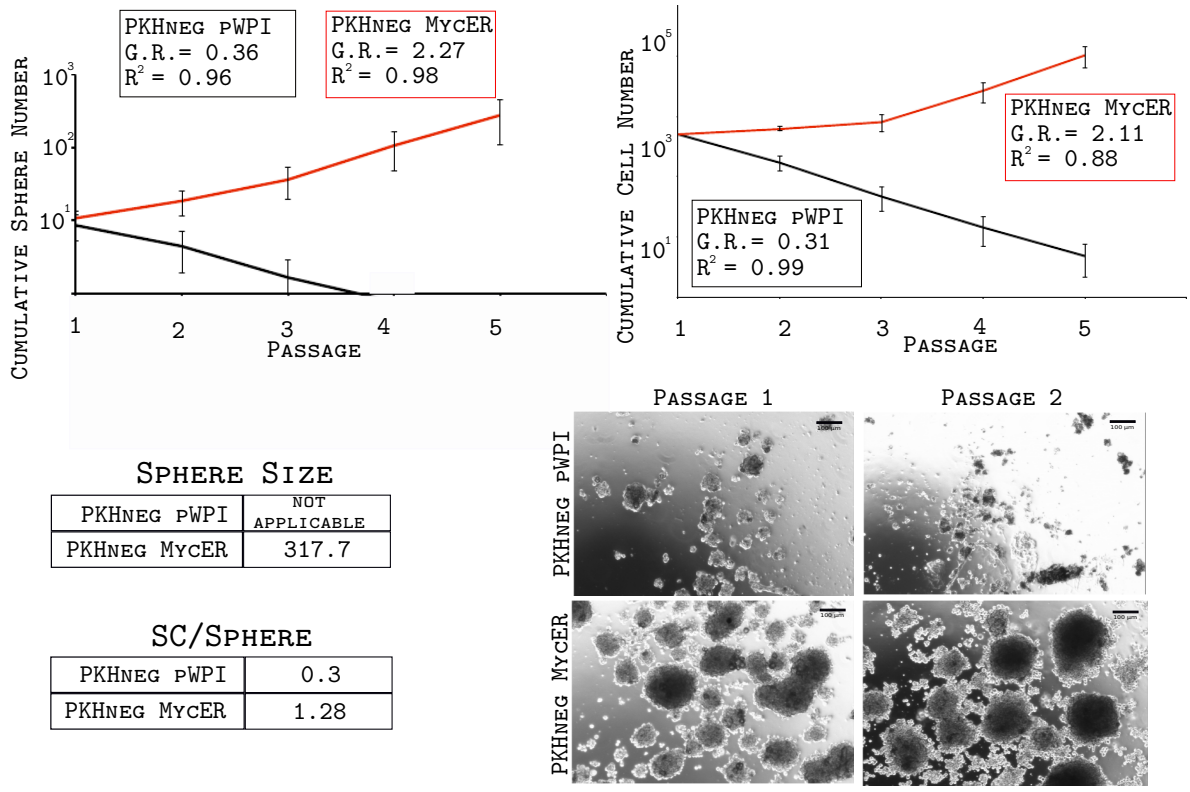

Sphere Size

PKHneg pWPI	not applicable
PKHneg MycER	317.7

SC/Sphere

PKHneg pWPI	0.3
PKHneg MycER	1.28

Figure 6.50: **Growth curves of progenitor cells expressing low levels of Myc.**
Upper panel: Semi-logarithmic plotting of Cumulative Sphere (left panel) and Cumulative Cell (right panel) Numbers were obtained from serial replating of mock-infected (black lines, PKH^{neg}pWPI) and MycER-infected (red lines, PKH^{neg} MycER) progenitor cells. Regression analysis of the data set was performed to obtain trend lines (light lines) that best approximate the curves. The growth rates (GR) and the coefficients of determination (R^2) for each trend line are reported inside the graph.
Tables: average mammosphere size during passages. We have demonstrated that mammosphere size remains constant at every passage (Cicalese et al., 2009). Mock-infected PKH^{neg} cells did not form mammospheres, but only small aggregates that could not be passaged further.MycER-expressing PKH^{neg}cells were able to form mammospheres. Average number of SCs per sphere is also reported. The number of SCs per sphere was estimated as ratio between the number of counted spheres and the number of plated spheres (equivalent to 5,000 cells, as estimated by the calculated sphere dimension).
Lower panel: representative images of mock-infected of low Myc-expressing primary and secondary mammospheres after infection. Scale bars as represented.

Again, to confirm that the phenotype was not due to the ER system, we infected progenitor cells with a constitutive Myc construct at low titers, and indeed we obtained similar results (Fig. 6.51).

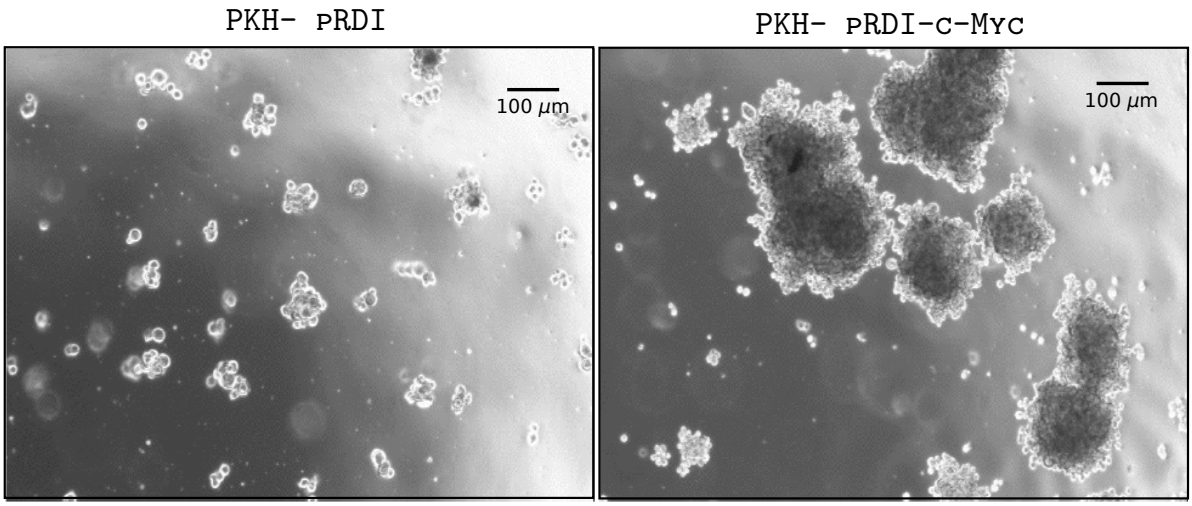

Figure 6.51: **Infection of progenitor cells with constitutive Myc at low titers.** Representative images of PKH^{neg}progenitor cells 6 days after infection with a control vector (pRDI) or a constitutive Myc (pRDI-Myc) at low titers. Scale bars as represented.

Adult SCs are defined by their ability to self-renew and to differentiate into all the cell types of the tissue of origin. We have demonstrated by *in vitro* culture assay that upon expression of Myc at low levels, mammary progenitor cells acquire self-renewing properties and can form mammospheres that can be serially passaged. To investigate whether these cells were able to differentiate into different cell types in the mammary gland, we transplanted these cells into the cleared fat-pad of recipient mice. After two months the mice were sacrificed and their inguinal mammary glands were collected for whole mount staining to evaluate the presence of positive outgrowths. Strikingly, we could observe, although with low frequencies, positive outgrowths resulting from the injection of low Myc-expressing cells. The epithelial tree that was formed showed no macroscopical differences compared to the epithelial tree that is formed upon transplantation of WT SCs (Fig. 6.52).

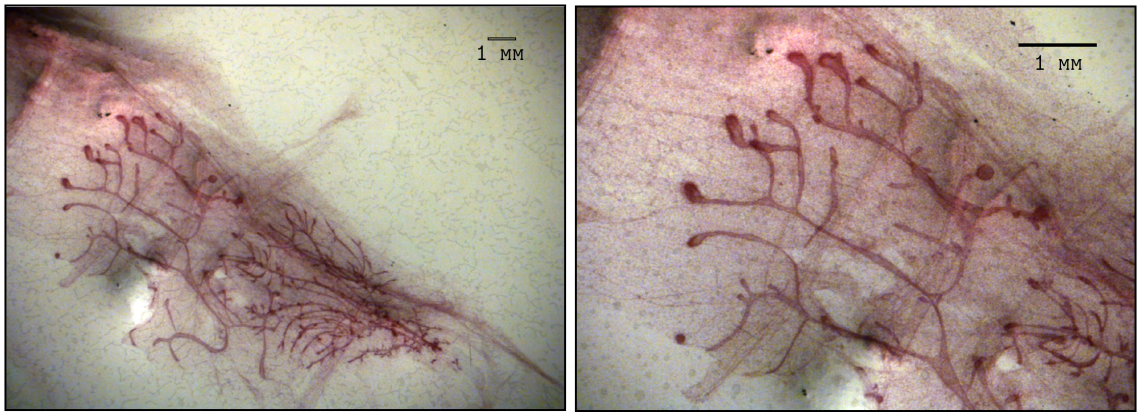

Figure 6.52: **Whole mount staining of a positive outgrowth resulting from the injection of low Myc expressing progenitor cells in the cleared fat-pad of recipient mice.**
Carmine-stained whole mount of typical outgrowths after injection of cell suspension from low Myc-expressing secondary mammospheres. Scale bars as indicated.

These data demonstrate that low levels of Myc expression are able to induce reprogramming of progenitor cells into cells with stem properties, although with low frequencies.

6.4.3 Low Myc-Induced Reprogramming is Associated With Genomic Instability

We have shown that high levels of Myc expression are associated with a p53-dependent apoptotic response, resulting in the rapid exhaustion of the mammosphere culture. Low levels of Myc expression do not trigger a p53-dependent response, however, we checked for the presence of genomic instability in these cells. To this end, we cultured for 9 passages low Myc-expressing mammospheres at which point the mammospheres were collected, disaggregated, and the cell suspension was serially diluted to obtain single SC clones that were plated in 48-well plates. These clones were expanded for further 3-6 weeks, and then genomic DNA was prepared. Comparative genomic hybridisation assays on chromosomes 10, 11, 12, 13 and part of chromosomes 9 and 14 (covering about a quarter of the mouse genome) were then performed using as control non-infected mammospheres at passage 5. Five clones of reprogrammed SCs were analysed and all five showed genomic aberrations. Interestingly, all aberrations were localised on known fragile sites. In particular, one clone presented the deletion of about 100 Kbp localised within the retinoic acid receptor-related orphan receptor A (Rora) on chromosome 9 (Fig. 6.53).

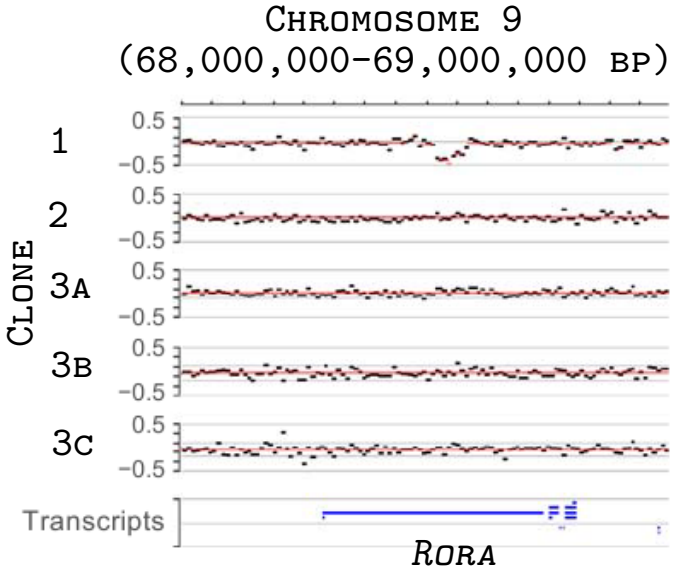

Figure 6.53: **Comparative genomic hybridisation chromosome 9.**
Comparative genomic hybridisation analysis of five MycER-reprogrammed stem cell clones. Clones 3a, 3b and 3c are considered to be subclones of the same original clone. Selected regions of chromosome 9 are indicated. The results are expressed as log2 ratios of the intensity signals of the stem cell clone DNA to the control DNA. Each black bar represents the average of 10 probes with 1,388 bp median spacing. The red lines represent the statistical average and show discontinuities, when a series of averaged probe data deviates in a statistically significant manner from its neighbours. Transcripts are indicated by blue lines and the names of select genes are indicated.

The Rora gene, in humans, maps to the common fragile site FRA15A (Bignell et al., 2010; Zhu et al., 2006). The second clone had a deletion of about 250 Kbp on chromosome 13 spanning within the phospohodiesterase 4D (Pde4D) gene (Fig.6.54).

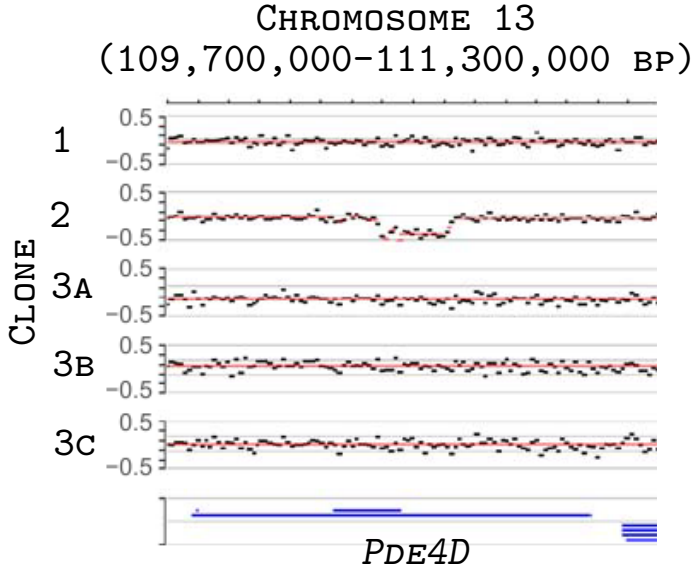

Figure 6.54: **Comparative genomic hybridisation chromosome 13.**
Comparative genomic hybridisation analysis of five MycER-reprogrammed stem cell clones. Clones 3a, 3b and 3c are considered to be subclones of the same original clone. Selected regions of chromosome 13 are indicated. The results are expressed as log2 ratios of the intensity signals of the stem cell clone DNA to the control DNA. Each black bar represents the average of 10 probes with 1,388 bp median spacing. The red lines represent the statistical average and show discontinuities, when a series of averaged probe data deviates in a statistically significant manner from its neighbours. Transcripts are indicated by blue lines and the names of select genes are indicated.

Again, the human homologue of Pde4D is situated within the common fragile site FRA5H (Zhu et al., 2006).

Interestingly, the remaining three clones had identical chromosomal rearrangements suggesting that they had originated from an identical clone prior to the serial dilution analysis. This rearrangement targeted telomeric regions of chromosomes 9 and 10 (Fig.6.55) and the breakpoints were within the high mobility group AT-hook2 (Hmga2) genes and the ubiquitin specific peptidase 4 (Usp4) gene respectively. These sites are often rearranged in human cancers (Gray et al., 1995; Cleynen and Van de Ven, 2008).

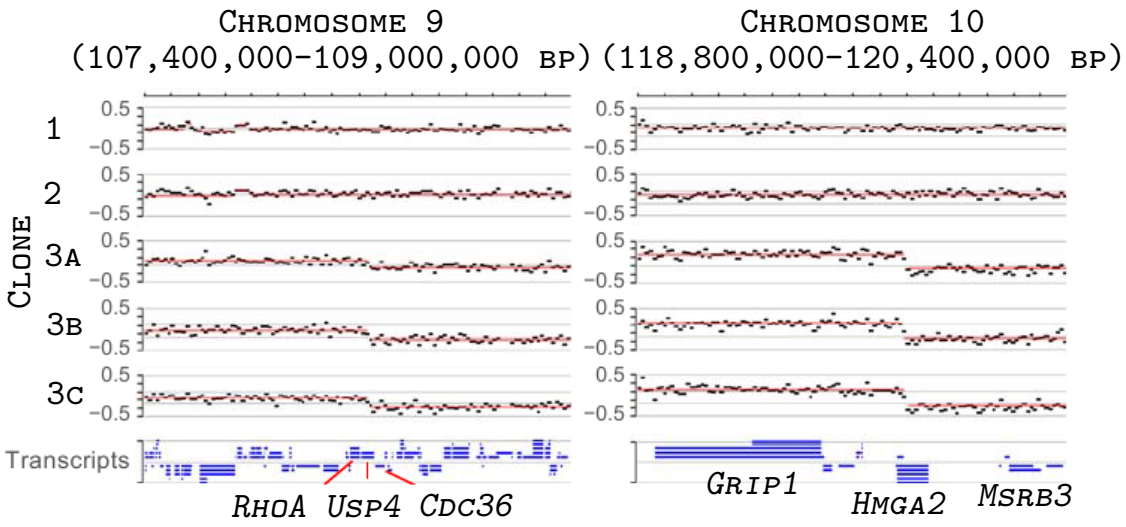

Figure 6.55: **Comparative genomic hybridisation chromosomes 9 and 10.** Comparative genomic hybridisation analysis of five MycER-reprogrammed stem cell clones. Clones 3a, 3b and 3c are considered to be subclones of the same original clone. Selected regions of chromosomes 9 and 10 are indicated. The results are expressed as log2 ratios of the intensity signals of the stem cell clone DNA to the control DNA. Each black bar represents the average of 10 probes with 1,388 bp median spacing. The red lines represent the statistical average and show discontinuities, when a series of averaged probe data deviates in a statistically significant manner from its neighbours. Transcripts are indicated by blue lines and the names of select genes are indicated.

Altogether these data show that the expression of low levels of Myc in mammary epithelial cells, that is associated with reprogramming of progenitor cells into cells with adult SC properties, induces genomic instability and results in chromosomal aberrations that are localised in common fragile sites. Strikingly, no further rearrangements were accumulated during the single clone expansion, suggesting that the genomic instability in mammary SCs had been a transient event, possibly associated with the reprogramming itself.

7 DISCUSSION

7.1 Self-Renewing Divisions in Mammary SCs

Stem cells are defined by their ability to self-renew and to differentiate into all the cell types that compose their tissue of origin. With these two fundamental abilities, SCs ensure the constant maintenance of homoeostasis in the hierarchically organised tissue, and, if needed, they can undergo several rounds of cell division without being lost. The failure of the mechanisms that regulate these processes inevitably results in an aberrant development of the tissue, and contributes to the formation of cancer. Interestingly, tumours are complex and heterogeneous tissues composed of a mass of diverse cell subtypes, sustained by a limited number of cells that for this reason are called CSCs. CSCs have been identified in several solid tumours as well as in haematopoietic diseases, yet their understanding is still very preliminar. Several important and unsolved questions are being addressed by numerous research groups, as, for example, what could be the origin of these cells and which are the mechanisms that are altered and render them transformed. Because of the properties that CSCs share with normal SCs, it is reasonable to hypothesise that they are generated following the loss of regulating mechanisms in normal SCs. After the identification and isolation of SCs in the haematopoietic system, which served as a paradigm for subsequent studies, cells endowed with the ability to sustain the balanced turnover of a tissue have been identified in several systems, including the mammary gland (Stingl et al., 2006; Shackleton et al., 2006). We took advantage of this system to investigate what are the alterations that characterise CSCs and that render them able to grow, insensitive to the regulatory mechanisms that normally control tissue homoeostasis.

7.1.1 Extended Replicative Potential and Increased Frequency of Symmetric Divisions in CSCs

Based on published protocols for the purification and culture of mammary SCs, we were able to set up a culturing system for the propagation of mouse mammary SCs, from both normal and tumour samples. In these cultures, the content in SCs was evaluated with assays *in vitro* (i.e. the ability of SCs to form mammospheres that could be propagated in culture and complex threedimentional structures in semisolid matrix) and *in vivo* (the ability to repopulate the cleared fat-pad of a mouse forming normal tissues or tumours with the same complexity of the tissue of origin). This characterisation led us to the observation that both *in vitro* and *in vivo*, CSCs show increased replicative potential, as they constantly expand in culture. The consequent analysis of the growth properties of these cells by a label retaining assay with the PKH26 dye confirmed that indeed CSCs possess increased proliferating capacity, as they were found also in the non-label retaining (PKH^{low}, PKH^{neg}) fractions. On the contrary, normal SCs remained in a quiescent or slowly proliferating state, and could be found only in the label-retaining PKH^{high}fraction.

Based on the property of normal SCs to remain mainly quiescent, we took advantage of the PKH26

label-retaining assay to isolate a subfraction of cells (PKH^{high}) that had retained the dye after 2 weeks in culture, and we confirmed that this subfraction is highly enriched in SCs, both in normal and tumour samples by limiting dilution transplantation. The visualisation of the cell division of PKH^{high}cells by time-lapse analysis during mammosphere formation showed that WT SCs mainly generate two cells with different proliferative fate: one cell that remains quiescent (the putative SC) and one that carries on proliferating, giving rise to the bulk of the mammosphere (progenitor cell). Indeed, this was consistent with the fact that the proliferating fractions of the PKH-sorted cells (PKH^{neg}) do not contain SCs. On the contrary, tumour SCs generate two daughter cells with the same proliferation potential and they can be found both in the non-proliferating and in the proliferating PKH subfractions. This, together with the observation that CSCs expand in number in culture, suggests that not only tumour SCs are able to divide symmetrically, but they have increased proliferative potential compared to WT SCs. These observations also correlated with the distribution of the cell fate determinant Numb on the cell membrane of dividing SCs. Numb was asymmetrically distributed on the cell membrane of dividing WT SCs, but was symmetrically partitioned in dividing CSCs. Altogether, these data suggest that an important acquired feature of CSCs is their ability to undergo several rounds of cell division without losing their self-renewal potential; furthermore, these cells adopt a symmetric mode of division that results in the amplification of the CSC pool.

Importantly, these acquired features in CSCs are not accompanied by the loss of the developmental potential, as their ability to form more differentiated cells is still maintained. In fact, both the mammospheres *in vitro* and the tumour tissue *in vivo* are not composed solely of CSCs. This implies that these cells are able to alternate the use of symmetric and asymmetric cell divisions, thus increasing the stem cell pool without losing the ability to generate new differentiated cells. Accordingly, the analysis of the symmetry of CSC divisions by time-lapse and Numb staining revealed that these cells are able to adopt both modes of divisions. Nevertheless, if we model the formation of tumour mammospheres assuming that the frequency of symmetric or asymmetric divisions remains constant throughout the sphere formation, we obtain tumour mammospheres with a predicted number of CSCs that is in fact highly overestimated compared to the experimentally generated numbers. In light of this, we corrected the modelling of the proliferative history of normal and CSCs during mammosphere formation based on the number of SCs that were measured empirically. According to the model reported in fig. 7.1, the relative frequency of symmetric divisions that a CSC undergoes decreases progressively during mammosphere formation, indicating that the mammosphere itself creates an environment for the SC that influences its behaviour with mechanisms that are yet unknown, favouring asymmetric cell divisions.

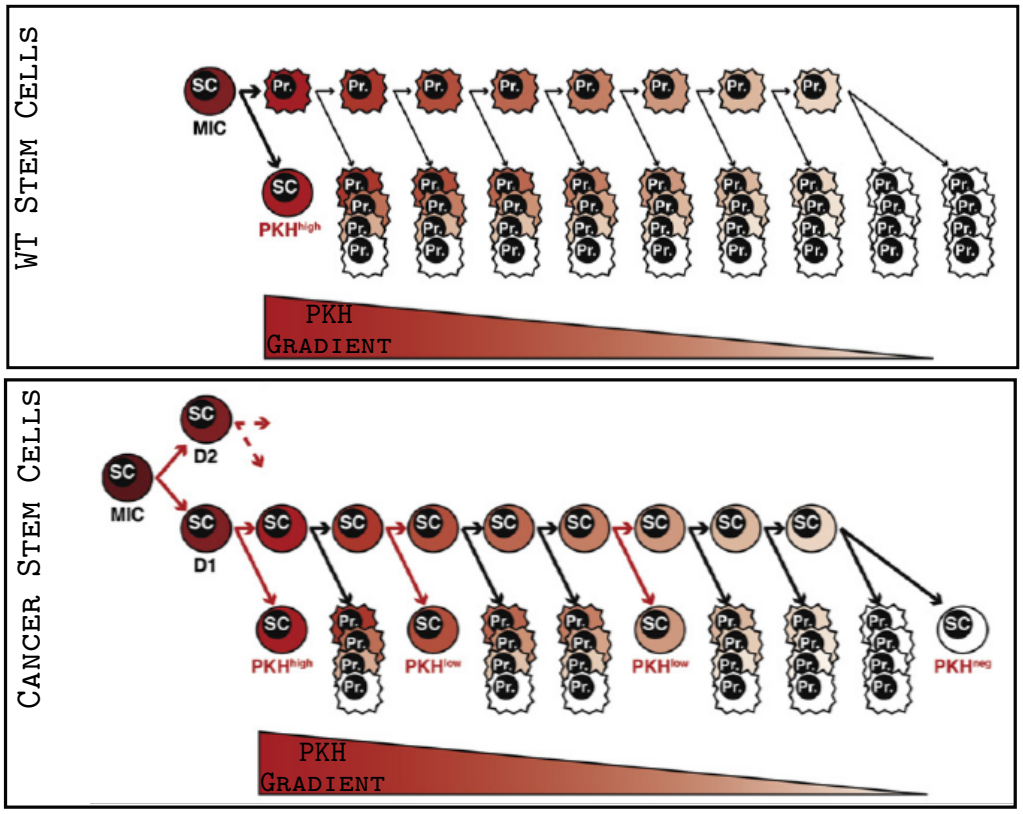

Figure 7.1: **Modelling the proliferative history of normal and cancer SCs.** The model represents the kinetics of cell divisions during the clonal expansion of one normal (upper panel) or ErbB2-tumour (lower panel) mammary initiating cell. Each (WT or tumour) scheme reports the proliferative history of one mammary initiating cell (upper part), the projected cellular composition of the formed mammosphere (middle part), and the progressive decrease of the PKH fluorescence intensity (PKH gradient). Mathematical modelling of WT or ErbB2 SC divisions within mammospheres was based on two predicted values: *i)* the number of SCs within each of the three PKH-subsets of the mammosphere; and *ii)* the number of prior divisions for each of the predicted SCs (proliferative history) within each PKH subset. These predictions were elaborated from the experimental data. The proliferative history of the WT mammary initiating cell was modelled to obtain one mammosphere containing 1 PKH^{high} SC, through 1 asymmetric division (bold black arrows). The proliferative history of the tumour mammosphere initiating cell was modelled to obtain a mammosphere containing 7 SCs, of which: 2 in the PKH^{high} subset (2 cell divisions), 4 in the PKH^{low} (4-7 divisions) and 1 in the PKH^{neg} (10 divisions). To accommodate these constrains, the model incorporated the following features: *i)* 1 symmetric division of the tumour mammosphere initiating cell (red arrow) to generate two daughter SCs with equal proliferative potential (D1 and D2; only the expansion of D1 is shown in the graph); *ii)* 1 symmetric division of D1 (red arrows) to generate 1 PKH^{high} SC and 1 SC that divided further to generate PKH^{low} and PKH^{neg} SCs; *iii)* alternation of 2 symmetric and 3 asymmetric (black arrows) divisions to generate 2 PKH^{low} SCs and 1 SC that proliferated further; and *iv)* 3 additional rounds of asymmetric divisions to generate 1 PKH^{neg} SC. The resulting model predicts that the frequency of symmetric divisions decreases with the growth of the mammosphere. Pr: Progenitors (overlapped progenitors project their expansion).

Another important acquired feature of CSCs is their extended replicative potential. In fact, while normal SCs can only undergo a restricted number of self-renewing divisions *in vitro* and exhaust in culture, and can only be serially transplanted for six to seven times(Daniel et al., 1968), tumour SCs are virtually immortal and can be indefinitely passaged in culture. This property, together with their increased frequency of symmetric divisions, explains the continuous geometric expansion of CSCs *in vivo*

and *in vitro*. On the other hand, their ability to divide asymmetrically and generate differentiated progeny, explains the continuous growth of the tumour mass and its cellular heterogeneity.

7.1.2 p53 and Regulation of SC Polarity

We have shown that SCs can divide symmetrically or asymmetrically and that the regulatory mechanisms that govern these processes appear to be altered in cancer SCs, that preferentially adopt a symmetric mode of division, thereby expanding in number and giving rise to ever-growing tumour masses. The mechanism by which SC divisions are regulated may involve asymmetric distribution of cell fate determinants (for example the Par proteins, Notch or Numb) or other cytoplasmic components like mRNAs. We have shown the involvement in this process of the tumour suppressor p53, which suggests that the cell stress and DNA-damage that result from proliferation may also play a role on the outcome of cell divisions. Interestingly, p53 has been recently found to be a key regulator of the reprogramming process that drives differentiated adult cells into a pluripotent stem-like state (iPS cells) by expression of different factors like Myc, Klf4, Oct4 and Sox2 (Utikal et al., 2009; Marion et al., 2009; Li et al., 2009; Hong et al., 2009; Kawamura et al., 2009). In particular, the absence of p53 is an important factor in enhancing the frequency of reprogramming of iPS cells.

The absence of p53 on mammary SCs increases their replicative potential and determines a switch in their mode of division from asymmetric to symmetric. The outcome of this is that p53 KO SCs behave like tumour SCs in terms of SC expansion, both in the mammary gland *in vivo* and in mammospheres *in vitro*.

These observations are in agreement with published data showing that in the presence of a p53 mutant with increased activity, mammary SCs undergo rapid exhaustion and have limited regenerative potential upon serial transplantation (Gatza et al., 2008). These data show how p53 has a role in the regulation of self-renewal in mammary SCs, and acts by maintaining their number constant in the mammary gland by imposing an asymmetric mode of division, thereby limiting the SC expansion.

Interestingly, this effect appears not to be restricted to mammary SCs, as the absence of p53 also increases self-renewal of neural SCs (Meletis et al., 2006), suggesting that its role in the regulation of SC division is common to different tissues.

7.1.3 Loss of p53 and Tumour Initiation

p53 is lost or functionally impaired in a vast number of cancers of various tissues. In the mammary gland, genetic alterations of the p53 locus result in an increased incidence of breast tumours. In the mouse, the absence of p53 results in the formation of an apparently normal mammary gland (Jerry et al., 1998) and p53 KO mice rarely develop mammary tumours, probably due to the premature development of lymphomas. Nevertheless, somatic inactivation of p53 in the mammary gland (Liu et al., 2007b) or

transplantation of p53 KO mammary tissues in WT mice result in the formation of mammary tumours with high incidence (Jerry et al., 2000; Kuperwasser et al., 2000). These observations suggest that an increase in the number of SCs due to p53 inactivation primes the mammary tissue to the formation of tumours, possibly by increasing the number of putative targets of transformation. Notably, amongst common risk factors for mammary tumour formation there is also the mass of the mammary gland itself, which is likely to correlate with the SC content (Trichopoulos et al., 2008).

In the MMTV-ErbB2 breast cancer model, the increased proliferative potential and symmetric SC divisions can be explained by the absence of a functional p53 pathway. We have shown, in fact, that in tumour mammospheres the p53-mediated response to stress is functionally attenuated compared to WT samples. It is therefore reasonable to conclude that the behaviour of tumours in terms of proliferating potential and SC division can be attributed to the absence of p53. In fact, we have shown that in these cells, the restoration of the levels of p53 by inhibition of its degradation pathway (with Mdm2-inhibitor Nutlin-3) results in a rapid exhaustion of the tumour mammospheres in culture due to the recovery of the asymmetry of SC division and the progressive reduction of the number of cancer SCs in tumour mammospheres (Fig. 7.2).

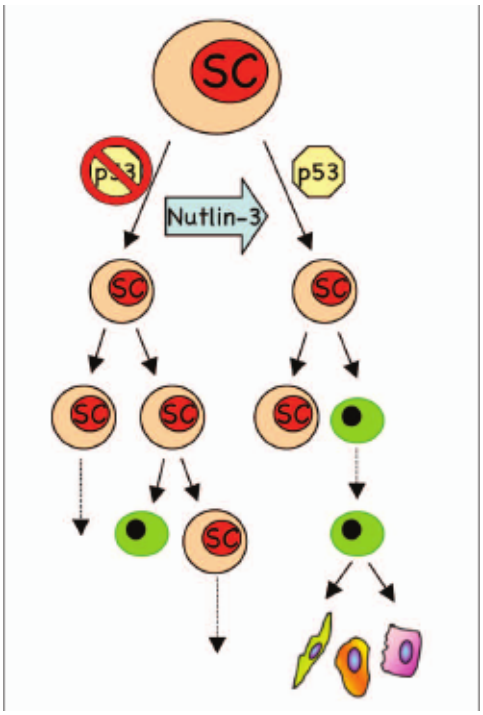

Figure 7.2: **Modelling the role of p53 in tumour development.**
In the absence of a functional p53 SCs divide symmetrically and contribute to the formation of a tumour mass. Restoration of p53 levels with Nutlin-3 treatment switches SC division from symmetric to asymmetric (adapted from Pasi et al., 2010).

This effect was also confirmed *in vivo*, as tumour mammospheres treated *in vitro* with Nutlin-3 gen-

erated tumours with reduced volumes compared to controls. Interestingly, this was not accompanied by an apoptotic response or by the reduction of proliferating cells, suggesting that the consequence of the restoration of p53 on the tumour mass is to be attributed solely on its effect on SC divisions.

Because tumour expansion is regulated by the proliferative potential and the mode of division of CSCs, and the presence of p53 ensures a tight control on these processes, the possibility to reactivate of the p53 pathway has important therapeutic implications in those cancers where it is altered. Recently, several groups have shown that re-expression of p53 in p53-null tumours results in an apoptotic or senescent response and in the rapid regression of the malignancy (Xue et al., 2007; Ventura et al., 2007; Martins et al., 2006). However, in tumours where p53 is present in its WT form, other mechanisms may be responsible for the impairment of its function. In our tumour model, a constitutively active ErbB2 acts on the localisation of Mdm2, an E3 ubiquitine-ligase that targets p53 for degradation, enhancing its activity. Indeed we have shown that the treatment of MMTV-ErbB2 mice with the Mdm-2 inhibitor Nutlin-3 and the consequent disruption of the p53-degrading pathway in tumour tissues results in an increase in the latency of tumour development and in a reduction of the mass. This is also accompanied by a reduction in the number of CSCs, the putative targets of new anticancer strategies. Favourable therapeutic outcomes can therefore also be achieved by enhancement of the p53 pathway also in the presence of WT p53 alleles, but with attenuated signalling, a situation that is common to approximately 50% of human cancers.

7.2 Myc and Self-Renewal

We have shown that p53 regulates self-renewing divisions in SCs, and imposes asymmetry in the cell fate of the two daughter cells. In the absence of p53, however, the asymmetry is lost and two daughter cells with identical stem properties are formed, thus amplifying the SC pool. Interestingly, the impaired function of p53 is responsible for the increased proliferative potential and the symmetric division in cancer SCs derived from MMTV-ErbB2 tumour tissues, as its restoration is sufficient to revert the phenotype. These findings have very important therapeutic implications for the establishment of new anticancer therapies aimed at the enhancement of the p53 function in the presence of WT alleles with impaired activity. Nevertheless, the mechanism with which p53 regulates SC self-renewal is still unknown, but of great interest for those cancers that lack a normal p53 allele but might follow similar pathways that result in the deregulated activity of SCs. We have investigated the mechanisms that govern SC self-renewal and symmetry of division, and have found that deregulated Myc may act as a putative effector for the increased self-renewal and symmetric divisions in CSCs.

7.2.1 The p53-Myc Axis in the Regulation of SC Self-Renewal

A role for Myc in regulating SC self-renewal has been described in several systems (Betschinger et al., 2006; Kerosuo et al., 2008; Nagao et al., 2008; Zheng et al., 2008).

Interestingly, we found high levels of Myc expression in our mammosphere models with increased self-renewing abilities (p53 KO and tumour mammospheres), which are characterised by absent or functionally impaired p53. This is consistent with the existing evidences for a p53-mediated negative regulation of the transcription of the Myc gene(Sachdeva et al., 2009; Ragimov et al., 1993; Ho et al., 2005). The function of p53 in favouring asymmetric cell division may therefore proceed through the inhibition of its target Myc, and Myc activation in the absence of a functional p53 may be responsible for the induction of symmetric divisions in cancer SCs as depicted in the model in fig. 7.3. We have investigated this pathway to confirm that the regulation of self-renewal and cell divisions in SCs is ascribable to the p53-Myc axis.

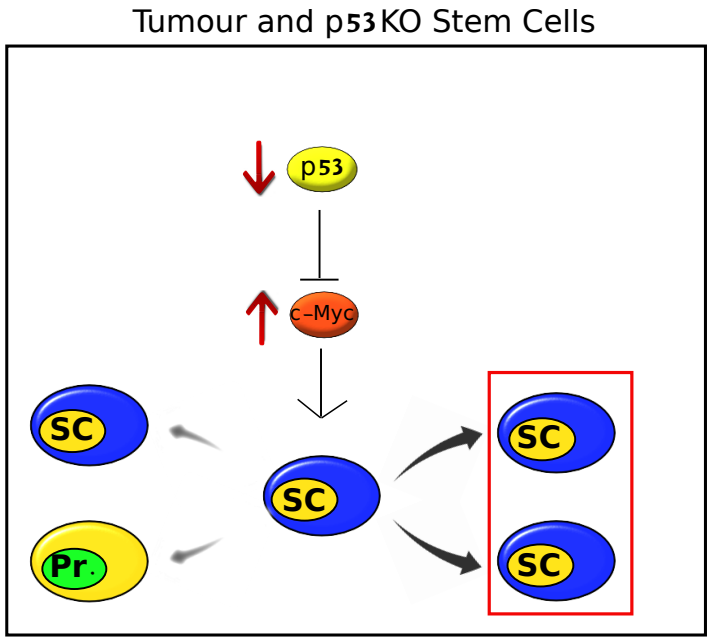

Figure 7.3: **The absence of p53 in cancer and p53 KO SCs promotes symmetric divisions through activation of c-Myc.**
Modelling of the effect of the absence of p53 on the regulation of Myc expression and its effect on SC division. In the absence of its negative regulator p53, Myc is overexpressed and induces SCs to divide symmetrically, a situation that is common to p53 KO and MMTV-ErbB2 SCs.

In this scenario it is reasonable to hypothesise, but still remains unshown, that the restoration of p53 levels in tumour SCs by Nutlin-3 treatment results in the inhibition of the expression of Myc and subsequently a switch in the mode of SC division from symmetric to asymmetric (fig. 7.4).

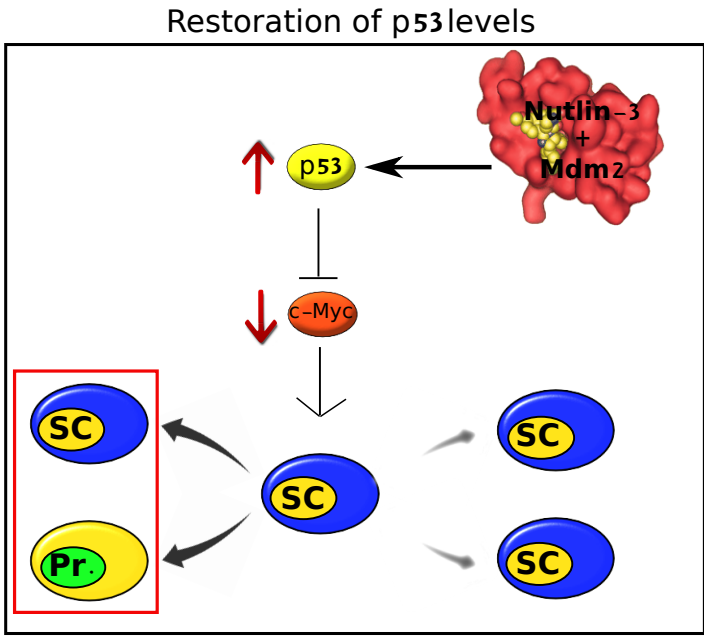

Figure 7.4: **Restoration of p53 levels by Nutlin-3 treatment results in downregulation of Myc and asymmetric SC division.**
Treatment of MMTV-ErbB2 SCs with Nutlin-3 restores the levels of p53 expression. This in turn results in the switch of the SC mode of division from symmetric to asymmetric. We have shown that Myc is responsible for the symmetric divisions of mammary SCs, it is therefore reasonable to hypothesise that Nutlin-3 treatment indirectly induces downregulation of Myc.

Reverse genetics approaches to confirm the function of Myc in controlling SC self-renewal resulted ineffective due to the fact that the silencing of Myc expression was not compatible with cell viability. Our approach was therefore an indirect one, and was aimed at the uncoupling of the p53 and Myc pathways in the regulation of SC divisions in tumour mammospheres. To achieve this, we rendered the expression of Myc independent from the p53-mediated regulation by infecting the cells with a lentiviral vector carrying the Myc protein under a strong promoter. We then treated the cells with Nutlin-3 to restore the levels of p53. Because the exogenous Myc was not negatively controlled by p53, we expected its levels to remain high, and therefore to induce symmetric division thus rendering the treatment with Nutlin-3 ineffective (fig. 7.5).

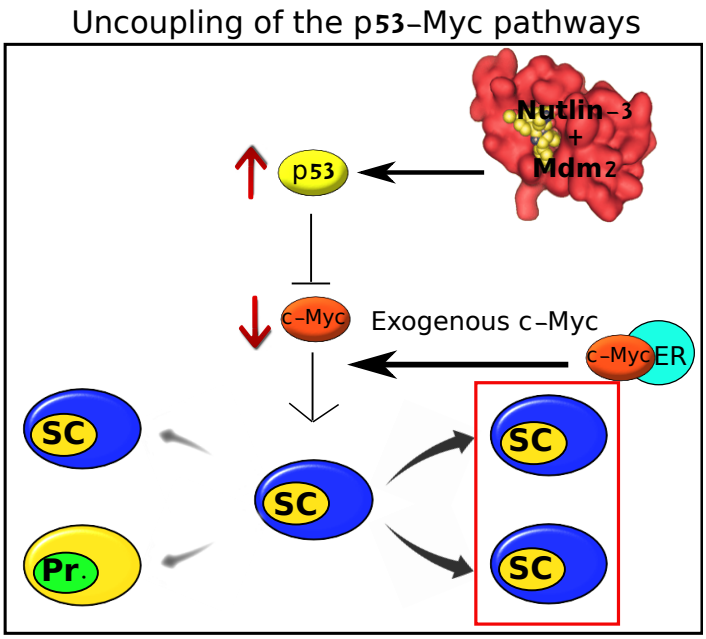

Figure 7.5: **Uncoupling of the p53 and Myc pathways in the regulation of SC divisions.** The expression of exogenous Myc renders the treatment with Nutlin-3 ineffective on SC division, as restored p53 cannot act on the regulation of Myc under a strong promoter. This results in the maintenance of a symmetric mode of SC division independently of the levels of p53 expression.

Indeed, we were able to demonstrate that exogenous Myc expression renders the treatment with Nutlin-3 ineffective, suggesting that indeed it acts downstream to p53 itself. In the context of cancer SCs, these are novel and interesting findings that may broaden the number of available treatments that can target specifically SCs, that may not be targeted by conventional anticancer treatments. To this end it will be of great interest to investigate if this mechanism that governs self-renewal in mammary CSCs is common also to other tumour types.

7.2.2 Different Thresholds of Myc Expression Have Different Effects on SCs

Deeper analysis on the involvement of Myc in self-renewal regulation led us to identify two diametrically opposed situations resulting from the overexpression of Myc in mammary SCs. In fact, depending on the levels of Myc expression we found that SCs responded either by activating a p53-mediated checkpoint (high levels) or by increasing their self-renewing properties (low levels). We have shown that expression of Myc at high levels triggers in SCs an apoptotic checkpoint associated with phosphorilation and stabilisation of p53, and the expression of p21/WAF1, a p53 transcriptional target(el-Deiry el Deiry, 1993) . This phenotype was indeed consistent with an oncogene-induced, p53-dependent apoptotic checkpoint (Ray et al., 2006; Halazonetis et al., 2008). Accordingly, the absence of p53 protected the SCs from apoptosis when expressing high levels of Myc. The robust DNA-damage response in the presence of high levels of Myc is consistent with the oncogene-induced DNA replication stress model, which postulates that aberrant

oncogene activation induces DNA replication fork collapse, formation of DNA double-strand breaks and genomic instability targeting preferentially specific sites in the genome that are referred to as common fragile sites (Halazonetis et al., 2008; Di Micco et al., 2006; Bartkova et al., 2006). Indeed, high levels of Myc have already been shown to induce genomic instability (Mai et al., 1996).

Conversely, low levels of Myc expression resulted in increased self-renewal and lifespan of normal mammary SCs, as they continuously expanded in culture and could be passaged virtually indefinitely. Interestingly, low levels of Myc activation did not induce the expression of checkpoint genes such as p53, or p21/WAP, suggesting that low levels of Myc do not act through the activation of p53. Accordingly, p53 was perfectly functional, as activation of stress induced its phosphorilation and stabilisation. Finally, p53 KO mammospheres transduced with the Myc lentivirus did not acquire additional self-renewing abilities upon expression of low levels of Myc. These observations suggest that low levels of Myc expression do not act through the activation of p53, and do not create selective pressure to lose the p53-mediated checkpoint. In fact, they are not sufficient to activate a p53-dependent oncogene-induced checkpoint.

A dual effect for Myc depending on the levels of its expression had been described previously by Murphy et al. by using a conditional mouse model for the expression of Myc in the Rosa26 locus, which allows for low levels of expression. Expression of low levels of Myc induced hyperproliferation but not apoptosis in several tissues including pancreas, liver, kidneys and lung. On the contrary, when expressed at high levels in a different model, Myc induced growth arrest and activation of ARF (Murphy et al., 2008). These and our observations show that the expression of Myc can have different effects depending on its expression levels. Interestingly, very preliminar data show that induction of high levels of Myc expression in MMTV-ErbB2 tumour SCs are sufficient to induce growth arrest of tumour mammospheres, indicating that the sensitivity to Myc thresholds is maintained in transformed SCs despite them already exhibiting higher levels of Myc expression compared to WT SCs (data not shown).

From a biological point of view, Myc does not transform normal SCs, as transplantation of these cells into recipient mice resulted in the formation of normal tissues two months after engraftment. Currently, transplanted mice do not show any formation of palpable masses in the transplantation sites (7 months). Interestingly, us and others have shown that p53 KO SCs transplanted into the cleared fat-pad of recipient mice form normal mammary tissues. However, it has been reported that these tissues undergo spontaneous transformation with a latency of about 50 weeks without any hormonal stimulation (Jerry et al., 2000). Because the absence of p53 and overexpression of Myc seem to be part of one single mechanism, it is reasonable to hypothesise that tumour formation in low Myc-expressing cells may occur with long latency, or even, due to the tumour-suppressor activity of p53 that is still present and active in these cells, it may even take longer than in the absence of p53.

7.3 Dual Effect of Myc on Stem and Progenitor Cells

The rapid expansion of the Myc-expressing mammosphere cultures suggests that each mammosphere contains more than one SC. Two possible mechanisms can account for this phenotype depending on whether Myc acts on SCs or progenitors. We have shown that Myc is responsible for the increased self-renewal in tumour SCs and p53 KO SCs, and it is reasonable to believe that a similar effect is found in WT SCs with enforced expression of Myc at low levels. Nevertheless, we could not exclude that Myc also acts on progenitor cells by reprogramming them into new SCs.

7.3.1 Effect of Myc on Mammary SCs

We have shown that Myc increases the lifespan of WT SCs if expressed at low levels, and that it also increases their replicative potential. The ever-expanding mammosphere culture in low Myc-expressing cells suggests that the SC pool is in continuous expansion. This is reflected in the continuous expansion of mammosphere initiating cell at every passage. Indeed we have demonstrated (Cicalese et al., 2009)that mammosphere-initiating cells and SCs coincide in normal and tumour mammospheres. We can therefore assume that the number of mammosphere-initiating cells in low Myc-expressing mammospheres corresponds to the frequency of SCs per mammosphere (~15 per sphere). We have shown that the expansion in the number of SCs is ascribable to a switch from an asymmetric to a symmetric mode of division of SCs. Indeed we show that a similar mechanism is activated upon expression of low levels of Myc. In fact, isolation of PKH^{high}cells and visualisation of the first few divisions during mammosphere formation led us to the conclusion that whereas SCs infected with a control vector showed proliferative asymmetry in the two daughter cells, the expression of Myc was sufficient to induce a switch in the mode of division, and SCs mainly generated two daughter cells with analogous proliferating capacities. Indeed, we confirmed this also by staining the dividing SC with an antibody that recognises the fate determinant Numb and found that it is indeed asymmetrically distributed in WT SCs but uniformly localised on the membrane of dividing SCs that express low levels of Myc. Interestingly, recent evidences have been published to show that Numb regulates the activity of p53, therefore representing an upstream link to the p53-Myc axis in the regulation of SC division (Colaluca et al., 2008). It will be of great interest to study this axis in relation to SC division regulation.

7.3.2 Effect of Myc Expression on Progenitor Cells

Myc enhances the efficiency of reprogramming of somatic cells into pluripotent cells by about a thousand-fold(Nakagawa et al., 2008). Induction of the pluripotent state requires genome-wide demethylation (Mikkelsen et al., 2008), which is difficult to achieve (Kim et al., 2010) therefore explaining the low frequency of reprogramming events in the transition from fibroblasts to iPS cells. It is reasonable to

assume that reprogramming of somatic cells to SCs of the same tissue type may not require such extensive genome-wide demethylation and might, therefore, be more readily achievable. To investigate the effect of low Myc expression on progenitor cells and its contribution to the increased self-renewing abilities of WT mammospheres expressing Myc, we deprived the mammosphere culture of the SCs by fractionating these cells with the already described PKH assay. We have demonstrated that in WT samples PKH^{high}cells are enriched in SCs (1 in 3), and that the PKH^{neg}do not contain any cells with stem properties, however, we refer to PKH^{neg} cells as progenitors but the formal demonstration that they are progenitors is still lacking in our system. Nevertheless, evidence obtained using human mammary PKH^{neg} cells show that upon plating in a collagen-based matrix (which allows differentiation), these cells can only form either epithelial or myoepithelial colonies (never mixed colonies as expected with SCs). Under the same experimental conditions, PKH^{high} cells form mixed colonies, confirming that they are indeed SCs (Pece et al., 2010).

Strikingly, we observed that upon expression of low levels of Myc, PKH^{neg} progenitor cells were able to survive anoikis and acquire self-renewing abilities. In fact, whereas control infected progenitors only formed small irregular aggregates that had no self-renewing abilities and could not be passaged in culture, low Myc-expressing progenitors formed mammospheres that could be serially passaged and possessed increased growth kinetics compared to WT mammospheres. Strikingly, we measured the regenerative potential of these cells by transplantation in cleared fat-pads of recipient mice and we found that these cells are able to form, albeit with low frequency, a normal mammary gland. Indeed their regenerative potential together with the acquired self-renewing abilities suggested that progenitor cells had undergone a cellular reprogramming that led to the formation of SCs. Interestingly, like iPS cells can be induced to differentiate into different tissues (Wernig et al., 2008; Hanna et al., 2007; Dimos et al., 2008), reprogrammed mammary progenitors can differentiate and give rise to a normal mammary gland, a process that is probably accompanied by epigenetic alterations and downregulation of the exogenously expressed Myc protein.

These data show that the effect of Myc on mammary epithelial cells acts on two levels: by inducing symmetric divisions in SCs thus expanding their pool, and by stochastically reprogramming progenitor cells into new SCs (Fig.7.6).

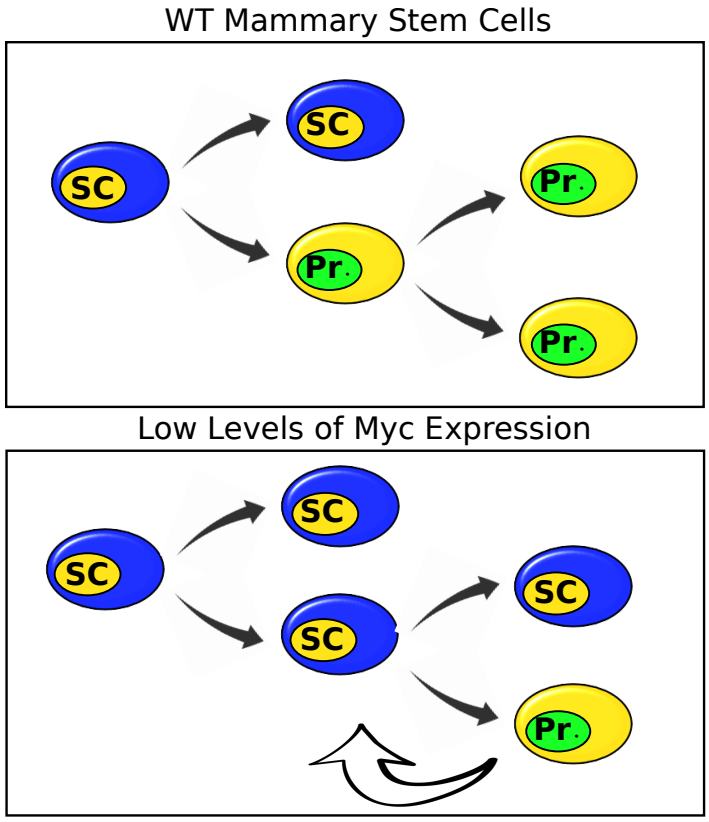

Figure 7.6: **Modelling of the effect of Myc on mammary epithelial cells.** Schematic representation of the SC division in normal cells (asymmetry of division) and in cells where Myc is overexpressed at low levels (symmetry of division and stochastic reprogramming). Normal SCs divide asymmetrically to generate a SC that remains quiescent and a progenitor cell that is able to proliferate and differentiate. When Myc is expressed at low levels, but still higher than the basal levels, SCs undergo symmetric divisions generating two daughter cells with stem properties. Moreover, the expression of Myc is sufficient to induce stochastic reprogramming of progenitor cells into new SCs. Together, these two mechanisms account for the continuous expansion of the SC pool in low Myc-expressing samples.

Indeed, newly reprogrammed SCs are subject to the same induction of symmetric divisions in response to low levels of Myc expression. In fact, if the only effect of Myc was that of reprogramming progenitors into SCs, then these cells would behave as WT mammospheres in serial re-plating experiments, and progressively exhaust or show a slight increase in the yield of mammospheres compared to normal SCs, proportional to the frequency of reprogramming in progenitors, which is very low. On the contrary, the experiments demonstrate that Myc, on top of its reprogramming effect, confers new properties to SCs, regardless whether they are obtained from PKH^{neg} cells or WT mammospheres: Myc, in fact, increases self-renewal (measured by the increased number of mammospheres at each passage, which is due to its ability to increase the frequency of symmetric divisions) and confers immortality (based on the fact that the mammosphere cultures do no exhaust). In summary, data suggest three separated effects of Myc: *i)* reprogramming of progenitors, *ii)* increased self-renewal of SCs (increased frequency of symmetric divisions), *iii)* immortalisation of SCs.

It still remains to be demonstrated whether these effects are part of the same phenotype (e.g. whether they are hierarchically linked) or whether they are three (mechanistically) independent effects. However, these findings challenge the current postulation of the cancer stem cell theory that identifies the target of transformation with normal SC, as the first stages of cellular immortalisation may induce progenitor reprogramming if they alter the expression of specific genes. The best fitting theory for cancer development to the model that we postulate is therefore the interconversion model, which stands between the clonal evolution model and the cancer SC theory, and takes into consideration that any cell may be the target of transformation and not only SCs, as the cancer SC theory postulates. On the other hand, targeting of any cell in a given tissue may proceed by reprogramming of this cell into a CSC with stem properties, thus accomodating recent evidences for the existence of SCs in the tumour bulk. From a clinical point of view, these findings have tremendous implications, as the eradication of tumours may require not only to target specifically the CSCs, but also those mechanisms that may induce reprogramming of tumour cells into cells with CSC properties.

7.3.3 Myc-Induced Reprogramming and Genomic Instability

The reprogramming of adult cells into SCs has been extensively developed in the last few years and has raised hopes for the treatment of several human diseases. The reprogramming involves the expression of different genes and Myc is typically included in this mix. However, expression of oncogenes leads to DNA replication stress and genomic instability that activate a p53-dependent response. We wondered if the reprogramming that results from the expression of proto-oncogene Myc can be associated with genomic instability and to this end we analysed five reprogrammed clones for genomic aberrations.

Interestingly, we show that all the analysed cloned had genomic alterations in regions of known fragile sites, based on the homology with the human common fragile sites (Helmrich et al., 2006). Given that we only analysed a quarter of the mouse genome, it is reasonable to assume that with this protocol one could only obtain reprogrammed SCs with genomic rearrangements. Two mechanisms may contribute to the observed genomic instability. The first may involve oncogene-induced DNA replication stress and the presence of deletions in common fragile sites in two of our clones suggest that this mechanism may be relevant(Halazonetis et al., 2008; Bartkova et al., 2006; Di Micco et al., 2006). The second mechanism may relate to the reprogramming process itself. Reprogramming requires DNA demethylation, which is currently thought to involve induction of DNA damage and subsequent DNA repair-mediated replacement of methylated cytosines by unmethylated cytosines (Gehring et al., 2009; Mikkelsen et al., 2008). Perhaps, the single-stranded DNA breaks generated during DNA repair lead to genomic instability in replicating cells, whereas DNA demethylation in primordial germ cells occurs in the G2 phase of the cell cycle (Hajkova et al., 2008).

A key question is whether a few genomic aberrations can compromise the function and utility of

reprogrammed SCs. In our case, the mammary SCs were capable of repopulating cleared fat pads and none of the mammary glands derived from these cells have become cancerous so far. This would be consistent with the apparent transient nature of the genomic instability during the reprogramming process itself. It would now be interesting to examine if iPS cells also exhibit genomic aberrations. Because reprogramming of somatic cells to pluripotent SCs is more efficient in a p53 KO background (Utikal et al., 2009; Hong et al., 2009; Kawamura et al., 2009; Marion et al., 2009), we speculate that reprogramming of those cells is also associated with some form of genomic instability. Indeed, these finding challenge the use of reprogrammed SCs in the clinic and may open new questions on the true identity of these cells.

8 References

References

Ahn, S., Joyner, A. L., Oct. 2005. In vivo analysis of quiescent adult neural stem cells responding to sonic hedgehog. Nature 437 (7060), 894–7.

Akala, O. O., Park, I.-K., Qian, D., Pihalja, M., Becker, M. W., Clarke, M. F., May 2008. Long-term haematopoietic reconstitution by trp53-/-p16ink4a-/-p19arf-/- multipotent progenitors. Nature 453 (7192), 228–32.

Al-Hajj, M., Wicha, M. S., Benito-Hernandez, A., Morrison, S. J., Clarke, M. F., Apr. 2003. Prospective identification of tumorigenic breast cancer cells. Proc Natl Acad Sci U S A 100 (7), 3983–8.

Alvi, A. J., Clayton, H., Joshi, C., Enver, T., Ashworth, A., d M Vivanco, M., Dale, T. C., Smalley, M. J., 2003. Functional and molecular characterisation of mammary side population cells. Breast Cancer Res 5 (1), R1–8.

Armesilla-Diaz, A., Bragado, P., Del Valle, I., Cuevas, E., Lazaro, I., Martin, C., Cigudosa, J. C., Silva, A., Feb. 2009. p53 regulates the self-renewal and differentiation of neural precursors. Neuroscience 158 (4), 1378–89.

Baas, A. F., Smit, L., Clevers, H., Jun. 2004. Lkb1 tumor suppressor protein: Partaker in cell polarity. Trends Cell Biol 14 (6), 312–9.

Barry, R. E., Krek, W., Sep. 2004. The von hippel-lindau tumour suppressor: a multi-faceted inhibitor of tumourigenesis. Trends Mol Med 10 (9), 466–72.

Bartkova, J., Rezaei, N., Liontos, M., Karakaidos, P., Kletsas, D., Issaeva, N., Vassiliou, L.-V. F., Kolettas, E., Niforou, K., Zoumpourlis, V. C., Takaoka, M., Nakagawa, H., Tort, F., Fugger, K., Johansson, F., Sehested, M., Andersen, C. L., Dyrskjot, L., Arntoft, T., Lukas, J., Kittas, C., Helleday, T., Halazonetis, T. D., Bartek, J., Gorgoulis, V. G., Nov. 2006. Oncogene-induced senescence is part of the tumorigenesis barrier imposed by dna damage checkpoints. Nature 444 (7119), 633–7.

Beachy, P. A., Karhadkar, S. S., Berman, D. M., Nov. 2004. Tissue repair and stem cell renewal in carcinogenesis. Nature 432 (7015), 324–31.

Betschinger, J., Mechtler, K., Knoblich, J. A., Mar. 2006. Asymmetric segregation of the tumor suppressor brat regulates self-renewal in drosophila neural stem cells. Cell 124 (6), 1241–53.

Bignell, G. R., Greenman, C. D., Davies, H., Butler, A. P., Edkins, S., Andrews, J. M., Buck, G., Chen, L., Beare, D., Latimer, C., Widaa, S., Hinton, J., Fahey, C., Fu, B., Swamy, S., Dalgliesh, G. L., Teh,

B. T., Deloukas, P., Yang, F., Campbell, P. J., Futreal, P. A., Stratton, M. R., Feb. 2010. Signatures of mutation and selection in the cancer genome. Nature 463 (7283), 893–8.

Bodine, D. M., Seidel, N. E., Orlic, D., Jul. 1996. Bone marrow collected 14 days after in vivo administration of granulocyte colony-stimulating factor and stem cell factor to mice has 10-fold more repopulating ability than untreated bone marrow. Blood 88 (1), 89–97.

Boman, B. M., Huang, E., Jun. 2008. Human colon cancer stem cells: a new paradigm in gastrointestinal oncology. J Clin Oncol 26 (17), 2828–38.

Bonnefoix, T., Bonnefoix, P., Verdiel, P., Sotto, J. J., Aug. 1996. Fitting limiting dilution experiments with generalized linear models results in a test of the single-hit poisson assumption. J Immunol Methods 194 (2), 113–9.

Campbell, L. L., Polyak, K., Oct. 2007. Breast tumor heterogeneity: cancer stem cells or clonal evolution? Cell Cycle 6 (19), 2332–8.

Cariati, M., Purushotham, A. D., Jan. 2008. Stem cells and breast cancer. Histopathology 52 (1), 99–107.

Cartwright, P., McLean, C., Sheppard, A., Rivett, D., Jones, K., Dalton, S., Mar. 2005. Lif/stat3 controls es cell self-renewal and pluripotency by a myc-dependent mechanism. Development 132 (5), 885–96.

Caussinus, E., Gonzalez, C., Oct. 2005. Induction of tumor growth by altered stem-cell asymmetric division in drosophila melanogaster. Nat Genet 37 (10), 1125–9.

Charafe-Jauffret, E., Ginestier, C., Iovino, F., Wicinski, J., Cervera, N., Finetti, P., Hur, M.-H., Diebel, M. E., Monville, F., Dutcher, J., Brown, M., Viens, P., Xerri, L., Bertucci, F., Stassi, G., Dontu, G., Birnbaum, D., Wicha, M. S., Feb. 2009. Breast cancer cell lines contain functional cancer stem cells with metastatic capacity and a distinct molecular signature. Cancer Res 69 (4), 1302–13.

Chenn, A., McConnell, S. K., Aug. 1995. Cleavage orientation and the asymmetric inheritance of notch1 immunoreactivity in mammalian neurogenesis. Cell 82 (4), 631–41.

Cho, R. W., Wang, X., Diehn, M., Shedden, K., Chen, G. Y., Sherlock, G., Gurney, A., Lewicki, J., Clarke, M. F., Feb. 2008. Isolation and molecular characterization of cancer stem cells in mmtv-wnt-1 murine breast tumors. Stem Cells 26 (2), 364–71.

Cicalese, A., Bonizzi, G., Pasi, C. E., Faretta, M., Ronzoni, S., Giulini, B., Brisken, C., Minucci, S., Di Fiore, P. P., Pelicci, P. G., Sep 2009. The tumor suppressor p53 regulates polarity of self-renewing divisions in mammary stem cells. Cell 138 (6), 1083–95.

Clarke, M. F., Fuller, M., Mar. 2006. Stem cells and cancer: two faces of eve. Cell 124 (6), 1111–5.

Clement, V., Sanchez, P., de Tribolet, N., Radovanovic, I., Ruiz i Altaba, A., Jan. 2007. Hedgehog-gli1 signaling regulates human glioma growth, cancer stem cell self-renewal, and tumorigenicity. Curr Biol 17 (2), 165–72.

Clevers, H., Oct. 2005. Stem cells, asymmetric division and cancer. Nat Genet 37 (10), 1027–8.

Cleynen, I., Van de Ven, W. J. M., Feb. 2008. The hmga proteins: a myriad of functions (review). Int J Oncol 32 (2), 289–305.

Colaluca, I. N., Tosoni, D., Nuciforo, P., Senic-Matuglia, F., Galimberti, V., Viale, G., Pece, S., Di Fiore, P. P., Jan. 2008. Numb controls p53 tumour suppressor activity. Nature 451 (7174), 76–80.

Conboy, I. M., Rando, T. A., Sep. 2002. The regulation of notch signaling controls satellite cell activation and cell fate determination in postnatal myogenesis. Dev Cell 3 (3), 397–409.

Cotterman, R., Jin, V. X., Krig, S. R., Lemen, J. M., Wey, A., Farnham, P. J., Knoepfler, P. S., Dec. 2008. N-myc regulates a widespread euchromatic program in the human genome partially independent of its role as a classical transcription factor. Cancer Res 68 (23), 9654–62.

Dalerba, P., Dylla, S. J., Park, I.-K., Liu, R., Wang, X., Cho, R. W., Hoey, T., Gurney, A., Huang, E. H., Simeone, D. M., Shelton, A. A., Parmiani, G., Castelli, C., Clarke, M. F., Jun. 2007. Phenotypic characterization of human colorectal cancer stem cells. Proc Natl Acad Sci U S A 104 (24), 10158–63.

Daniel, C. W., De Ome, K. B., Young, J. T., Blair, P. B., Faulkin, L. J., Sep. 1968. The in vivo life span of normal and preneoplastic mouse mammary glands: a serial transplantation study. Proc Natl Acad Sci U S A 61 (1), 53–60.

Dave, B., Chang, J., Mar. 2009. Treatment resistance in stem cells and breast cancer. J Mammary Gland Biol Neoplasia 14 (1), 79–82.

Davis, A. C., Wims, M., Spotts, G. D., Hann, S. R., Bradley, A., Apr. 1993. A null c-myc mutation causes lethality before 10.5 days of gestation in homozygotes and reduced fertility in heterozygous female mice. Genes Dev 7 (4), 671–82.

DEOME, K. B., FAULKIN, L. J., BERN, H. A., BLAIR, P. B., Jun. 1959. Development of mammary tumors from hyperplastic alveolar nodules transplanted into gland-free mammary fat pads of female c3h mice. Cancer Res 19 (5), 515–20.

Dho, S. E., Trejo, J., Siderovski, D. P., McGlade, C. J., Sep. 2006. Dynamic regulation of mammalian numb by g protein-coupled receptors and protein kinase c activation: Structural determinants of numb association with the cortical membrane. Mol Biol Cell 17 (9), 4142–55.

Di Micco, R., Fumagalli, M., Cicalese, A., Piccinin, S., Gasparini, P., Luise, C., Schurra, C., Garre', M., Nuciforo, P. G., Bensimon, A., Maestro, R., Pelicci, P. G., d'Adda di Fagagna, F., Nov. 2006. Oncogene-induced senescence is a dna damage response triggered by dna hyper-replication. Nature 444 (7119), 638–42.

Dimos, J. T., Rodolfa, K. T., Niakan, K. K., Weisenthal, L. M., Mitsumoto, H., Chung, W., Croft, G. F., Saphier, G., Leibel, R., Goland, R., Wichterle, H., Henderson, C. E., Eggan, K., Aug. 2008. Induced pluripotent stem cells generated from patients with als can be differentiated into motor neurons. Science 321 (5893), 1218–21.

Doetsch, F., Petreanu, L., Caille, I., Garcia-Verdugo, J. M., Alvarez-Buylla, A., Dec. 2002. Egf converts transit-amplifying neurogenic precursors in the adult brain into multipotent stem cells. Neuron 36 (6), 1021–34.

Dontu, G., Abdallah, W. M., Foley, J. M., Jackson, K. W., Clarke, M. F., Kawamura, M. J., Wicha, M. S., May 2003. In vitro propagation and transcriptional profiling of human mammary stem/progenitor cells. Genes Dev 17 (10), 1253–70.

el-Deiry el Deiry, W., Nov. 1993. Waf1, a potential mediator of p53 tumor suppression. Cell 75 (4), 817–25.

Fan, X., Khaki, L., Zhu, T. S., Soules, M. E., Talsma, C. E., Gul, N., Koh, C., Zhang, J., Li, Y.-M., Maciaczyk, J., Nikkhah, G., Dimeco, F., Piccirillo, S., Vescovi, A. L., Eberhart, C. G., Jan. 2010. Notch pathway blockade depletes cd133-positive glioblastoma cells and inhibits growth of tumor neurospheres and xenografts. Stem Cells 28 (1), 5–16.

Fan, X., Matsui, W., Khaki, L., Stearns, D., Chun, J., Li, Y.-M., Eberhart, C. G., Aug. 2006. Notch pathway inhibition depletes stem-like cells and blocks engraftment in embryonal brain tumors. Cancer Res 66 (15), 7445–52.

Farnie, G., Clarke, R. B., Spence, K., Pinnock, N., Brennan, K., Anderson, N. G., Bundred, N. J., Apr. 2007. Novel cell culture technique for primary ductal carcinoma in situ: role of notch and epidermal growth factor receptor signaling pathways. J Natl Cancer Inst 99 (8), 616–27.

Gatza, C. E., Dumble, M., Kittrell, F., Edwards, D. G., Dearth, R. K., Lee, A. V., Xu, J., Medina, D., Donehower, L. A., Jan. 2008. Altered mammary gland development in the p53+/m mouse, a model of accelerated aging. Dev Biol 313 (1), 130–41.

Gehring, M., Bubb, K. L., Henikoff, S., Jun. 2009. Extensive demethylation of repetitive elements during seed development underlies gene imprinting. Science 324 (5933), 1447–51.

Gera, J. F., Mellinghoff, I. K., Shi, Y., Rettig, M. B., Tran, C., hsin Hsu, J., Sawyers, C. L., Lichtenstein, A. K., Jan. 2004. Akt activity determines sensitivity to mammalian target of rapamycin (mtor) inhibitors by regulating cyclin d1 and c-myc expression. J Biol Chem 279 (4), 2737–46.

Gil, J., Stembalska, A., Pesz, K. A., Sasiadek, M. M., 2008. Cancer stem cells: the theory and perspectives in cancer therapy. J Appl Genet 49 (2), 193–9.

Ginestier, C., Hur, M. H., Charafe-Jauffret, E., Monville, F., Dutcher, J., Brown, M., Jacquemier, J., Viens, P., Kleer, C. G., Liu, S., Schott, A., Hayes, D., Birnbaum, D., Wicha, M. S., Dontu, G., Nov. 2007. Aldh1 is a marker of normal and malignant human mammary stem cells and a predictor of poor clinical outcome. Cell Stem Cell 1 (5), 555–67.

Godar, S., Ince, T. A., Bell, G. W., Feldser, D., Donaher, J. L., Bergh, J., Liu, A., Miu, K., Watnick, R. S., Reinhardt, F., McAllister, S. S., Jacks, T., Weinberg, R. A., Jul. 2008. Growth-inhibitory and tumor- suppressive functions of p53 depend on its repression of cd44 expression. Cell 134 (1), 62–73.

Gonzalez, C., Jun. 2007. Spindle orientation, asymmetric division and tumour suppression in drosophila stem cells. Nat Rev Genet 8 (6), 462–72.

Grange, C., Lanzardo, S., Cavallo, F., Camussi, G., Bussolati, B., Dec. 2008. Sca-1 identifies the tumor-initiating cells in mammary tumors of balb-neut transgenic mice. Neoplasia 10 (12), 1433–43.

Gray, D. A., Inazawa, J., Gupta, K., Wong, A., Ueda, R., Takahashi, T., Jun. 1995. Elevated expression of unph, a proto-oncogene at 3p21.3, in human lung tumors. Oncogene 10 (11), 2179–83.

Grifoni, D., Garoia, F., Schimanski, C. C., Schmitz, G., Laurenti, E., Galle, P. R., Pession, A., Cavicchi, S., Strand, D., Nov. 2004. The human protein hugl-1 substitutes for drosophila lethal giant larvae tumour suppressor function in vivo. Oncogene 23 (53), 8688–94.

Gupta, P. B., Chaffer, C. L., Weinberg, R. A., Sep. 2009. Cancer stem cells: mirage or reality? Nat Med 15 (9), 1010–2.

Guzman, M. L., Swiderski, C. F., Howard, D. S., Grimes, B. A., Rossi, R. M., Szilvassy, S. J., Jordan, C. T., Dec. 2002. Preferential induction of apoptosis for primary human leukemic stem cells. Proc Natl Acad Sci U S A 99 (25), 16220–5.

Hajkova, P., Ancelin, K., Waldmann, T., Lacoste, N., Lange, U. C., Cesari, F., Lee, C., Almouzni, G., Schneider, R., Surani, M. A., Apr. 2008. Chromatin dynamics during epigenetic reprogramming in the mouse germ line. Nature 452 (7189), 877–81.

Halazonetis, T. D., Gorgoulis, V. G., Bartek, J., Mar. 2008. An oncogene-induced dna damage model for cancer development. Science 319 (5868), 1352–5.

Hanna, J., Wernig, M., Markoulaki, S., Sun, C.-W., Meissner, A., Cassady, J. P., Beard, C., Brambrink, T., Wu, L.-C., Townes, T. M., Jaenisch, R., Dec. 2007. Treatment of sickle cell anemia mouse model with ips cells generated from autologous skin. Science 318 (5858), 1920–3.

Helmrich, A., Stout-Weider, K., Hermann, K., Schrock, E., Heiden, T., Oct. 2006. Common fragile sites are conserved features of human and mouse chromosomes and relate to large active genes. Genome Res 16 (10), 1222–30.

Hennighausen, L., Robinson, G. W., Oct. 2001. Signaling pathways in mammary gland development. Dev Cell 1 (4), 467–75.

Hennighausen, L., Robinson, G. W., Sep. 2005. Information networks in the mammary gland. Nat Rev Mol Cell Biol 6 (9), 715–25.

Herrera-Merchan, A., Cerrato, C., Luengo, G., Dominguez, O., Piris, M. A., Serrano, M., Gonzalez, S., Aug. 2010. mir-33-mediated downregulation of p53 controls hematopoietic stem cell self-renewal. Cell Cycle 9 (16).

Ho, J. S. L., Ma, W., Mao, D. Y. L., Benchimol, S., Sep. 2005. p53-dependent transcriptional repression of c-myc is required for g1 cell cycle arrest. Mol Cell Biol 25 (17), 7423–31.

Hong, H., Takahashi, K., Ichisaka, T., Aoi, T., Kanagawa, O., Nakagawa, M., Okita, K., Yamanaka, S., Aug. 2009. Suppression of induced pluripotent stem cell generation by the p53-p21 pathway. Nature 460 (7259), 1132–5.

Huang, S., Law, P., Francis, K., Palsson, B. O., Ho, A. D., Oct. 1999. Symmetry of initial cell divisions among primitive hematopoietic progenitors is independent of ontogenic age and regulatory molecules. Blood 94 (8), 2595–604.

Huff, C. A., Matsui, W., Smith, B. D., Jones, R. J., Jan. 2006. The paradox of response and survival in cancer therapeutics. Blood 107 (2), 431–4.

Hugo, H., Ackland, M. L., Blick, T., Lawrence, M. G., Clements, J. A., Williams, E. D., Thompson, E. W., Nov. 2007. Epithelial–mesenchymal and mesenchymal–epithelial transitions in carcinoma progression. J Cell Physiol 213 (2), 374–83.

Hutchin, M. E., Kariapper, M. S. T., Grachtchouk, M., Wang, A., Wei, L., Cummings, D., Liu, J., Michael, L. E., Glick, A., Dlugosz, A. A., Jan. 2005. Sustained hedgehog signaling is required for basal cell carcinoma proliferation and survival: conditional skin tumorigenesis recapitulates the hair growth cycle. Genes Dev 19 (2), 214–23.

Huttner, W. B., Kosodo, Y., Dec. 2005. Symmetric versus asymmetric cell division during neurogenesis in the developing vertebrate central nervous system. Curr Opin Cell Biol 17 (6), 648–57.

Ikushima, H., Todo, T., Ino, Y., Takahashi, M., Miyazawa, K., Miyazono, K., Nov. 2009. Autocrine tgf-beta signaling maintains tumorigenicity of glioma-initiating cells through sry-related hmg-box factors. Cell Stem Cell 5 (5), 504–14.

Illmensee, K., Mintz, B., Feb. 1976. Totipotency and normal differentiation of single teratocarcinoma cells cloned by injection into blastocysts. Proc Natl Acad Sci U S A 73 (2), 549–53.

Ito, K., Bernardi, R., Morotti, A., Matsuoka, S., Saglio, G., Ikeda, Y., Rosenblatt, J., Avigan, D. E., Teruya-Feldstein, J., Pandolfi, P. P., Jun. 2008. Pml targeting eradicates quiescent leukaemia-initiating cells. Nature 453 (7198), 1072–8.

Januschke, J., Gonzalez, C., Nov. 2008. Drosophila asymmetric division, polarity and cancer. Oncogene 27 (55), 6994–7002.

Jerry, D. J., Kittrell, F. S., Kuperwasser, C., Laucirica, R., Dickinson, E. S., Bonilla, P. J., Butel, J. S., Medina, D., Feb. 2000. A mammary-specific model demonstrates the role of the p53 tumor suppressor gene in tumor development. Oncogene 19 (8), 1052–8.

Jerry, D. J., Kuperwasser, C., Downing, S. R., Pinkas, J., He, C., Dickinson, E., Marconi, S., Naber, S. P., Nov. 1998. Delayed involution of the mammary epithelium in balb/c-p53null mice. Oncogene 17 (18), 2305–12.
URL 1

Jin, L., Lee, E. M., Ramshaw, H. S., Busfield, S. J., Peoppl, A. G., Wilkinson, L., Guthridge, M. A., Thomas, D., Barry, E. F., Boyd, A., Gearing, D. P., Vairo, G., Lopez, A. F., Dick, J. E., Lock, R. B., Jul. 2009. Monoclonal antibody-mediated targeting of cd123, il-3 receptor alpha chain, eliminates human acute myeloid leukemic stem cells. Cell Stem Cell 5 (1), 31–42.

Jordan, C. T., Guzman, M. L., Noble, M., Sep. 2006. Cancer stem cells. N Engl J Med 355 (12), 1253–61.

Kammerer, S., Roth, R. B., Hoyal, C. R., Reneland, R., Marnellos, G., Kiechle, M., Schwarz-Boeger, U., Griffiths, L. R., Ebner, F., Rehbock, J., Cantor, C. R., Nelson, M. R., Braun, A., Feb. 2005. Association of the numa region on chromosome 11q13 with breast cancer susceptibility. Proc Natl Acad Sci U S A 102 (6), 2004–9.

Kastan, M. B., Berkovich, E., May 2007. p53: a two-faced cancer gene. Nat Cell Biol 9 (5), 489–91.

Kawamura, T., Suzuki, J., Wang, Y. V., Menendez, S., Morera, L. B., Raya, A., Wahl, G. M., Belmonte, J. C. I., Aug. 2009. Linking the p53 tumour suppressor pathway to somatic cell reprogramming. Nature 460 (7259), 1140–4.

Kerosuo, L., Fox, H., PerÃÂ€lÃÂ€, N., Ahlqvist, K., Suomalainen, A., Westermarck, J., Sariola, H., Wartiovaara, K., Jul. 2010. Cip2a increases self-renewal and is linked to myc in neural progenitor cells. Differentiation 80 (1), 68–77.

Kerosuo, L., Piltti, K., Fox, H., Angers-Loustau, A., Hayry, V., Eilers, M., Sariola, H., Wartiovaara, K., Dec. 2008. Myc increases self-renewal in neural progenitor cells through miz-1. J Cell Sci 121 (Pt 23), 3941–50.

Kim, K., Doi, A., Wen, B., Ng, K., Zhao, R., Cahan, P., Kim, J., Aryee, M. J., Ji, H., Ehrlich, L. I. R., Yabuuchi, A., Takeuchi, A., Cunniff, K. C., Hongguang, H., McKinney-Freeman, S., Naveiras, O., Yoon, T. J., Irizarry, R. A., Jung, N., Seita, J., Hanna, J., Murakami, P., Jaenisch, R., Weissleder, R., Orkin, S. H., Weissman, I. L., Feinberg, A. P., Daley, G. Q., Sep. 2010. Epigenetic memory in induced pluripotent stem cells. Nature 467 (7313), 285–90.

KLEINSMITH, L. J., PIERCE, G. B., Oct. 1964. Multipotentiality of single embryonal carcinoma cells. Cancer Res 24, 1544–51.

Klezovitch, O., Fernandez, T. E., Tapscott, S. J., Vasioukhin, V., Mar. 2004. Loss of cell polarity causes severe brain dysplasia in lgl1 knockout mice. Genes Dev 18 (5), 559–71.

Knoblich, J. A., Dec. 1997. Mechanisms of asymmetric cell division during animal development. Curr Opin Cell Biol 9 (6), 833–41.

Knoepfler, P. S., Cheng, P. F., Eisenman, R. N., Oct. 2002. N-myc is essential during neurogenesis for the rapid expansion of progenitor cell populations and the inhibition of neuronal differentiation. Genes Dev 16 (20), 2699–712.

Kordon, E. C., Smith, G. H., May 1998. An entire functional mammary gland may comprise the progeny from a single cell. Development 125 (10), 1921–30.

Kuperwasser, C., Hurlbut, G. D., Kittrell, F. S., Dickinson, E. S., Laucirica, R., Medina, D., Naber, S. P., Jerry, D. J., Dec. 2000. Development of spontaneous mammary tumors in balb/c p53 heterozygous mice. a model for li-fraumeni syndrome. Am J Pathol 157 (6), 2151–9.

kyung Park, I., Qian, D., Kiel, M., Becker, M. W., Pihalja, M., Weissman, I. L., Morrison, S. J., Clarke, M. F., May 2003. Bmi-1 is required for maintenance of adult self-renewing haematopoietic stem cells. Nature 423 (6937), 302–5.

Lanzkron, S. M., Collector, M. I., Sharkis, S. J., Mar. 1999. Hematopoietic stem cell tracking in vivo: a comparison of short-term and long-term repopulating cells. Blood 93 (6), 1916–21.

Lapidot, T., Sirard, C., Vormoor, J., Murdoch, B., Hoang, T., Caceres-Cortes, J., Minden, M., Paterson, B., Caligiuri, M. A., Dick, J. E., Feb. 1994. A cell initiating human acute myeloid leukaemia after transplantation into scid mice. Nature 367 (6464), 645–8.

Laurenti, E., Varnum-Finney, B., Wilson, A., Ferrero, I., Blanco-Bose, W. E., Ehninger, A., Knoepfler, P. S., Cheng, P.-F., MacDonald, H. R., Eisenman, R. N., Bernstein, I. D., Trumpp, A., Dec. 2008. Hematopoietic stem cell function and survival depend on c-myc and n-myc activity. Cell Stem Cell 3 (6), 611–24.

Laurenti, E., Wilson, A., Trumpp, A., Dec. 2009. Myc's other life: stem cells and beyond. Curr Opin Cell Biol 21 (6), 844–54.

Lechler, T., Fuchs, E., Sep. 2005. Asymmetric cell divisions promote stratification and differentiation of mammalian skin. Nature 437 (7056), 275–80.

Lee, C.-Y., Andersen, R. O., Cabernard, C., Manning, L., Tran, K. D., Lanskey, M. J., Bashirullah, A., Doe, C. Q., Dec. 2006. Drosophila aurora-a kinase inhibits neuroblast self-renewal by regulating apkc/numb cortical polarity and spindle orientation. Genes Dev 20 (24), 3464–74.

Lee, G., Papapetrou, E. P., Kim, H., Chambers, S. M., Tomishima, M. J., Fasano, C. A., Ganat, Y. M., Menon, J., Shimizu, F., Viale, A., Tabar, V., Sadelain, M., Studer, L., Sep. 2009. Modelling pathogenesis and treatment of familial dysautonomia using patient-specific ipscs. Nature 461 (7262), 402–6.

Lessard, J., Sauvageau, G., May 2003. Bmi-1 determines the proliferative capacity of normal and leukaemic stem cells. Nature 423 (6937), 255–60.

Li, H., Collado, M., Villasante, A., Strati, K., Ortega, S., Canamero, M., Blasco, M. A., Serrano, M., Aug. 2009. The ink4/arf locus is a barrier for ips cell reprogramming. Nature 460 (7259), 1136–9.

Liao, M.-J., Zhang, C. C., Zhou, B., Zimonjic, D. B., Mani, S. A., Kaba, M., Gifford, A., Reinhardt, F., Popescu, N. C., Guo, W., Eaton, E. N., Lodish, H. F., Weinberg, R. A., Sep. 2007. Enrichment of a population of mammary gland cells that form mammospheres and have in vivo repopulating activity. Cancer Res 67 (17), 8131–8.

Lin, T., Chao, C., Saito, S., Mazur, S. J., Murphy, M. E., Appella, E., Xu, Y., Feb. 2005. p53 induces differentiation of mouse embryonic stem cells by suppressing nanog expression. Nat Cell Biol 7 (2), 165–71.

Littlewood, T. D., Hancock, D. C., Danielian, P. S., Parker, M. G., Evan, G. I., May 1995. A modified oestrogen receptor ligand-binding domain as an improved switch for the regulation of heterologous proteins. Nucleic Acids Res 23 (10), 1686–90.

Liu, J. C., Deng, T., Lehal, R. S., Kim, J., Zacksenhaus, E., Sep. 2007a. Identification of tumorsphere- and tumor-initiating cells in her2/neu-induced mammary tumors. Cancer Res 67 (18), 8671–81.

Liu, S., Dontu, G., Wicha, M. S., 2005. Mammary stem cells, self-renewal pathways, and carcinogenesis. Breast Cancer Res 7 (3), 86–95.

Liu, X., Holstege, H., van der Gulden, H., Treur-Mulder, M., Zevenhoven, J., Velds, A., Kerkhoven, R. M., van Vliet, M. H., Wessels, L. F. A., Peterse, J. L., Berns, A., Jonkers, J., Jul. 2007b. Somatic loss of brca1 and p53 in mice induces mammary tumors with features of human brca1-mutated basal-like breast cancer. Proc Natl Acad Sci U S A 104 (29), 12111–6.

Liu, Y., Elf, S. E., Miyata, Y., Sashida, G., Liu, Y., Huang, G., Di Giandomenico, S., Lee, J. M., Deblasio, A., Menendez, S., Antipin, J., Reva, B., Koff, A., Nimer, S. D., Jan. 2009. p53 regulates hematopoietic stem cell quiescence. Cell Stem Cell 4 (1), 37–48.

Mai, S., Fluri, M., Siwarski, D., Huppi, K., Aug. 1996. Genomic instability in mycer-activated rat1a-mycer cells. Chromosome Res 4 (5), 365–71.

Malanchi, I., Peinado, H., Kassen, D., Hussenet, T., Metzger, D., Chambon, P., Huber, M., Hohl, D., Cano, A., Birchmeier, W., Huelsken, J., Apr. 2008. Cutaneous cancer stem cell maintenance is dependent on beta-catenin signalling. Nature 452 (7187), 650–3.

Mani, S. A., Guo, W., Liao, M.-J., Eaton, E. N., Ayyanan, A., Zhou, A. Y., Brooks, M., Reinhard, F., Zhang, C. C., Shipitsin, M., Campbell, L. L., Polyak, K., Brisken, C., Yang, J., Weinberg, R. A., May 2008. The epithelial-mesenchymal transition generates cells with properties of stem cells. Cell 133 (4), 704–15.

Marion, R. M., Strati, K., Li, H., Murga, M., Blanco, R., Ortega, S., Fernandez-Capetillo, O., Serrano, M., Blasco, M. A., Aug. 2009. A p53-mediated dna damage response limits reprogramming to ensure ips cell genomic integrity. Nature 460 (7259), 1149–53.

Martins, C. P., Brown-Swigart, L., Evan, G. I., Dec. 2006. Modeling the therapeutic efficacy of p53 restoration in tumors. Cell 127 (7), 1323–34.

Meletis, K., Wirta, V., Hede, S.-M., NistÃÂ©r, M., Lundeberg, J., FrisÃÂ©n, J., Jan. 2006. p53 suppresses the self-renewal of adult neural stem cells. Development 133 (2), 363–9.

Mikkelsen, T. S., Hanna, J., Zhang, X., Ku, M., Wernig, M., Schorderet, P., Bernstein, B. E., Jaenisch, R., Lander, E. S., Meissner, A., Jul. 2008. Dissecting direct reprogramming through integrative genomic analysis. Nature 454 (7200), 49–55.

Miller, L. D., Smeds, J., George, J., Vega, V. B., Vergara, L., Ploner, A., Pawitan, Y., Hall, P., Klaar, S., Liu, E. T., Bergh, J., Sep. 2005. An expression signature for p53 status in human breast cancer predicts mutation status, transcriptional effects, and patient survival. Proc Natl Acad Sci U S A 102 (38), 13550–5.

Molofsky, A. V., Pardal, R., Iwashita, T., Park, I.-K., Clarke, M. F., Morrison, S. J., Oct. 2003. Bmi-1 dependence distinguishes neural stem cell self-renewal from progenitor proliferation. Nature 425 (6961), 962–7.

Momand, J., Wu, H. H., Dasgupta, G., Jan. 2000. Mdm2–master regulator of the p53 tumor suppressor protein. Gene 242 (1-2), 15–29.

Morel, A.-P., LiÃÂšvre, M., Thomas, C., Hinkal, G., Ansieau, S., Puisieux, A., 2008. Generation of breast cancer stem cells through epithelial-mesenchymal transition. PLoS One 3 (8), e2888.

Morrison, S. J., Hemmati, H. D., Wandycz, A. M., Weissman, I. L., Oct. 1995. The purification and characterization of fetal liver hematopoietic stem cells. Proc Natl Acad Sci U S A 92 (22), 10302–6.

Morrison, S. J., Kimble, J., Jun. 2006. Asymmetric and symmetric stem-cell divisions in development and cancer. Nature 441 (7097), 1068–74.

Morrison, S. J., Wright, D. E., Weissman, I. L., Mar. 1997. Cyclophosphamide/granulocyte colony-stimulating factor induces hematopoietic stem cells to proliferate prior to mobilization. Proc Natl Acad Sci U S A 94 (5), 1908–13.

Muller, W. J., Sinn, E., Pattengale, P. K., Wallace, R., Leder, P., Jul. 1988. Single-step induction of mammary adenocarcinoma in transgenic mice bearing the activated c-neu oncogene. Cell 54 (1), 105–15.

Murphy, D. J., Junttila, M. R., Pouyet, L., Karnezis, A., Shchors, K., Bui, D. A., Brown-Swigart, L., Johnson, L., Evan, G. I., Dec. 2008. Distinct thresholds govern myc's biological output in vivo. Cancer Cell 14 (6), 447–57.

Nagao, M., Campbell, K., Burns, K., Kuan, C.-Y., Trumpp, A., Nakafuku, M., Dec. 2008. Coordinated control of self-renewal and differentiation of neural stem cells by myc and the p19arf-p53 pathway. J Cell Biol 183 (7), 1243–57.

Nakagawa, M., Koyanagi, M., Tanabe, K., Takahashi, K., Ichisaka, T., Aoi, T., Okita, K., Mochiduki, Y., Takizawa, N., Yamanaka, S., Jan. 2008. Generation of induced pluripotent stem cells without myc from mouse and human fibroblasts. Nat Biotechnol 26 (1), 101–6.

Nishimura, T., Fukata, Y., Kato, K., Yamaguchi, T., Matsuura, Y., Kamiguchi, H., Kaibuchi, K., Sep. 2003. Crmp-2 regulates polarized numb-mediated endocytosis for axon growth. Nat Cell Biol 5 (9), 819–26.

Noctor, S. C., Martinez-Cerdeno, Ivic, L., Kriegstein, A. R., Feb. 2004. Cortical neurons arise in symmetric and asymmetric division zones and migrate through specific phases. Nat Neurosci 7 (2), 136–44.

O'Brien, M. J., Dec. 2007. Hyperplastic and serrated polyps of the colorectum. Gastroenterol Clin North Am 36 (4), 947–68, viii.

Okabe, M., Ikawa, M., Kominami, K., Nakanishi, T., Nishimune, Y., May 1997. 'green mice' as a source of ubiquitous green cells. FEBS Lett 407 (3), 313–9.

Okita, K., Ichisaka, T., Yamanaka, S., Jul. 2007. Generation of germline-competent induced pluripotent stem cells. Nature 448 (7151), 313–7.

Pasi, C. E., Bonizzi, G., Pelicci, P., Jun 2010. Setting sights on the right target: p53 and stem cell division. Cell Cycle 9 (12).

Pece, S., Tosoni, D., Confalonieri, S., Mazzarol, G., Vecchi, M., Ronzoni, S., Bernard, L., Viale, G., Pelicci, P. G., Di Fiore, P. P., Jan. 2010. Biological and molecular heterogeneity of breast cancers correlates with their cancer stem cell content. Cell 140 (1), 62–73.

Penuelas, S., Anido, J., Prieto-Sanchez, R. M., Folch, G., Barba, I., Cuartas, I., GarcÃÂa-Dorado, D., Poca, M. A., Sahuquillo, J., Baselga, J., Seoane, J., Apr. 2009. Tgf-beta increases glioma-initiating cell self-renewal through the induction of lif in human glioblastoma. Cancer Cell 15 (4), 315–27.

Piccirillo, S. G. M., Reynolds, B. A., Zanetti, N., Lamorte, G., Binda, E., Broggi, G., Brem, H., Olivi, A., Dimeco, F., Vescovi, A. L., Dec. 2006. Bone morphogenetic proteins inhibit the tumorigenic potential of human brain tumour-initiating cells. Nature 444 (7120), 761–5.

Piltti, K., Kerosuo, L., Hakanen, J., Eriksson, M., Angers-Loustau, A., LeppÃÂ€, S., Salminen, M., Sariola, H., Wartiovaara, K., Aug. 2006. E6/e7 oncogenes increase and tumor suppressors decrease the proportion of self-renewing neural progenitor cells. Oncogene 25 (35), 4880–9.

Pinner, S., Jordan, P., Sharrock, K., Bazley, L., Collinson, L., Marais, R., Bonvin, E., Goding, C., Sahai, E., Oct. 2009. Intravital imaging reveals transient changes in pigment production and brn2 expression during metastatic melanoma dissemination. Cancer Res 69 (20), 7969–77.

Ponti, D., Costa, A., Zaffaroni, N., Pratesi, G., Petrangolini, G., Coradini, D., Pilotti, S., Pierotti, M. A., Daidone, M. G., Jul. 2005. Isolation and in vitro propagation of tumorigenic breast cancer cells with stem/progenitor cell properties. Cancer Res 65 (13), 5506–11.

Quintana, E., Shackleton, M., Sabel, M. S., Fullen, D. R., Johnson, T. M., Morrison, S. J., Dec. 2008. Efficient tumour formation by single human melanoma cells. Nature 456 (7222), 593–8.

Ragimov, N., Krauskopf, A., Navot, N., Rotter, V., Oren, M., Aloni, Y., May 1993. Wild-type but not mutant p53 can repress transcription initiation in vitro by interfering with the binding of basal transcription factors to the tata motif. Oncogene 8 (5), 1183–93.

Rambhatla, L., Bohn, S. A., Stadler, P. B., Boyd, J. T., Coss, R. A., Sherley, J. L., 2001. Cellular senescence: Ex vivo p53-dependent asymmetric cell kinetics. J Biomed Biotechnol 1 (1), 28–37.

Ray, S., Atkuri, K. R., Deb-Basu, D., Adler, A. S., Chang, H. Y., Herzenberg, L. A., Felsher, D. W., Jul. 2006. Myc can induce dna breaks in vivo and in vitro independent of reactive oxygen species. Cancer Res 66 (13), 6598–605.

Raya, A., RodrÃÂguez-PizÃ, I., Guenechea, G., Vassena, R., Navarro, S., Barrero, M. J., Consiglio, A., CastellÃ, M., RÃÂo, P., Sleep, E., GonzÃ¡lez, F., Tiscornia, G., Garreta, E., Aasen, T., Veiga, A., Verma, I. M., SurrallÃÂ©s, J., Bueren, J., IzpisÃÂºa Belmonte, J. C., Jul. 2009. Disease-corrected haematopoietic progenitors from fanconi anaemia induced pluripotent stem cells. Nature 460 (7251), 53–9.

Reya, T., Morrison, S. J., Clarke, M. F., Weissman, I. L., Nov. 2001. Stem cells, cancer, and cancer stem cells. Nature 414 (6859), 105–11.

Reynolds, B. A., Weiss, S., Apr. 1996. Clonal and population analyses demonstrate that an egf-responsive mammalian embryonic cns precursor is a stem cell. Dev Biol 175 (1), 1–13.

Ricci-Vitiani, L., Lombardi, D. G., Pilozzi, E., Biffoni, M., Todaro, M., Peschle, C., De Maria, R., Jan. 2007. Identification and expansion of human colon-cancer-initiating cells. Nature 445 (7123), 111–5.

Sachdeva, M., Zhu, S., Wu, F., Wu, H., Walia, V., Kumar, S., Elble, R., Watabe, K., Mo, Y.-Y., Mar. 2009. p53 represses c-myc through induction of the tumor suppressor mir-145. Proc Natl Acad Sci U S A 106 (9), 3207–12.

Santolini, E., Puri, C., Salcini, A. E., Gagliani, M. C., Pelicci, P. G., Tacchetti, C., Di Fiore, P. P., Dec. 2000. Numb is an endocytic protein. J Cell Biol 151 (6), 1345–52.

Satoh, Y., Matsumura, I., Tanaka, H., Ezoe, S., Sugahara, H., Mizuki, M., Shibayama, H., Ishiko, E., Ishiko, J., Nakajima, K., Kanakura, Y., Jun. 2004. Roles for c-myc in self-renewal of hematopoietic stem cells. J Biol Chem 279 (24), 24986–93.

Sears, R., Nuckolls, F., Haura, E., Taya, Y., Tamai, K., Nevins, J. R., Oct. 2000. Multiple ras-dependent phosphorylation pathways regulate myc protein stability. Genes Dev 14 (19), 2501–14.

Shackleton, M., Quintana, E., Fearon, E. R., Morrison, S. J., Sep. 2009. Heterogeneity in cancer: cancer stem cells versus clonal evolution. Cell 138 (5), 822–9.

Shackleton, M., Vaillant, F., Simpson, K. J., Stingl, J., Smyth, G. K., Asselin-Labat, M.-L., Wu, L., Lindeman, G. J., Visvader, J. E., Jan. 2006. Generation of a functional mammary gland from a single stem cell. Nature 439 (7072), 84–8.

Shen, Q., Zhong, W., Jan, Y. N., Temple, S., Oct. 2002. Asymmetric numb distribution is critical for asymmetric cell division of mouse cerebral cortical stem cells and neuroblasts. Development 129 (20), 4843–53.

Shinin, V., Gayraud-Morel, B., GomÃÂšs, D., Tajbakhsh, S., Jul. 2006. Asymmetric division and cosegregation of template dna strands in adult muscle satellite cells. Nat Cell Biol 8 (7), 677–87.

Shipitsin, M., Polyak, K., May 2008. The cancer stem cell hypothesis: in search of definitions, markers, and relevance. Lab Invest 88 (5), 459–63.

Singh, S. K., Hawkins, C., Clarke, I. D., Squire, J. A., Bayani, J., Hide, T., Henkelman, R. M., Cusimano, M. D., Dirks, P. B., Nov. 2004. Identification of human brain tumour initiating cells. Nature 432 (7015), 396–401.

Sleeman, K. E., Kendrick, H., Ashworth, A., Isacke, C. M., Smalley, M. J., 2006. Cd24 staining of mouse mammary gland cells defines luminal epithelial, myoepithelial/basal and non-epithelial cells. Breast Cancer Res 8 (1), R7.

Smalley, M., Ashworth, A., Nov. 2003. Stem cells and breast cancer: A field in transit. Nat Rev Cancer 3 (11), 832–44.

Smith, C. A., Dho, S. E., Donaldson, J., Tepass, U., McGlade, C. J., Aug. 2004. The cell fate determinant numb interacts with ehd/rme-1 family proteins and has a role in endocytic recycling. Mol Biol Cell 15 (8), 3698–708.

Soucek, L., Helmer-Citterich, M., Sacco, A., Jucker, R., Cesareni, G., Nasi, S., Nov. 1998. Design and properties of a myc derivative that efficiently homodimerizes. Oncogene 17 (19), 2463–72.

Sridharan, R., Tchieu, J., Mason, M. J., Yachechko, R., Kuoy, E., Horvath, S., Zhou, Q., Plath, K., Jan. 2009. Role of the murine reprogramming factors in the induction of pluripotency. Cell 136 (2), 364–77.

St-Jacques, B., Dassule, H. R., Karavanova, I., Botchkarev, V. A., Li, J., Danielian, P. S., McMahon, J. A., Lewis, P. M., Paus, R., McMahon, A. P., Sep. 1998. Sonic hedgehog signaling is essential for hair development. Curr Biol 8 (19), 1058–68.

Stadtfeld, M., Hochedlinger, K., Oct. 2010. Induced pluripotency: history, mechanisms, and applications. Genes Dev 24 (20), 2239–63.

Stadtfeld, M., Maherali, N., Borkent, M., Hochedlinger, K., Jan. 2010. A reprogrammable mouse strain from gene-targeted embryonic stem cells. Nat Methods 7 (1), 53–5.

Stingl, J., Eaves, C. J., Kuusk, U., Emerman, J. T., Aug. 1998. Phenotypic and functional characterization in vitro of a multipotent epithelial cell present in the normal adult human breast. Differentiation 63 (4), 201–13.

Stingl, J., Eirew, P., Ricketson, I., Shackleton, M., Vaillant, F., Choi, D., Li, H. I., Eaves, C. J., Feb. 2006. Purification and unique properties of mammary epithelial stem cells. Nature 439 (7079), 993–7.

Straight, A. F., Cheung, A., Limouze, J., Chen, I., Westwood, N. J., Sellers, J. R., Mitchison, T. J., Mar. 2003. Dissecting temporal and spatial control of cytokinesis with a myosin ii inhibitor. Science 299 (5613), 1743–7.

Sukhai, M. A., Wu, X., Xuan, Y., Zhang, T., Reis, P. P., Dube, K., Rego, E. M., Bhaumik, M., Bailey, D. J., Wells, R. A., Kamel-Reid, S., Pandolfi, P. P., Jan. 2004. Myeloid leukemia with promyelocytic features in transgenic mice expressing hcg-numa-raralpha. Oncogene 23 (3), 665–78.

Takahashi, K., Yamanaka, S., Aug. 2006. Induction of pluripotent stem cells from mouse embryonic and adult fibroblast cultures by defined factors. Cell 126 (4), 663–76.

Tan, B. T., Park, C. Y., Ailles, L. E., Weissman, I. L., Dec. 2006. The cancer stem cell hypothesis: a work in progress. Lab Invest 86 (12), 1203–7.

Tokuzawa, Y., Kaiho, E., Maruyama, M., Takahashi, K., Mitsui, K., Maeda, M., Niwa, H., Yamanaka, S., Apr. 2003. Fbx15 is a novel target of oct3/4 but is dispensable for embryonic stem cell self-renewal and mouse development. Mol Cell Biol 23 (8), 2699–708.

Trichopoulos, D., Adami, H.-O., Ekbom, A., Hsieh, C.-C., Lagiou, P., Feb. 2008. Early life events and conditions and breast cancer risk: from epidemiology to etiology. Int J Cancer 122 (3), 481–5.

Uchida, N., Buck, D. W., He, D., Reitsma, M. J., Masek, M., Phan, T. V., Tsukamoto, A. S., Gage, F. H., Weissman, I. L., Dec. 2000. Direct isolation of human central nervous system stem cells. Proc Natl Acad Sci U S A 97 (26), 14720–5.

Utikal, J., Polo, J. M., Stadtfeld, M., Maherali, N., Kulalert, W., Walsh, R. M., Khalil, A., Rheinwald, J. G., Hochedlinger, K., Aug. 2009. Immortalization eliminates a roadblock during cellular reprogramming into ips cells. Nature 460 (7259), 1145–8.

Vaillant, F., Asselin-Labat, M.-L., Shackleton, M., Forrest, N. C., Lindeman, G. J., Visvader, J. E., Oct. 2008. The mammary progenitor marker cd61/beta3 integrin identifies cancer stem cells in mouse models of mammary tumorigenesis. Cancer Res 68 (19), 7711–7.

Varlakhanova, N. V., Cotterman, R. F., deVries deVries deVries deVries deVries deVries, W. N., Morgan, J., Donahue, L. R., Murray, S., Knowles, B. B., Knoepfler, P. S., Jul. 2010. myc maintains embryonic stem cell pluripotency and self-renewal. Differentiation 80 (1), 9–19.

Vassilev, L. T., Vu, B. T., Graves, B., Carvajal, D., Podlaski, F., Filipovic, Z., Kong, N., Kammlott, U., Lukacs, C., Klein, C., Fotouhi, N., Liu, E. A., Feb. 2004. In vivo activation of the p53 pathway by small-molecule antagonists of mdm2. Science 303 (5659), 844–8.

Ventura, A., Kirsch, D. G., McLaughlin, M. E., Tuveson, D. A., Grimm, J., Lintault, L., Newman, J., Reczek, E. E., Weissleder, R., Jacks, T., Feb. 2007. Restoration of p53 function leads to tumour regression in vivo. Nature 445 (7128), 661–5.
URL 2

Vintersten, K., Monetti, C., Gertsenstein, M., Zhang, P., Laszlo, L., Biechele, S., Nagy, A., Dec. 2004. Mouse in red: red fluorescent protein expression in mouse es cells, embryos, and adult animals. Genesis 40 (4), 241–6.

Visvader, J. E., Lindeman, G. J., Oct. 2008. Cancer stem cells in solid tumours: accumulating evidence and unresolved questions. Nat Rev Cancer 8 (10), 755–68.

Vogelstein, B., Lane, D., Levine, A. J., Nov. 2000. Surfing the p53 network. Nature 408 (6810), 307–10.

von Stein, W., Ramrath, A., Grimm, A., MÃÂŒller-Borg, M., Wodarz, A., Apr. 2005. Direct association of bazooka/par-3 with the lipid phosphatase pten reveals a link between the par/apkc complex and phosphoinositide signaling. Development 132 (7), 1675–86.

Vousden, K. H., Prives, C., Jan. 2005. P53 and prognosis: new insights and further complexity. Cell 120 (1), 7–10.

Wang, H., Lathia, J. D., Wu, Q., Wang, J., Li, Z., Heddleston, J. M., Eyler, C. E., Elderbroom, J., Gallagher, J., Schuschu, J., MacSwords, J., Cao, Y., McLendon, R. E., Wang, X.-F., Hjelmeland, A. B., Rich, J. N., Oct. 2009. Targeting interleukin 6 signaling suppresses glioma stem cell survival and tumor growth. Stem Cells 27 (10), 2393–404.

Watkins, D. N., Berman, D. M., Burkholder, S. G., Wang, B., Beachy, P. A., Baylin, S. B., Mar. 2003. Hedgehog signalling within airway epithelial progenitors and in small-cell lung cancer. Nature 422 (6929), 313–7.

Watt, F. M., Frye, M., Benitah, S. A., Mar. 2008. Myc in mammalian epidermis: how can an oncogene stimulate differentiation? Nat Rev Cancer 8 (3), 234–42.

Weiss, S., Dunne, C., Hewson, J., Wohl, C., Wheatley, M., Peterson, A. C., Reynolds, B. A., Dec. 1996. Multipotent cns stem cells are present in the adult mammalian spinal cord and ventricular neuroaxis. J Neurosci 16 (23), 7599–609.

Wernig, M., Meissner, A., Foreman, R., Brambrink, T., Ku, M., Hochedlinger, K., Bernstein, B. E., Jaenisch, R., Jul. 2007. In vitro reprogramming of fibroblasts into a pluripotent es-cell-like state. Nature 448 (7151), 318–24.

Wernig, M., Zhao, J.-P., Pruszak, J., Hedlund, E., Fu, D., Soldner, F., Broccoli, V., Constantine-Paton, M., Isacson, O., Jaenisch, R., Apr. 2008. Neurons derived from reprogrammed fibroblasts functionally integrate into the fetal brain and improve symptoms of rats with parkinson's disease. Proc Natl Acad Sci U S A 105 (15), 5856–61.

Wodarz, A., Gonzalez, C., Mar. 2006. Connecting cancer to the asymmetric division of stem cells. Cell 124 (6), 1121–3.

Wright, D. E., Cheshier, S. H., Wagers, A. J., Randall, T. D., Christensen, J. L., Weissman, I. L., Apr. 2001. Cyclophosphamide/granulocyte colony-stimulating factor causes selective mobilization of bone marrow hematopoietic stem cells into the blood after m phase of the cell cycle. Blood 97 (8), 2278–85.

Wright, M. H., Calcagno, A. M., Salcido, C. D., Carlson, M. D., Ambudkar, S. V., Varticovski, L., 2008. Brca1 breast tumors contain distinct cd44+/cd24- and cd133+ cells with cancer stem cell characteristics. Breast Cancer Res 10 (1), R10.

Xu, D., Alipio, Z., Fink, L. M., Adcock, D. M., Yang, J., Ward, D. C., Ma, Y., Jan. 2009. Phenotypic correction of murine hemophilia a using an ips cell-based therapy. Proc Natl Acad Sci U S A 106 (3), 808–13.

Xue, W., Zender, L., Miething, C., Dickins, R. A., Hernando, E., Krizhanovsky, V., Cordon-Cardo, C., Lowe, S. W., Feb. 2007. Senescence and tumour clearance is triggered by p53 restoration in murine liver carcinomas. Nature 445 (7128), 656–60.
URL 1933

Yilmaz, O. H., Valdez, R., Theisen, B. K., Guo, W., Ferguson, D. O., Wu, H., Morrison, S. J., May 2006. Pten dependence distinguishes haematopoietic stem cells from leukaemia-initiating cells. Nature 441 (7092), 475–82.

Zanet, J., Pibre, S., Jacquet, C., Ramirez, A., de AlborÃ¡n, I. M., Gandarillas, A., Apr. 2005. Endogenous myc controls mammalian epidermal cell size, hyperproliferation, endoreplication and stem cell amplification. J Cell Sci 118 (Pt 8), 1693–704.

Zhang, M., Behbod, F., Atkinson, R. L., Landis, M. D., Kittrell, F., Edwards, D., Medina, D., Tsimelzon, A., Hilsenbeck, S., Green, J. E., Michalowska, A. M., Rosen, J. M., Jun. 2008. Identification of tumor-initiating cells in a p53-null mouse model of breast cancer. Cancer Res 68 (12), 4674–82.

Zhang, R., Zhang, Z., Zhang, C., Zhang, L., Robin, A., Wang, Y., Lu, M., Chopp, M., Jun. 2004. Stroke transiently increases subventricular zone cell division from asymmetric to symmetric and increases neuronal differentiation in the adult rat. J Neurosci 24 (25), 5810–5.

Zhao, C., Chen, A., Jamieson, C. H., Fereshteh, M., Abrahamsson, A., Blum, J., Kwon, H. Y., Kim, J., Chute, J. P., Rizzieri, D., Munchhof, M., VanArsdale, T., Beachy, P. A., Reya, T., Apr. 2009. Hedgehog signalling is essential for maintenance of cancer stem cells in myeloid leukaemia. Nature 458 (7239), 776–9.

Zhao, Z., Zuber, J., Diaz-Flores, E., Lintault, L., Kogan, S. C., Shannon, K., Lowe, S. W., Jul. 2010. p53 loss promotes acute myeloid leukemia by enabling aberrant self-renewal. Genes Dev 24 (13), 1389–402.

Zheng, H., Ying, H., Yan, H., Kimmelman, A. C., Hiller, D. J., Chen, A.-J., Perry, S. R., Tonon, G., Chu, G. C., Ding, Z., Stommel, J. M., Dunn, K. L., Wiedemeyer, R., You, M. J., Brennan, C., Wang, Y. A., Ligon, K. L., Wong, W. H., Chin, L., DePinho, R. A., Oct. 2008. p53 and pten control neural and glioma stem/progenitor cell renewal and differentiation. Nature 455 (7216), 1129–33.

Zheng, L., Ren, J. Q., Li, H., Kong, Z. L., Zhu, H. G., Dec. 2004. Downregulation of wild-type p53 protein by her-2/neu mediated pi3k pathway activation in human breast cancer cells: its effect on cell proliferation and implication for therapy. Cell Res 14 (6), 497–506.

Zhu, Y., McAvoy, S., Kuhn, R., Smith, D. I., May 2006. Rora, a large common fragile site gene, is involved in cellular stress response. Oncogene 25 (20), 2901–8.

9 Appendix and Acknowledgements

The setting up of the mammosphere culture and the characterisation of CSCs, as well as the study of the role of p53 in regulating SC division were performed together with Giuseppina Bonizzi and Angelo Cicalese at the European Institute of Oncology. The analysis of genomic instability in reprogrammed mammary clones was performed by the group of Thanos Halazonetis in the Department of Biochemistry at the University of Geneva, Switzerland.

I thank my boss Pier Giuseppe Pelicci for being an amazing scientific guide throughout this PhD, all the collegues and friends who have helped me technically and spiritually over the years, all my family for support and trust.